Dissertation

Precise Sr Isotope Ratio Measurements by Multiple Collector-Inductively Coupled Plasma Mass Spectrometry

ausgeführt zum Zwecke der Erlangung des akademischen Grades eines Doktors der Bodenkultur bzw. Doctor rerum naturalium technicarium unter der Leitung und Betreuung von

Ao.Univ.Prof. DI Dr. Thomas Prohaska

eingereicht an der Universität für Bodenkultur Wien

von

DI Patrick Galler
Matr. Nr.: 9925953
Trostsrasse 98/3/35
A-1100 Wien

Wien, April 2008

People I want to thank

It is my top priority to acknowledge my supervisor Thomas Prohaska who has made all of this happen. He was the one making it possible for me to co-operate with and learn from great scientific minds like Takafumi Hirata, Sergei F. Boulyga, Andreas Limbeck and Maria Teschler-Nicola. Also did he sponsor my numerous science related travels to destinations all over the world including the Czech Republic, Germany, Great Britain, Hungary, Italy, Japan, Russia, Switzerland, Turkey and the US. If it wasn't for him, the time in the VIRIS group would have been much less exciting and salutary. He really is a scientific daredevil!

Dear Andreas, thank you for being understanding and supportive in equal shares. It will be difficult not having you around for most fruitful conversations. I deeply appreciate what you have done for me during the course of this work.

Lucky are the ones who have a chance of co-operating with Sergei F. Boulyga. His knowledge is vast, his skills are superb and his humour is razor-sharp. There is definitely a lot to learn from a man like him. Thank you!

Takafumi Hirata is one of my personal heroes in the field of (LA)-ICP-MS. I was in the fortunate position of having been able to work in his laboratory at the "Tokyo Institute for Technology" for a period of 2 months. There I received a more than comprehensive introduction to isotope ratio analysis. His contribution to my work was and still is significant.

I acknowledge Maria for the permanent, positive feedback, the challenging tasks and highly interesting samples I received. May this cooperation last forever!

I thank all my friends, mates and colleagues in the VIRIS team and on the BOKU, especially Siegfried Swoboda, Marion Brunner, Steffi Kappel and Alexandra Pederzolli. I will miss Siegfried's sparkling humour and Marion's witty remarks certainly a lot. I became accustomed to Sigi like to an older brother during the course of this work.

I deeply appreciate the positive feedback I almost constantly received from Prof. Gerhard Stingeder, Stephan Hann and Gunda Köllensperger. This made things a lot easier.

These lines go to my familiy, especially to my beloved mother Marianne, my dear father Harald and my inestimable brother Joachim. Dear brother, a thousand thanks for always being encouraging, supportive, interested in my work and listening to me whenever I was troubled. Acknowledgement goes also to my little brother Benedikt and my aunt Regina.

Hereby I acknowledge my versatile circle of friends. Anja, Betty, Christian, Christoph, Didl, Erkan, Harald, Helga, Irmi, Oliver, Peter, Taku, Thomas, Ulrike and Wolfgang are only a few names I want to mention. You are truly great people! I especially enjoyed the rock climbing sessions with some of you.

Finally I acknowledge all the governments of the world that are currently putting so much effort into uninstalling our hard-fought for civil rights, so we all don't have to think too much ourselves!

Kurzfassung

Die vorgelegte Dissertation befasst sich mit hochpräziser Sr Isotopenanalytik mittels „Multiple Collector-Inductively Coupled Plasma Mass Spectrometry" (MC-ICPMS). Der Inhalt dieser Dissertation umfasst das Testen zweier kommerziell erwerblicher Geräte dieses Typs die im Zuge dieser Arbeit bezüglich Ihrer Performance überprüft wurden. Weiters wird der routinemässige Ablauf von Sr Isotopenmessungen mit „dem „Nu Plasma" MC-ICP-MS beschrieben. Unter anderem werden dabei praktische Aspekte der Probenvorbereitung wie auch die Korrektur der generierten Daten bezüglich Basislinie, Interferenzen und Massenfraktionierung diskutiert. Typische Resultate für routinemässige Sr Isotopenanalytik werden anhand von archäologischen Proben gezeigt.

Ein weiterer Teil dieser Arbeit ist der Entwicklung einer on-line Fliess-Injektions (FI) Sr/Matrix Trennmethode zur interferenzfreien Bestimmung von $^{87}Sr/^{86}Sr$ Isotopenverhältnissen mittels MC-ICPMS gewidmet. Dazu wird das sog. "Sr Resin"; ein selektives Sorptionsmittels für in HNO_3 gelöstes Sr; verwendet um Säulen mit einem internen Volumen von 100 µL herzustellen. Diese Säulen können für multiple, hoch-effiziente Sr/Matrix Trennungen und nachfolgende on-line Sr Isotopen Messungen verwendet werden. In einem weiterführenden Teil dieser Arbeit wird diese Methode mit Hilfe eines Autosamplers und programmierbaren Ventilen sowie Pumpen vollständig automatisiert und das Säulenvolumen auf etwa 40 µL reduziert. Die Verwendung eines Membran Desolvators zur Probenzufuhr in das MC-ICPMS erlaubt eine sensitive, präzise und akkurate $^{87}Sr/^{86}Sr$ Bestimmungen von flüssigen Probenmengen von ungefähr 100 µL bei einer Sr Konzentration von 20-40 ng*g^{-1}. Die Applikation dieses Setups für die Charakterisierung von ungarischen und österreichischen Spargelproben wird gezeigt. Abschliessend wird ein Ansatz zur Untersuchung eventueller methodeninduzierter Isotopenfraktionierung sowie die potentielle Möglichkeit zur Untersuchung massenabhängiger $^{86}Sr/^{88}Sr$ Isotopenfraktionierung mittels dieses Ansatzes erläutert.

Im letzten Teil der Arbeit wird die Entwicklung einer Methode zur semi-invasiven Sr Isotopenanalytik in archäologischen Zahnproben mittels laser ablations (LA)-MC-ICPMS beschrieben. Der Einfluss methodenrelevanter Parameter wie des Ablationsgasflusses, des Ablationsgastypus (He und Ar) oder die Verwendung eines Partikelabscheiders auf das Messergebnis wird untersucht. Interferenzstudien und der potentielle Einfluss isobarer Überlagerungen in den generierten Massenspektren werden besprochen. Ein neuartiges Referenzmaterial; ähnlich der menschlichen Knochenmatrix; zur Qualitätskontrolle dieser Messungen wird vorgestellt. Die Tauglichkeit der Methode wird anhand der Untersuchung von archäologischen Zahnfunden aus dem Mladeč Funkomplex überprüft.

Abstract

This thesis addresses the issue of high precision Sr isotope ratio analysis using multiple collector-inductively coupled plasma mass spectrometry (MC-ICPMS). The content of this work includes the testing of two commercially available MC-ICP mass spectrometers. The decision process which apparatus was finally installed on the BOKU Vienna will be described briefly.

A routine procedure for Sr isotope ratio measurements using the "Nu Plasma" MC-ICPMS will be described. Practical aspects of sample preparation as well as data processing with respect to correction of baseline, interferences and mass bias will be discussed. Typical results of routine Sr isotope analysis by means of investigation of archaeological samples are shown.

A part of this work is dedicated to the development of an on-line flow-injection (FI) Sr/matrix separation method for interference free determination of $^{87}Sr/^{86}Sr$ isotope ratios via MC-ICPMS. "Sr Resin"; a highly selective sorbent for Sr dissolved in HNO_3; is used to produce separation columns possessing an internal volume of 100 µL. These columns may be used for multiple, highly efficient Sr/matrix separations and subsequent on-line Sr isotope ratio measurement. In a continuative part of this project the developed method was fully automated using an auto-sampler, programmable valves and pumps. Additionally the column volume was reduced to approximately 40 µL. Use of a desolvating membrane nebuliser for sample introduction to the MC-ICPMS allows sensitive, precise and accurate $^{87}Sr/^{86}Sr$ ratio measurements of liquid sample volumes of 100 µL at Sr concentrations of 20-40 ng*g^{-1}. The application of this set-up is demonstrated for the characterisation of Hungarian and Austrian asparagus samples. Finally an approach for investigation of potential method induced isotopic fractionation as well as the possibility for investigation of mass dependent $^{86}Sr/^{88}Sr$ isotope fractionation using automated FI Sr/matrix separation is illustrated.

The last part of this work is dedicated to the development of a method for semi-invasive Sr isotope analysis in archaeological tooth samples by laser ablation (LA)-MC-ICPMS. The influence of method relevant parameters such as ablation gas flow, ablation gas type (He and Ar) or the use of a particle separation/signal stabilisation device on the final measurement result are investigated. Potential isobaric interferences in the recorded mass spectra owing to the human bone matrix are discussed. A novel reference material, chemically similar to the human bone matrix, for quality control of Sr isotope ratio measurements by LA-MC-ICPMS is presented. The potentials and limits of the method are demonstrated by investigation of archaeological tooth samples from the Mladeč findings.

Introduction

Since the introduction of the first commercial inductively coupled plasma mass spectrometers (ICPMS) in 1983 (Potter, 2008), this analytical technique has spread throughout laboratories worldwide at an increasing rate (Jarvis et al., 1993). The possibility to analyse samples in gas (Krupp and Donard, 2005), liquid (Serapinas et al., 2008) and solid form (Saetveit et al., 2008) at unrivalled sample throughput rates, combined with multi-element capabilities and high detection power (Jarvis et al., 1993) makes this technology very attractive for a large variety of scientific fields. Countless applications may be found, including environmental sciences (Prohaska et al., 1995; Reimann et al., 2007), medical research (Walczyk and Blanckenburg, 2002; Smith et al., 2000), geological studies (Simon et al., 2007; Tanaka et al., 2007) and archaeological investigations (Åberg et al., 1998, Budd et al., 2004), to cite a limited number of selected applications. In addition to the capability of reliable quantification of elemental concentrations, ICPMS comprises the potential of comparably precise and accurate determination of isotope ratios. The adequacy of ICPMS for this purpose was already demonstrated quite early during the history of development of this technology (Jarvis et al., 1993). The potential advantages of employing ICPMS for measurement of isotope ratios and abundances over traditional approaches, such as thermal ionisation mass spectrometry (TIMS) (Albarède et al, 2004) or secondary ionisation mass spectrometry (SIMS) (Košler at al., 2002), are significant. First of all, sample pre-treatment preceding ICPMS measurements is usually less labour intensive than sample pre-treatment required for TIMS or SIMS (Jarvis et al., 1993). Additionally, using ICPMS will result in reduced measurement time, which becomes noticeable as increased sample throughput (Jarvis et al., 1993; Albarède at al., 2004; Košler at al., 2002). Furthermore, the physical characteristics of an ion source used in TIMS limit its application to elements with low first ionisation potentials (Jarvis et al., 1993). This is in strong contrast to ICPMS, as the inductively coupled plasma ion source is capable of ionising virtually all elements within the periodic system (Jarvis et al., 1993). Despite the excellent suitability of an inductively coupled Ar-plasma as ion source, its use for isotope ratio determination and isotope abundance quantification was hampered by short term signal fluctuations, also termed as "plasma flicker noise" (Meija and Mester, 2007; Weiss et al., 2000). This and the sequential nature of most ICP-ion source based mass analysers restricted measurement of isotope ratios to studies where, isotopic variation between investigated samples were expected to be sufficiently large (Prohaska et al., 2005; Eis et al., 2001) or quantification of elemental contents was achieved via isotope dilution mass spectrometry (IDMS) (Boulyga and Heumann, 2005). In the latter application the precision of measured isotope ratios has only limited influence on the measurement uncertainty associated with the final measurement result , i.e. the absolute elemental content of a given sample (Klingbeil et al., 2001).

It was in 1992 when successful coupling of an inductively coupled plasma ion source to a magnetic sector analyser, equipped with seven Faraday detectors was reported for the first time (Walder and Freedman, 1992). This novel instrumental configuration allowed simultaneous detection of multiple ion currents on an array of parallel detectors, opening up a new paradigm in the world of ICPMS. The great interest of the scientific community to study variation of isotopic abundances with high accuracy and precision in a large variety of samples led to the launch of the first commercial multiple collector-ICP-mass spectrometers (MC-ICPMS) a few years later (Belshaw et al., 1998; Heumann et al., 1998). Exemplary figure 1 shows the occurrence of the search-term "MC-ICPMS" in the literature database provided by www.sciencedirect.com (Elsevier Publishing). It is evident from this data, that MC-ICPMS is a relatively recent technological development which did not level of yet to a constant number of publications per year. A similar trend can be found in a recent publication concerning the evolution and applications of MC-ICPMS (Douthitt, 2008) It can be estimated, that a lot more studies applying MC-ICPMS will follow during the next years. It may also be assumed, that the understanding of the true nature of data produced by this technology is not yet fully developed.
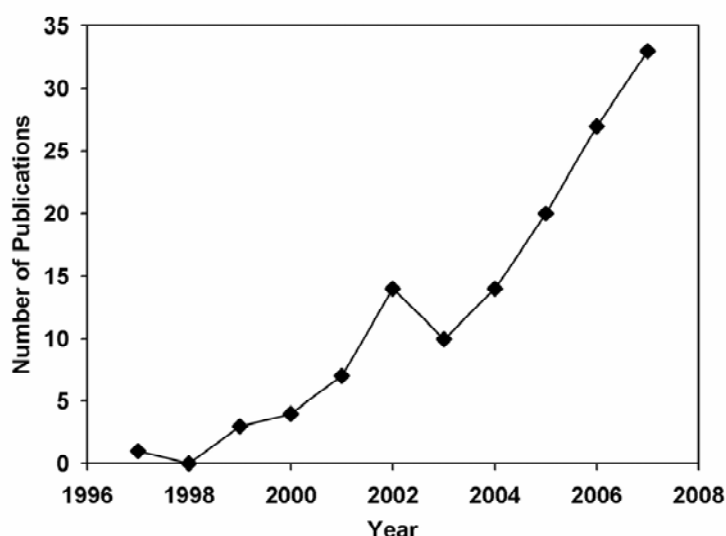
Fig. 1 Occurrence of MC-ICPMS related publications

As soon as MC-ICPMS technology emerged to meet the demands of high throughput, accurate, high precision isotope ratio and abundance analysis, it was clear that such measurements are significantly affected by spectral interferences and other matrix related effects (Albarède et al., 2004, Ingle et al., 2003, Andrén et al., 2004, Leya et al., 2007). Spectral interferences; as indicated by their name; are usually found to adulterate the "true" mass spectrum of elemental isotopes by contribution of atomic singly and doubly charged as

well as charged molecular species to the recorded analyte signals. Different strategies are proposed for avoiding influence of spectral interferences which include increase of the mass spectrometric resolution power "m/Δm" (Ingle et al., 2003) and chemical or physical analyte/matrix separation (Gale, 1996; Latkoczy et al., 2001; Rowland et al., 2008). Usually the separation of the analyte from the matrix is performed "off-line" as part of the sample preparation procedure before the actual isotope measurement. Samples are pre-treated accordingly, so that finally solutions; ideally containing only dissolved analyte; are placed into a rack of an auto sampler and measured in a sequential manner. Due to the fast rate of data acquisition possible by MC-ICPMS, common "off-line" sample preparation can become a limiting factor with respect to sample throughput. On-line sample pre-treatment as a programmable part of the measurement procedure offers several advantages. First of all the expenditure of human labour can be significantly reduced, thereby also decreasing, if not eliminating, the likeliness of human error. Furthermore the risk of sample contamination can be reduced, as sample preparation is performed under highly reproducible conditions within a closed system (Wang and Hansen, 2003).

The measurement of isotope abundances and isotope ratios becomes even more challenging when analyte/matrix separation is unfavourable. This can be the case for very valuable samples to be analysed in a preferably non-invasive manner. Laser ablation (LA) (Ramos et al., 2004; Hattendorf et al., 2003) hyphenated to MC-ICPMS offers a very elegant way to analyse very small amounts of an arbitrary specimen, leaving damage in the μm range. A small quantity of material; typically some μg; is ablated from the specimen by a focussed laser beam and swept into the detector. Depending on the experimental parameters and sample properties, very precise and accurate results may be derived from such measurements. It is clear however, that analyte/matrix separation is very difficult to achieve for LA-MC-ICPMS measurements and no commercial technology is available for this purpose yet. Given the fact, that during these types of measurements essentially all of the matrix as well as the analyte are introduced into the ICPMS, makes proper understanding of interference contributions essential.

In this work the development of a fully automated on-line flow injection (FI) Sr/matrix separation method will be presented. This method allows reducing sample preparation for Sr isotope ratio determinations to a suitable digestion and dilution of the sample prior to on-line processing. Moreover, recent advances in $^{87}Sr/^{86}Sr$ isotope ratio analysis by LA-MC-ICPMS will be reported in detail.

The significance of Sr for tracing

The Sr isotope system

Natural Sr consists of 4 isotopes of the approximate atomic weights 84, 86, 87 and 88 (De Bievre and Taylor, 1993). Isotope abundances as recommended by the International Union of Pure and Applied Chemistry (IUPAC) can be found in table 1. It is a fact however, that natural isotope abundances may vary significantly owing to either radioactive decay processes or mass dependent chemical and physical processes such as dissolution or precipitation of Sr containing minerals. Sr is among the most abundant trace elements found on earth (Capo et al., 1998). Additionally the artificial radionuclide ^{90}Sr ($t_{1/2}$ = 29.1 a) may appear in very low concentrations in nature due to nuclear accidents and weapon testing (Vonderheide et al., 2004). The artificial radionuclides ^{85}Sr ($t_{1/2}$ = 64.8 d) and ^{89}Sr ($t_{1/2}$ = 50.5 d) are used solely for medical purposes and do not occur in nature (Nielsen, 2004). ^{87}Sr is the only radiogenic of all 4 naturally occurring Sr isotopes. ^{87}Sr is the product of the radioactive β^- decay of ^{87}Rb (equation 1), with an approximate half life of $t_{1/2}$ = 4.88 ± 0.05 x 10^{10} a (Holden, 1990).

Isotope	Abundance [%]
^{84}Sr	0.56
^{86}Sr	9.86
^{87}Sr	7
^{88}Sr	82.58

Tab. 1 Natural Sr isotope abundances

^{87}Rb → ^{87}Sr + β- + Q (decay constant λ = 1.42 x 10^{-11} a^{-1}) (Steiger and Jäger, 1977)   **Equ. 1**
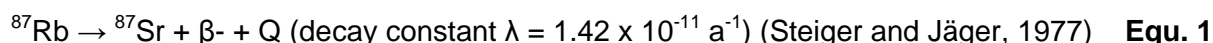
Evolution of Sr isotope patterns in nature

The ubiquitous trace elements Rb and Sr are both incorporated in various geologic matrices (Melgunov et al., 1995). Within a given geologic matrix, the radioactive decay of ^{87}Rb will lead to an increase of the ^{87}Sr abundance over time, while the abundances of ^{84}Sr, ^{86}Sr and ^{88}Sr remain constant. The absolute amount of ^{87}Sr within a geologic matrix is therefore a function of the initial Rb/Sr concentration ratio as well as the time Rb and Sr spent together within the given geologic matrix. "Rb/Sr age determination" of geologic materials represents a practical application of this knowledge (Moens et al., 2001; Pinson et al., 1958). The measurand for estimation of ^{87}Sr abundance is traditionally the ^{87}Sr/^{86}Sr isotope ratio (Choi et

al., 2008; Pinson et al., 1958). $^{87}Sr/^{86}Sr$ isotope ratios exhibit significant variation in nature and are typically close to 0.7. The lowest natural $^{87}Sr/^{86}Sr$ isotope ratio representative for the upper mantle of the Earth is 0.703. It is assumed that the evolution of the isotopic composition of Sr in the earth, caused by the decay of ^{87}Rb, started with an initial $^{87}Sr/^{86}Sr$ isotope ratio of 0.69908. This value is also referred to as BABI (basaltic achondrite best initial) and was found in whole-rock achondrite meteorites (Faure and Mensing, 2005). Ratios > 1 are reported for geologic matrices containing high levels of Rb, like mica, K-feldspar or biotite. (Capo et al., 1998; Nebel and Mezger 2006; Jeong et al., 2006). For comprehensive information concerning $^{87}Sr/^{86}Sr$ isotope ratios and their evolution in different types of rocks and minerals; including lunar rocks and meterorites; it is highly recommended to study Faure and Mensing, 2005.

Cycling of Sr in nature

Sr is released from geologic matrices by weathering processes, dissipated and subsequently cycled in nature. The isotopic composition of Sr in soils is defined by the underlying bedrock and atmospheric deposition (Capo et al., 1998; Stewart et al., 2001). Application of fertilizers to agriculturally used soils has additional impact on the Sr isotope signature of soils (Hosono et al., 2007). Soil is the interface between litho- and biosphere and provides nutrients for plant growth. Only labile or exchangeable Sr will be taken up by plants. It was demonstrated, that a total digest of a soil delivers different $^{87}Sr/^{86}Sr$ isotope ratios than a leachate of the same soil (Swoboda et al., 2007). The fact that Sr is a chemical proxy for Ca has great significance for application of Sr for tracing purposes (Capo et al., 1998). Ca is an essential element for the development of most life forms (Komiya et al., in press). Therefore Sr is cycled through the food chain as well.

Sr isotope tracing

The fact that Sr is ubiquitous, exhibits significant variation of its isotopic composition and is constantly released from the lithosphere by weathering processes enables tracing of large scale ecologic processes (Capo et al., 1998). Recent examples on the variety of applications are tracing of dust sources (Chavagnac et al., 2008; Chen et al., 2007; Grousset and Biscaye, 2005), tracing of water sources (Jørgensen et al., 2008; Brenot et al., 2008; Négrel and Petelet-Giraud, 2005) environmental sciences (Prohaska et al., 2005; Hosono et al., 2007; Nakano et al., 2008; Burton et al., 2006), archaeometry (Simonetti et al., in press; Benson et al., in press; Evans et al., 2006), migration tracing (Milton et al., in press; Font et al., 2007; Weber et al., 2005), forensic chemistry (Rauch et al., 2007; Montgomery et al., 2006) and provenance studies (Swoboda et al., 2007; Rodushkin et al., 2007; Fortunato et al., 2004; Almeida and Vasconcelos, 2001). It shall be commented here, that the

instrumental development within this work was applied for archaeometric purposes as well as identification of the authenticity of food via the Sr isotopic fingerprint.

Archaeological migration studies exploit the effect of incorporation of a locally specific Sr isotope signature into the human hard tissues bone and teeth via the food chain. These types of studies assume a well defined Sr isotope signature of bones and teeth among groups of people sharing the same habitat, food and water sources. When examining pre-historic burial grounds different groups of people may be identified by specific similarities, like e.g. different grave goods or a specific burial style. Affiliation to different groups can potentially be reflected by different Sr isotope signatures in investigated bone or tooth fragments (Evans et al., 2006; Knudson et al., 2005).

Monitoring of the Sr isotope signature of food products together with other parameters shall ensure traceability of food from "farm to fork" (Swoboda et al., 2007) in order to guarantee, that customers are receiving food quality they are actually paying for. A potential advantage of the application of Sr for isotope tracing is, that isotope ratios of "heavy elements" like Sr or Pb are believed to be less affected by seasonal variations during a year.than isotope ratios of "bio elements" like H, C, N and O (Swoboda et al., 2007).

Sr in the human body

A regular human diet contains approximately 2-4 mg Sr per day (Nielsen et al., 2004). A part of ingested Sr will be incorporated into the human skeleton, which is mainly composed of hydroxyl-apatite and collagen. Sr concentrations of 174 ± 127 µg*g^{-1} for bone (Tandon et al., 1998) and 81 ± 11 µg*g^{-1} for teeth (Losee et al., 1974) are suggested in literature. Sr in human teeth plays a special role. A human tooth basically consists of a hard protective outer part called enamel, and a softer inner core, termed dentine (He et al., 2006; Zaslansky et al., 2006). Enamel is growing in increments of a few µm per day during tooth formation in childhood (Smith, in press). Unlike bone and dentine, mineralized tooth enamel does not undergo a Sr turnover and therefore preserves the elemental and isotopic composition incorporated during the first few living years of an individual during tooth formation (Price et al., 2000). Thus a change of residence between child- and adulthood can potentially be reflected by different Sr isotope signatures in tooth enamel and dentine or skeletal bone.

Further difference exists with respect to the porosity of the different materials comprising the human skeleton. Whereas enamel is a very densely packed mineral phase with minimum organic content, dentine and skeletal bone exhibit high porosities (Sealy et al., 1995; Camargo et al., 2008). A table listing certain chemical features of skeletal bone, dental enamel and dentine is given below (table 2) (Martin et al., 1998; White and Folkens, 2005; Berkovitz et al., 1989; Schumacher and Schmidt, 1983). Not quoted in table 2 is the fact, that dentine in contrary to enamel has piezo- and pyro-electric properties. Several studies

indicate that dental enamel is much less susceptible to diagenetic alteration of the native Sr isotope signature than other parts of the human skeleton (Kohn et al., 1999; Budd et al., 2000; Lee-Thorp and Sponheimer, 2003). Enamel is therefore a frequently analysed part of human skeletal remains in archaeological studies (Åberg et al., 1998; Wright 2005). Moreover, the incremental nature of enamel growth and the fact, that different teeth start mineralization at different times within one and the same individual, theoretically allows reconstruction of an individual's nutritional history that covers a significantly longer time span than provided by a single tooth (Smith, in press; Wright 2005; Bentaleb et al., 2006). A comprehensive review on the relation between Sr and the human skeleton with respect to archaeological applications is provided in literature (Bentley, 2006).

Compartment	Suggested empiricial formula	Approximate relative content [% w/w]		
		Inorganic	Organic	H_2O
Bone	$(OH)_2C_6[(P_{5.9}C_{0.1})O_{24}](Ca_{3.3}Mg_{0.1}C_{0.6})$	68	17	15
Dentine	$(OH)_2C_6[(P_{5.6}C_{0.4})O_{24}](Ca_{2.9}Mg_{0.4}C_{0.7})$	70	20	10
Enamel	$(OH)_2C_6[(P_{5.3}C_{0.7})O_{24}](Ca_{3.4}Mg_{0.2}C_{0.4})$	99.5	0.4	0.1

Tab. 2 Selected chemical features of human bone, dentine and enamel

From the sample to the Sr isotope ratio

Preface

This section is dedicated to a brief overview of the sequence of processes necessary to determine Sr isotope signatures of any given sample. It is intended to serve as an orientation or guideline.

Sample preparation – digestion

The aim of sample preparation preceding solution based measurements is to finally obtain the sample in a form, suitable for the employed mass spectrometric technique. Ideally the sample digest is a clear, colourless solution without presence of suspended or sedimented particulate matter. Depending on the application, samples can undergo a drying step prior to digestion. Digestion of samples can be performed in open or closed vessels. Energy for sample digestion can be delivered by e.g. UV-lamps, microwave systems or simple hot plates. Alkali fusions are avoided as they usually result in high levels of impurities by the employed reagents or a high final salt content of the sample digest. Ideally a digestion method is adapted in a way, that labour effort is reduced and the measurement system will not be negatively affected by the final sample condition. Additionally it should be kept in

14

mind, that the amount of samples that can be readily prepared within a defined time span has significant impact on the economy of the whole analytical procedure, including the sampling as well as the measurement itself. A variety of samples has been digested prior to Sr isotope analysis in the presented work: archaeological bone and tooth fragments, recent bone and tooth fragments, asparagus, basalts and human hair. Three different digestion procedures for archaeological tooth, asparagus and basalt will be described in the experimental part of this work.

Sample preparation – Sr/matrix separation

Generally analyte/matrix separation is a pre-requisite for solution based high precision isotope ratio measurements to avoid interferences or matrix effects (Albarède et al., 2004; Andrén et al., 2004; Leya et al., 2007). This is specifically true when analysing $^{87}Sr/^{86}Sr$ isotope ratios. Here, the signal for ^{87}Sr is interfered by the isobar ^{87}Rb (Balcaen et al., 2005). These two signals may only be resolved by mass spectrometers possessing a mass spectrometric resolution of approximately 300 000, or accelerator mass spectrometry (AMS) (Müller, 2003). As AMS instrumentation is not easily accessible if at all available, and commercial inductively coupled plasma- and thermal ionisation mass spectrometers are restricted to a maximum mass spectrometric resolution power of ~ 10 000, alternative strategies for Sr/matrix separation are used. The main routes for routinely achieving proper Sr/matrix separation are currently the use of ion exchange chromatographic methods (Almeida and Vasconcelos, 2001; van Geldern et al., 2006; Korte et al., 2006), application of a Sr specific solid phase extraction procedure (Balcaen et al., 2005; Burton et al., 2006; Fantle and DePaolo, 2006) or a mixture of both (Waight et al., 2002a; Waight et al., 2002b). Traditionally Sr/matrix separation is performed off-line as batch procedure before the actual sample investigation.

Off-line Sr/matrix separation using the Sr specific resin

In this work Sr/matrix separation was achieved exclusively by using the Sr specific solid phase extraction as originally proposed by Horwitz et al. (1991). This procedure is performed using a commercially available product called "Sr Resin" (Eichrom, Bruz, France). For obtaining optimum separation efficiency using the Sr resin, a few things have to be taken care of. The resin is received in dry form and has to be soaked prior to use for at least 30 minutes in a 0.1 mol*L^{-1} nitric acid solution. When transferring the resin slurry into a convenient column with a pipette it has to be well taken care that the resin is under liquid all the time. Otherwise formation of air bubbles within the column bed may occur. It was found that it is worthwhile pre-cleaning the Sr resin with a few mL of water before conditioning the material with the sample media (Vonderheide et al., 2004). Sr retention is strongly increasing

with the nitric acid concentration of the sample and washing solution (Horwitz et al., 1992). Typically nitric acid concentrations between 6 and 8 mol*L^{-1} were found to be sufficient for the sample medium and the washing solution (Galler et al., 2007). It is crucial to show patience when loading the sample onto the extraction column. Flow rates should not exceed 0.5 mL*min^{-1} in order to allow the sample solution to equilibrate with the sorbent. Washing cycles necessary for removing essentially all matrix components depend on the Sr/Rb concentration ratio as well as on their absolute concentrations and may have to be optimised for each sample type. After sample elution, the resin is washed well with several column volumes of water and stored as slurry in PE vessels at 4°C in dilute nitric acid. The shelf life of Sr resin once suspended and soaked is limited (Charlier et al., 2006). Several blanks should be run with each batch of samples prepared, as the Sr resin is known to show a significant memory effect (Vonderheide et al., 2004). A description of problems occurring when using a not fully optimized method for a large number of samples can be found in literature (Swoboda et al., 2007). It is therefore strongly recommended not to use columns equipped with glass wool plugs instead of frits, as this can lead to irreproducible separation conditions.

On-line Sr/matrix separation

It is clear from the authors point of view that the larger number of samples processed in the VIRIS laboratory in the near future will be separated employing batch off-line Sr/matrix separation. This has the advantage, that the method does not demand much equipment and is a straightforward exercise. It can therefore be easily taught to students in a short time. Nonetheless does the research focus of the VIRIS group demand a discussion of current methods for on-line Sr/matrix separation in ICPMS.

As pointed out earlier, application of on-line sample pre-treatment in a preferably automated manner has several advantages. Only few publications demonstrating on-line Sr/matrix separation are currently available and the methods proposed show a broad spectrum of physical and chemical principles being applied. The use of ion-molecule gas phase reaction chemistry (Moens et al., 2001) and hyphenation of ion chromatography (Latkoczy et al., 2001) represent pioneering works in this field. Sr/matrix separation by ion-molecule gas phase reaction chemistry is based on the exothermal reaction of Sr$^+$ with CH$_3$F (equation 2) (Moens et al., 2001).

$$^{84\text{-}88}Sr^+ + CH_3{}^{19}F \rightarrow {}^{103\text{-}107}(SrF)^+ + CH_3 \cdot \quad \Delta H = -31.2 \text{ kcal/mol} \quad \textbf{Equ. 2}$$

No thermodynamic data is available for the formation of RbF$^+$, but based on the endothermic character of the reaction of Rb$^+$ with CH$_3$Cl, it is assumed to be endothermic as well. The

reaction quoted in equation 2 enables a quantitative shift of the Sr isotope pattern to a higher, un-interfered mass region by formation of a molecular ion consisting of mono-isotopic fluorine and strontium. However, the method was designed for a quadrupole ICPMS equipped with a dynamic reaction cell and it is known that such systems generally deliver poor precisions with respect to isotope ratio measurements (Meija and Mester, 2007).

The ion chromatographic method as proposed by Latkoczy et al. (2001) begins with 14 successive and exactly timed injections of a sample into a chromatographic system. The separation conditions are modified in a way that Rb elutes before Sr, and a steady state signal is provided in the form of a plateau for the elution of Sr. Full separation of Ca and Sr could not be obtained and the measurement time for a single sample is at least 40 minutes. On-line chromatographic separation of Sr from Rb experienced minor improvement later on by replacing several successive injections of small sample volumes with a single injection of a significantly increased sample volume of typically 3-5 mL (García-Ruiz et al., 2007 and 2008). Measurement time is roughly 20 minutes, influence of severe matrix effects has been reported and blank levels are put at stake by addition of an organic complexing agent to the sample solution and the eluent.

The most recent approach for separating Sr from Rb on-line, is application of electrothermal vaporization (ETV), exploiting the different volatilities of Sr and Rb (Rowland et al., 2008). This method is an impressive demonstration of how Sr and Rb can quantitatively be separated within a matter of a few seconds. The reported precision levels are pretty poor though and will probably restrict further application to screening purposes. Improvement of precision may be achieved by stretching the peak profile as discussed in the corresponding publication (Rowland et al., 2008).

A part of this work was dedicated to the development of a novel on-line Sr/matrix separation method (Galler et al., 2007). This was achieved by modifying the manual off-line Sr/matrix separation procedure; employing the Sr resin provided by Eichrom; as described above by means of flow injection (FI). Miniaturized separation columns containing approximately 100 µL of Sr resin were successfully used for quantitative on-line Sr/matrix separation in less than 10 minutes. Solvent consumption compared to the manual off-line Sr/matrix separation procedure was reduced by half. Memory effects, usually a major restriction to the repetitive use of Sr resin, can efficiently be reduced by repetitive blank measurements. In a first attempt a single 100 µL column was used for 40 Sr/matrix separations with subsequent measurement of the Sr isotope signature by MC-ICPMS. Precision levels remained constant throughout the measurement sequence although the Sr retention was observed to drop by approximately 50%. In a follow-up project the method was fully automated by replacing the employed manual valves with programmable valves and coupling of an auto sampler to the FI system. The volume of the separation columns was

reduced to a bed volume of approximately 40 µL while the injected sample volume was reduced from originally 500 µL to 100 µL. Use of a desolvating membrane nebuliser ("DSN 100", Nu Instruments, Wrexham, Wales, Great Britain) led to great improvement of the sensitivity, thus enabling investigation of samples with Sr concentrations of approximately 30 ng*g^{-1}. Applied flow rates for sample loading, washing and elution are around 100 µL*minute^{-1}. A single separation column was successfully employed for 66 measurements and the developed system worked 36 consecutive hours without any need for maintenance. It is apparent that the discussed method bears great economic potential, which is further underlined by application of peristaltic pumps instead of high performance chromatographic pumps. A corresponding publication draft concerning this work can be found in the appendix of this thesis.

Measurement of Sr isotope ratios

As pointed out earlier, TIMS and MC-ICPMS are the "working horses" with respect to high precision isotope ratio determination (Alabrède et al., 2004; Andrén et al., 2004; Ponzevera et al., 2006; Irisawa and Hirata, 2006). Data presented in this thesis are based on MC-ICPMS measurements. Thus, the following paragraphs are discussing the basic background of data acquisition and handling using the "Nu Plasma" MC-ICP-MS system.

Arrangement of analyte signals in the faraday detectors

The fact that two different collector arrangements; i.e. the "standard - " and the "U/Th/Pb - collector block"; are used in our laboratories with the Nu Plasma makes a discussion of peak alignment in the desired faraday detectors necessary.

regular collector block														
H6	H5	H4	H3	H2	H1	Ax	L1	L2	IC0	L3	IC1	L4	IC2	L5
		88		87		86		85		84		83		82
U/Th/Pb collector block														
Ex-H		H6	H5	H4	H3	H2	H1	Ax	L1	L2		IC0	IC1	L3	IC2	Ex-L
				88		87		86		85					

Tab. 3 Arrangement of Sr isotope signals relative to faraday cups

Changing the collector blocks will alter the position of the faraday cups. The outer faraday cups H6 and L5 are placed closer to the high and low mass side in the U/Th/Pb collector block than in the regular collector block to be able to cover the whole mass range from ^{204}Pb to ^{238}U (table 3). Alternatively these cups are then called extra high (Ex-H) and extra low (Ex-L). The mass spacing in case of Sr isotope analysis between cups Ex-H and H6, as well as L2 and IC0 is 2 atomic mass units. For the regular collector block mass spacing between H6 and H5 as well as H5 and H4 is only one atomic mass unit. The result is that only masses

88-85 can be covered when using the U/Th/Pb collector block for Sr isotope ratio measurements. This proved to be sufficient for all applications and is the minimum requirement for Sr isotope ratio analysis. Monitoring of masses 83 and 82, representative for Kr interferences on ^{86}Sr, can be omitted for the reason that all measurements were on peak baseline corrected. Potential Kr contamination levels coming from the Ar gas are stable as long as no liquid Ar tank is used for gas supply. In case of liquid Ar being used, Kr can become enriched at the bottom of the tank which will be noticeable as drifting baseline at mass 86. Mass 84 is proposed as monitor for molecular Ca interferences (Ramos et al., 2004; Waight et al., 2002b) in literature but was not evaluated during this work.

Solution based Sr isotope ratio measurements by MC-ICPMS

Solution based measurements of Sr isotope ratios can either be performed under "dry" or "wet plasma" conditions. The main difference consists of the fact that for dry plasma measurements a desolvating membrane nebuliser "DSN 100" (Nu Instruments) is used which enables efficient removal of water from the sample aerosol. The sample solution is introduced via a conventional low flow nebuliser into a heated spray chamber and subsequently introduced into a heated membrane, were water vapour is removed from the sample aerosol by permeation through the membrane. Outside the membrane a heated counter current Ar gas flow is removing the water vapour. The sample leaves the membrane desolvating nebuliser as dried aerosol and is directly introduced into the ICP. With such a set up a few hundred V*ppm^{-1} instrumental sensitivity can be obtained, enabling precise isotopic analysis of solutions containing a few ng*g^{-1} of analyte. Measuring under wet plasma conditions demands little alteration of the sample introduction system. The Nu Plasma MC-ICPMS is then equipped with a default, peltier cooled cinnabar spray chamber. A grounded plasma shield made of stainless steel is installed between the rf-load coil and the torch and wired up to the interface to increase instrumental sensitivity. Typically a few dozen V*ppm^{-1} instrumental sensitivity can be obtained for such a set up. A high capacity interface rotary pump "E2M80" (BOC Edwards, West Sussex, Great Britain) is permanently installed, resulting in lower pressure in the interface region between sampler and skimmer cone compared to when a default interface pump with lower evacuation capacity is installed. This has a favourable effect on instrumental sensitivity as a significantly smaller number of ions will be scattered due to collision with neutral species in the interface region.

Laser ablation based Sr isotope ratio measurements by MC-ICPMS

There are numerous reports of successful Sr isotope ratio determinations by LA-MC-ICPMS in a variety of mostly geologic matrices (Ramos et al., 2004; Woodhead et al., 2005; Barker et al., 2006; Vroon et al., 2008). One of the tasks of this work was the development of a

method, allowing reliable determination $^{87}Sr/^{86}Sr$ isotope ratios in archaeological tooth samples. Two reports applying LA-(MC)-ICPMS for this purpose are currently found in literature, but none of the methods proposed managed to deliver results suitable for archaeometric tracing purposes (Simonetti et al., in press; Prohaska et al., 2002). However, successful measurement of $^{87}Sr/^{86}Sr$ isotope ratios in apatite; a matrix similar to human the human dental matrix; was reported, likely resulting from the comparably high Sr concentration (> 3000 µg*g^{-1}) of this material (Bizzarro et al., 2003).

Sr signal intensity during LA-MC-ICPMS is critical for obtaining accurate and precise Sr isotope data in human teeth. Another important issue is the nature of the transient signal from which isotope data is derived. It is evident, that signal spikes; i.e. high temporal variation of the transient signal on a short time scale; can significantly contribute to the analytical uncertainty (Hirata 2007). Introduction of a "signal smoothing device" in the form of an increased flow path diameter between ablation cell and plasma torch can tremendously improve the quality of transient signals (Tunheng and Hirata, 2004). The use of a glass wool plug in the transfer line between ablation cell and ICP is frequently recommended to reduce signal spikes by filtering of large particles (Russo et al., 2004; Schultheis et al., 204; Guillong and Günther, 2002). Despite the benefits following from filtration of the LA aerosol (Guillong et al., 2003) the author does not recommend application of this practice. When ablating large quantities of sample at high repetition rates (e.g. 20 Hz) and large spot sizes (e.g. 300 µm) clogging of the glass wool filter plug was often observed. So was unpredictable, casual release of particles during measurement of gas blanks when the filter was not changed regularly. Application of high repetition rates combined with large spot sizes can be required by low abundance of the target analyte in the sample, as is the case for Sr in human dental material. Furthermore it turned out to be quite difficult to insert such a filtration device that performs in a reproducible manner.

Data reduction – preface

Data correction of MC-ICPMS measurements is a complex matter. Given below are only the steps that are routinely performed when processing a set of raw data. Some of the corrections of the data are performed automatically by the instrument software of the "Nu Plasma HR" MC-ICPMS as is the correction for gains between faraday cups. As no ion counting systems were involved in this work, corresponding corrections for non-linear effects are omitted (Hoffmann et al., 2005; Richter et al., 2005). Correction for cup efficiency (Makishima and Nakamura, 1991); i.e. the physical capability of a faraday detector to convert an impacting ion into a signal; was considered to be of minor influence with respect to the problems addressed in this work (Fortunato et al., 2004).

Data reduction – blank correction

Signal intensities may be recorded from steady state signals like in solution nebulisation based analysis or from transient signals as observed for laser ablation (LA) or flow injection (FI) based measurements. In any case the data reduction procedure is essentially the same. The first step is a blank or baseline correction of the raw signals. LA based measurements are corrected for blank by subtracting the intensities of a corresponding gas blank. The gas blank should be statistically representative with respect to its mean value. It should therefore be measured for at least 30 seconds and should ideally be measured prior to every ablation event. This will ensure that re-volatilisation of cone deposits can be corrected for more accurately. Transient signals from FI measurements can either be corrected with a pure water eluent baseline blank or via measurement of a corresponding procedural blank. If procedural blanks are managed to be kept low, both methods do not differ significantly from each other with respect to the final $^{87}Sr/^{86}Sr$ isotope ratio. Solution based measurements of samples formerly processed by off-line batch Sr/matrix separation are baseline corrected with procedural blanks in any case. It is necessary to introduce sufficiently long washing times between the measurement of samples and blanks to minimize influence of memory effects from the sample introduction system.

Data reduction – mass bias correction

Space charge is believed to be the main cause for preferential transmission of heavy masses in ICP mass spectrometers (Niu and Houk, 1996). The observed effect is called mass bias and usually in the range of a few percent for Sr on the "Nu Plasma" MC-ICPMS. Measured isotope ratios will therefore significantly deviate from their "true ratios" if no proper correction algorithm is applied. Mass bias can be externally corrected for by monitoring and evaluating the mass bias drift of a standard solution of known isotopic composition, measured before and after samples. In this case matrices of standard and sample solutions should be matched as close as possible, as matrix components can lead to a change of mass bias behaviour by affecting the charge density in the ICP (Ingle et al., 2003). If the investigated isotopic system provides a stable, invariable isotope ratio that is constant in nature, internal mass bias correction may be applied by evaluating the mass bias of this ratio. Subsequently the observed mass bias for this isotope pair may be applied for mass bias correction of another isotope pair of the same element. If the isotope system of interest does not provide a naturally constant isotope ratio, such a pair of isotopes with known isotopic composition may be added to the sample by spiking the sample with an isotope pair of known composition. This approach is suggested for example for high precision S isotope measurements where an isotope pair of Si is used for mass bias correction of S isotopes (Mason et al., 2006; Clough et al., 2006). Comparable procedures for Pb isotope measurements and a

corresponding Tl spike (Weiss et al., 2004), Rb as well as Sr isotope studies and a corresponding Zr spike (Waight et al., 2002b; Ohno et al., in press) or W isotope determinations using a Re spike for mass bias correction (Irisawa and Hirata, 2006) can be found in literature. Despite the excellent uncertainty levels that can be obtained by these methods, it is questionable whether the assumption of the same mass bias for different elements is valid (Ingle et al., 2003; Irisawa and Hirata, 2006; Hirata, 1996).

In the case of Sr the presumably invariant ^{86}Sr/^{88}Sr isotope ratio is routinely applied for internal mass bias correction of the measurand ^{87}Sr/^{86}Sr (Cavazzini, 2005). The use of an ^{86}Sr/^{88}Sr isotope ratio of 0.1194 for this purpose has a long history in literature and can be considered as convention (Bizzarro et al., 2003; Arriens and Compston, 1968; Steiger and Jäger, 1977). It was not until recently, that potential fractionation of ^{86}Sr/^{88}Sr isotope ratios in nature was started being discussed (Cavazzini, 2005). Even though this fractionation was reported to be significant (Ohno et al., in press), a constant ^{86}Sr/^{88}Sr isotope ratio of 0.1194 was assumed throughout this work.

Linear, power and exponential functions are commonly used for mass bias correction of ICPMS measurements (Ingle et al., 2003; Heumann et al., 1998). More refined methods like the mass dependent correction proposed by Russell (Russell et al., 1970) or polynomial mass response functions (Ingle et al., 2003) may be applied but do go beyond the scope of this work. There seems to be some confusion about the nomenclature of the exponential law, as the exponential law as applied by Balcaen et al. (2005) looks very similar to the Russell correction algorithm as quoted by Ingle et al. (2003). However, the exponential law quoted in the latter work has not very much in common with the exponential law found in the first groups' work or in Heumann et al. (1998). For this thesis exponential mass bias correction was performed using a mass dependent exponential correction algorithm, identical to the one used by Balcaen et al. (2005) or Archer and Vance (2004). Corresponding equations are quoted below. In these equations f is the fractionation coefficient and m the true mass of the respective Sr nuclide.

$$\left(\frac{^{87}\text{Sr}}{^{86}\text{Sr}}\right)_{corr} = \left(\frac{^{87}\text{Sr}}{^{86}\text{Sr}}\right)_{meas} \times \left(\frac{m_{87}}{m_{86}}\right)^{f} \qquad \textbf{Equ. 3}$$

$$f = \frac{\ln\left[\left(\frac{^{86}\text{Sr}}{^{88}\text{Sr}}\right)_{true} \Big/ \left(\frac{^{86}\text{Sr}}{^{88}\text{Sr}}\right)_{meas}\right]}{\ln\left(\frac{m_{86}}{m_{88}}\right)} \qquad \textbf{Equ. 4}$$

When analysing the literature, the choice of mass bias correction is usually based on the criterion how well an expected and certified isotope ratio of a reference material correlate after mass bias correction (Ingle et al., 2003). In the case of Sr isotope ratio analysis the reference $^{87}Sr/^{86}Sr$ isotope ratio is somewhat ambiguous. A frequently used reference material for control of Sr isotope measurement quality is the NIST standard reference material (SRM) 987 (National Institute of Standards and Technology, Gaithersburg, USA). This is a $SrCO_3$ with defined isotopic composition. There are actually 3 different values for the $^{87}Sr/^{86}Sr$ that are frequently quoted in literature and referred to as "accepted" or "adopted" ratios. Interestingly the certified $^{87}Sr/^{86}Sr$ isotope ratio of 0.71034 ± 0.00026 enjoys much less quotation frequency than do the "accepted" or "adopted" values of 0.71026 (Balcaen et al., 2006; Faure and Mensing, 2005) and 0.710245 (Faure and Mensing, 2005; Müller at al., 2003). One publication was found, were the certified $^{87}Sr/^{86}Sr$ isotope ratio for the NIST SRM 987 is quoted with 0.71025 (Revel-Rolland et al., 2006) although the certificate clearly states a different value. Mostly these "reference" values are quoted in any piece of literature reviewed without a corresponding uncertainty. However, the majority of published, measured $^{87}Sr/^{86}Sr$ isotope ratios for the NIST SRM 987 $SrCO_3$ are lower than the certified value and close to the accepted values (Stein et al., 1997; Petelet-Giraud and Negrel, 1997; Ntaflos and Richter, 2003; Wang et al., 2007; Ishikawa et al., 2007). The issue about the "true" $^{87}Sr/^{86}Sr$ isotope ratio of the NIST SRM 987 $SrCO_3$ however remains unresolved (Petelet-Giraud and Negrel, 1997; Schmitz et al., 1997). A good reference concerning the historical development of the "accepted" $^{87}Sr/^{86}Sr$ is provided by Thirlwall (1991). In order to allow comparison of different measurement results the isotope masses and ratios used for mass bias correction or normalisation should always be quoted.

Data reduction – Rb interference correction

Rb Interference correction is actually performed before mass bias correction, but thorough understanding of mass bias correction and knowledge of corresponding equations is necessary for this task. When measuring $^{87}Sr/^{86}Sr$ isotope ratios, ^{87}Sr and ^{87}Rb will overlap at the same mass-to-charge ratio in the mass spectrum. As Rb and Sr are both ubiquitous, this is quite often the case (Melgunov et al., 1995). The signals of ^{87}Sr and ^{87}Rb may only be resolved by mass spectrometers possessing a resolution of approximately 300 000 or AMS as was discussed before (Müller, 2003). Not properly taking care of the isobaric interference of ^{87}Rb on ^{87}Sr will inevitably lead to inaccurate measurement results. The Rb correction procedure is based on the knowledge of the measured intensity of a non interfered Rb isotope (^{85}Rb) and calculation of the contribution of ^{87}Rb to the total measured intensity at mass 87. Natural Rb consists of the isotopes ^{85}Rb and ^{87}Rb with relative isotope abundances

of 72.165 % and 27.835 % respectively (De Bievre and Taylor, 1993). In contrary to verified mass dependent $^{86}Sr/^{88}Sr$ isotope fractionation (Ohno et al., in press), such an effect was not yet found for Rb isotopes (Waight et al., 2002b; Nebel et al., 2005) although opinions with respect to this topic are observed to deviate (Garciá-Ruiz, 2008). The $^{87}Rb/^{85}Rb$ isotope ratio is therefore a well defined constant and may be used to estimate the ^{87}Rb signal intensity from the measured ^{85}Rb intensity. Only the ^{85}Rb isotope being available for interference free measurement, the mass bias between ^{87}Rb and ^{85}Rb has to be estimated from the measured mass bias for $^{86}Sr/^{88}Sr$. Rearrangement of equation 3 leads to equation 5 below. The fractionation coefficient remains essentially the same as for equation 3. The calculated ^{87}Rb intensity is then subtracted from the blank corrected intensity ($^{87}I_{Intensity}$) at mass 87, thus giving a reliable estimation of the actual signal intensity of ^{87}Sr ($^{87}Sr_{meas}$). The blank and ^{87}Rb corrected ^{87}Sr signal intensity ($^{87}Sr_{meas}$) is subsequently used for calculating an $^{87}Sr/^{86}Sr$ isotope ratio which will be corrected for mass bias using equation 2.

$$^{87}Rb_{meas} = \frac{\left(\frac{^{87}Rb}{^{85}Rb}\right)_{true} \times ^{85}Rb_{meas}}{\left(\frac{m_{87}}{m_{85}}\right)^{f}} \qquad \textbf{Equ. 5}$$

$$^{87}Sr_{meas} = {}^{87}I_{Intensity} - {}^{87}Rb_{meas} \qquad \textbf{Equ. 6}$$

Although it is possible to correct for the isobaric ^{87}Rb interference, Rb levels should be kept as low as possible by thorough conduction of Sr/matrix separation as described before. It is known from experience and literature that increase of the Rb/Sr concentration ratio will lead not only to larger measurement uncertainties as a result of the uncertainty of the $^{87}Rb/^{85}Rb$ isotope ratio, but also to a linear increase of the finally determined $^{87}Sr/^{86}Sr$ isotope ratio (Fortunato et al., 2004; Galler et al., 2007). Exemplary results of a long term study that were already published are given in figure 2 below (Galler et al., 2007).
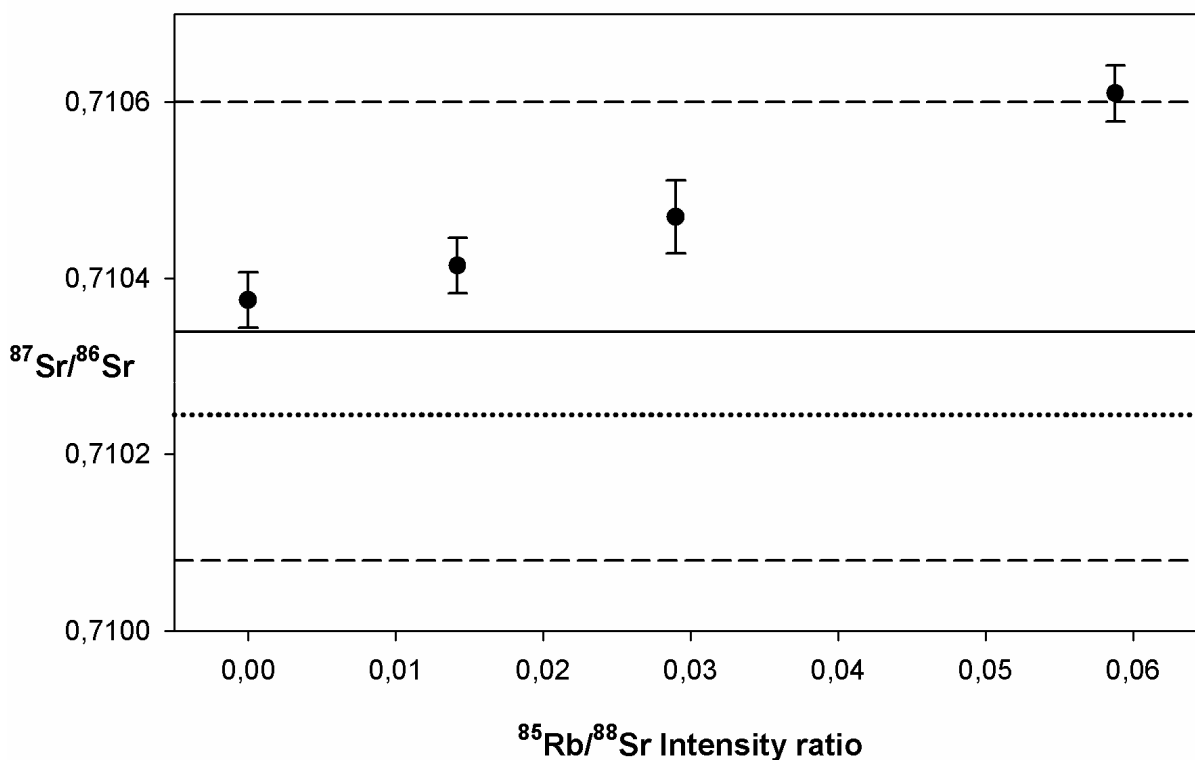
Fig. 2 Linear increase of corrected $^{87}Sr/^{86}Sr$ isotope ratio with increasing Rb concentrations; solid black line corresponds to certified isotope ratio, dashed black lines correspond to certified uncertainties, dotted black line corresponds to "accepted" value of 0.710245

Possible reasons for the increase of the finally determined $^{87}Sr/^{86}Sr$ isotope ratio are the actual inappropriateness of assuming identical mass bias for two different elements, inappropriateness of the employed correction algorithm, formation of molecular hydride interferences among investigated isotopes or incorrect reference isotope ratios for either $^{88}Sr/^{86}Sr$ or $^{85}Rb/^{87}Rb$. For the data presented in figure 2 an $^{87}Rb/^{85}Rb$ isotope ratio of 2.593 was assumed in agreement with isotope abundances recommended by the IUPAC (De Bievre and Taylor, 1993). Data presented in figure 2 was collected over a period of 8 weeks in 9 measurement sessions. Each data point corresponds to 90 measurements and is reproducible with 40-50 ppm. A linear regression fits these data points with a correlation coefficient of $R^2 = 0.99$. The slope of the linear regression is reproducible with only 20 % (1 RSD, n=9), whereas the intercept is reproducible with 40 ppm (1 RSD, n=9). Assuming an $^{87}Rb/^{85}Rb$ isotope ratio of 2.589 or a mass bias of Rb being approximately only 99.87 % of $^{86}Sr/^{88}Sr$, the residual slope in figure 2 can be eliminated. It was stated before, that so far no mass dependent fractionation of Rb isotopes was observed in nature. An $^{87}Rb/^{85}Rb$ isotope ratio of 2.589 would however be significantly different from 2.593, employing a measurement protocol as proposed by Nebel et al. (2005). But it should also be clear, that the proposed $^{87}Rb/^{85}Rb$ isotope ratio of 2.589 is only an assumption without quantified uncerbanties.

Application of a Rb mass bias determined in an individual measurement session later on as well as of a mass dependent mass bias as proposed by Hirata (1996) for Rb interference correction lead to even bigger residual slopes of a linear regression through the data points in figure 2. The absolute increase of the $^{87}Sr/^{86}Sr$ isotope ratio with increasing Rb/Sr concentration ratios determined in this work (Galler et al., 2007) and by Fortunato et al. (2004) is very similar despite the fact that corresponding experiments have been performed on different MC-ICPMS instruments under different plasma conditions. While Fortunato et al., were employing a membrane desolvating nebuliser, a conventional liquid nebulisation set up consisting of a Meinhard type nebuliser and peltier cooled cinnabar spray chamber was used for this work.

Data reduction – Kr interference correction

Kr interference correction of the isobar ^{86}Kr interfering with ^{86}Sr may be omitted, provided Kr levels are stable during measurement. It is mentioned nevertheless as this correction is different from Rb interference correction due to the fact, that the Kr mass bias can be determined directly from the non interfered isotopes ^{82}Kr and ^{83}Kr. Based on the discussion above it is suggested, that this approach is more accurate as no element-independent mass bias has to be assumed.

Experimental part

A brief comparison of the "Neptun" and "Nu Plasma" MC-ICPMS

Background

In the context of the FWF Start project "VIRIS" conducted at the BOKU Vienna (University of Applied Life Sciences and Natural Resources) a new MC-ICPMS was acquired for the purpose of high precision isotope ratio analysis. In the course of instrument selection the products of the two commercial providers have been tested. The "Nu Plasma HR" from Nu Instruments Ltd. (Wrexham, Wales, Great Britain) and the "Neptun" from Thermo Fisher Scientific (Bremen, Germany) have been investigated for their performances in Sr, Pb, Fe and S isotope analysis. In addition to solution analysis, solid samples (archaeological tooth samples of 3 individuals (Prohaska et al., 2006)) have been investigated for their Sr isotopic signatures via laser ablation. All measurements have been conducted at the mentioned manufacturer's production sites in Bremen and Wrexham.

Materials and reagents

All standards have been prepared gravimetrically inside a class 10000 clean room at the Division for Analytical Chemistry on the BOKU Vienna. Stock solutions in the µg*L^{-1} range have been prepared. Standards for measurements have been prepared via dilution of these stock solutions on site. Demineralised (F+L GmbH, Vienna, Austria) and sub-boiled (Milestone-MLS GmbH, Leutkirch, Germany) H_2O as well as doubly sub-boiled p.a. grade HNO_3 (Merck, Darmstadt, Germany) have been used for preparation of the stock solutions. All standards have been prepared in 1% (v/v) HNO_3 except for the sulphur standard. The sulphur standard was prepared from concentrated H_2SO_4 (Aldrich, St. Louis, USA) via dilution with H_2O. Prepared solutions have been stored in PE bottles (Semadeni, Ostermundigen, Switzerland). The Sr stock solution was gravimetrically prepared from NIST SRM 987 $SrCO_3$ (National Institute for Standards and Technology, Gaithersburg, USA). NIST SRM 981 and 982 Pb wire and NIST SRM 1486 bone meal (NIST) digestions have been conducted under appliance of a microwave system (Milestone-MLS). Hydroxyl-apatite (Aldrich) has been gravimetrically added to the standards in solid form to simulate for bone like matrices. The Fe standards „Mix 1" and „Mix 2" have been provided by Thomas Prohaska. The true concentration values of these synthetically prepared Fe standards are not reported in this study. The Palaeolithic tooth samples for investigation by LA-MC-ICPMS have been provided by Maria Teschler-Nicola from the Natural History Museum in Vienna. A list of all standards, including their concentrations, which have been measured on both of the MC-ICPMS instruments can be found in the appendix. No remarks about elemental contents of the tooth samples from the Mladeč excavation site can be made due to a lack of quantification. More detailed information on the background and measurement results of the Mladeč tooth samples can be found in the experimental part of this work dedicated to the development of a LA-MC-ICPMS method for Sr isotope signatures in archaeological tooth samples or in literature (Prohaska et al., 2006; Wild et al., 2005).

Motivation behind the development of MC-ICPMS

As stressed before in the introduction, the attractiveness of ICP mass spectrometry can be explained by the large number of elements that can be detected at low concentration levels simultaneously (Jarvis et al., 1993). The effortlessness of sample preparation and the high sample throughput compare favourably to the alternative methods of thermal ionisation mass spectrometry (TIMS) and secondary ionisation mass spectrometry (SIMS) (Jarvis et al., 1993; Albarède et al., 2004; Košler et al., 2002). In ICP mass spectrometry a gaseous, liquid or solid sample is injected into an Ar plasma as a sprayed aerosol. Due to the high plasma temperature around 7000K the sample aerosol is dried, vaporised and ideally fully atomised.

Subsequently sample atoms are ionised and electronically excited. While optical emission spectroscopy (OES) takes advantage of the information behind emitted, element specific radiation generated due to the decay of excited electronic states, ions are extracted from the plasma in mass spectrometry. The extracted ions are then separated according to their mass to charge ratio (m/z) in the analyser part of the mass spectrometer. The following principles are used for the separation of ions: quadrupole-MS (Q-MS), sector field-MS (S-MS or HR-MS), time of flight-MS (TOF-MS), Fourier transform-ion cyclotron-MS (FT-ICR-MS) and ion trap-MS (IT-MS). While most instruments are Q- or HR-MS devices, TOF-, FT-ICR- and IT-MS devices are rarely encountered. One major reason can be found in the lack of sensitivity of the last three devices. Highest accuracy for determination of elemental contents and isotope ratios can be reached with HR-ICPMS instruments, mainly due to the lower relative energy spread of the analysed ions and the higher acceleration voltage in comparison to Q-ICP-MS devices. Furthermore HR-ICPMS can reach mass resolutions $m/\Delta m$ of up to 10 000 while commercial Q-ICPMS instruments are operated at unit mass resolution. This is a critical parameter if the spectral separation of isobaric interferences from analyte signals is concerned.

While the beginning of ICPMS was limited to single detector instruments, multi collector ICP instruments are now more and more on the rise. In single detector mass spectrometers using a magnetic sector field as mass analyzer, ions with different m/z are sequentially scanned relative to a detector. This can be accomplished by variation of the magnetic field, the variation of the acceleration voltage and/or the electrostatic field. Due to the magnet's hysteresis the variation of the acceleration voltage is preferred for the determination of isotope ratios. Therefore all masses of interest are measured periodically for only a few milliseconds to compensate for fluctuations of the plasma. This is called a "quasi simultaneous" detection (Prohaska et al., 2005). Nevertheless the accuracy for isotope ratio measurements in this case is limited by fluctuations of the plasma on an even shorter time scale (Meija and Mester, 2007; Heumann et al., 1998). An improvement can be accomplished by a true simultaneous detection of the ion currents on a detector array (Meija and Mester, 2007). Using an array of multiple collectors will not compensate for short term signal fluctuations in ICPMS, but significantly enhances signal correlation of measured isotope pairs. This is the main reason for the excellent precision obtained for isotope ratio measurements by multiple collector-inductively coupled plasma mass spectrometry (MC-ICPMS). Typically the precision of a measurement can be improved by 1 to 2 orders of magnitude, resulting from increased signal correlation. This is the true motivation behind the development of MC-ICPMS. It is clear that the information content of analytical measurements is significantly enhanced if the uncertainties on the way to a result can be reduced, as this will reduce the distribution of the mean value of a set of data.

Instrumental differences between the "Neptun" and the "Nu Plasma" MC-ICPMS

Both instruments offer the possibility to measure in three different mass resolution modes. The resolving power $m/\Delta m$ is more or less the same for both systems and can be adjusted to approximate values of 400, 3000 and up to 10 000, going from low to high mass resolution. The resolution is adjusted by means of pre-selectable entrance slit. If no imaging slit is used in front of the detector, the obtained mass resolution is called "pseudo high resolution". It is based on the systematic of the nuclear mass defect. According to this, all molecular interferences in the low and medium mass range are heavier than the elemental species. This has the effect that all molecular interferences will appear on the same side of elemental peaks in a mass spectrum. The working principle of the pseudo high resolution is presented in figure 3. As presented Fe isotopes can be measured free of interferences from ArO^+ and $ArOH^+$ because just the elemental peaks enter the faraday cups while the interferences are prevented from entering the detector by the collector slits.

$^{56}Fe^+$ $^{16}O^{40}Ar^+$ $^{57}Fe^+$ $^{16}O^{40}Ar^1H^+$

collector slit   collector slit

Faraday 1   Faraday 2
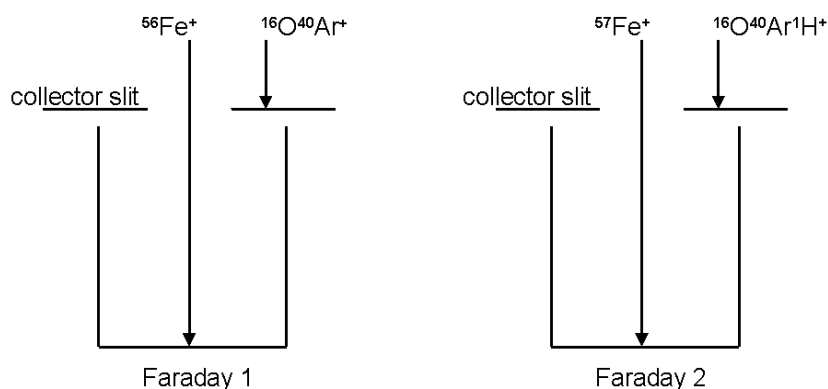
Fig. 3 Principle of pseudo high resolution

Difference exists in the applied electric potential at the plasma interface of the two instruments. While the "Neptun's" plasma interface is on ground potential, the "Nu Plasma" has a grounded analyser and collector part. A grounded plasma interface may be preferable since it allows manipulations of the sample introduction system at the interface without the need for turning of the instrument. The "Neptun" is solely evacuated by turbo pumps. The "Nu Plasma" additionally has got 3 ion pumps installed along the analyser part, allowing maintenance of the vacuum in case the turbo pumps accidentally break down.

The software for instrument controlling is very much different for both systems beginning with its history. Relating to experiences of Thomas Prohaska and his cooperation partner Urs Kloetzli, the "Neptun" software is a hybrid of the "Element 2" and "Triton" software. Both exhibit specific problems as far as transparency and data reprocessing is

concerned. Thermo Fisher Scientific was very assuring in response to the question whether the software will work offline for data reprocessing. Finally it was not possible to reprocess the data generated on the "Neptun" MC-ICPMS off-line. Additionally it has to be mentioned that the source code for the "Neptun" software is secret and cannot be amended by the operator. All problems that occur have to be corrected by Thermo Fisher Scientific. The software delivered with the "Nu Plasma" is open source and base on visual basic. Improvements can be accomplished if programming knowledge is available.

The largest difference between the "Neptun" and the "Nu Plasma" exists in the construction of the collector array. The "Nu Plasma" has got a fixed array of 12 faraday cups and three ion counters (discrete SEM) which are not moveable. Alignment of the analyte ion current with the detectors (peak centering) is achieved via a patented zoom optic. Most isotope systems can be measured with the standard collector set up provided by Nu Instruments. The collector array has to be changed though for measurement of U/Th/Pb isotope series, which requires a downtime of approximately 24 hours since the analyser part has to be vented for this operation. Additionally the zoom optic allows rapid switching between measured isotope systems within one method. This way the measured isotopes are not limited to the number of detectors available. An example from the authors experience is the following: It was impossible to dynamically measure all rare earth elements of a prepared liquid standard with the "Neptun" in Bremen within one run, because the detectors would have to be mechanically adjusted within the run to switch between the separate elements, while it was possible for the "Nu Plasma" using the zoom optic. The approach of the collector array design is very different for the "Neptun". The "Neptun" is equipped with 9 faraday cups and 3 ion counters (microchanneltrons) but has additional capacities for either up to 17 parallel faraday cups or 9 parallel ion counters at the time of testing. The detectors of the "Neptun" are moveable. The alignment of analyte ion currents with the detectors is achieved via moving the detectors mechanically. The fine tuning is accomplished with an ion optic. However, the mass range from mass 52 to 60 for Fe isotope (^{54}Fe, ^{56}Fe, ^{57}Fe, ^{58}Fe) measurements, which can be easily covered by the "Neptun", is un-coverable by the "Nu Plasma". ^{52}Cr needs to be monitored for ^{54}Cr interference on mass 54 and ^{60}Ni needs to be monitored because of ^{58}Ni interferences on mass 58.

Comment on instrument performance

It was found, that both instruments performed equally well with respect to accuracy and precision of the data generated. Both mass spectrometers exhibit the same mass bias stability, while the sensitivity for the "Neptun" was better by a factor of 1.5-1.8 for each analyte measured. However, the different experimental set ups used, make a direct comparison of sensitivity difficult. While a concentric glass nebuliser with an approximate

sample uptake rate of 200 µL*min^{-1} was employed for measurements with the "Nu Plasma", a low flow PFA nebuliser with an uptake rate of 50 µL*min^{-1} was used for measurements with the "Neptun". It is known, that the uptake rate of a nebuliser shows little correlation with the final sensitivity which can be accredited to nebulisation efficiency and resulting size distribution of the sample droplets. The results of the measurements of the archaeological tooth samples (Prohaska et al., 2006) by LA-MC-ICPMS with the "Nu Plasma" can be found in form a book chapter in the appendix of this work as can be the results together with experimental conditions of Sr, Pb, Fe and S isotope measurements on both instruments.

Sample digestion methods

Preface

The sample digestion is an essential part of the analytical scheme on the way to a measurement result. It shall allow reproducible conversion of the sample into a form that will allow investigation by the desired analytical method. The efficiency and sample throughput resulting from sample digestion have direct impact on the economy of an analytical method. As the selection of samples dealt with in this work included very different matrices, exemplary 3 different digestion methods will be described in this section. The method for digestion of archaeological tooth samples could be significantly improved with respect to sample throughput, which was formerly a major limitation for this type of sample.

Materials and reagents

All operational steps were performed inside a class 100 000 clean room. Doubly sub-boiled (Milestone-MLS GmbH, Leutkirch, Germany) p.a. grade HNO$_3$ (Merck, Darmstadt, Germany), 40 % suprapure HF (Merck), sub-boiled p.a. grade HCl (Merck), 30 % suprapure H$_2$O$_2$ (Merck) and doubly sub-boiled H$_2$O; pre-cleaned by reverse osmosis and subsequent demineralisation (F+L GmbH, Vienna, Austria); were used for sample digestion and dilution. A ceramic knife (Kyocera, Esslingen, Germany) was used for cutting the asparagus samples. An "Alpha 1-2/LD" freeze dryer (Martin Christ GmbH, Osterode, Germany) was used for freeze drying of asparagus samples. Asparagus and basalt samples were digested using microwave assisted (MLS 1200mega, Milestones-MLS) digestion procedures. Pre-cleaned PE ware (Semadeni, Ostermundigen, Switzerland) was used for sample dilution and storage. An ancient dental drill of unknown origin was used for sampling of archaeological tooth material. PFA screw cap vials (Savillex, Minnetonka, USA) were used for digestion and evaporation of part of the sample matrices. Hot plates (IKA, Staufen, Germany) were used for evaporation or thermal treatment of sample digests.

Digestion of asparagus

The digestion procedure is based on Swoboda et al. (2007). Samples of asparagus were cut into thin slices, followed by freeze-drying of the sample slices for approximately 24 h until the sample weight was constant. Approximately 200 mg of the freeze-dried sample was directly weighed into a Teflon bomb for microwave assisted digestion. 3 mL of concentrated double-sub-boiled HNO_3 and 0.5 mL of 30 % H_2O_2 were added as digestion reagents. The microwave time and temperature programme was performed as indicated in table 4.

time [min]	MW power [W]
5	250
5	400
10	600
5	250
10	vent

Tab. 4 Microwave digestion program

The samples were transferred into pre-cleaned 50 mL polyethylene (PE) containers after digestion, topped up with 1 % (w/w) nitric acid to a final amount of 25 g and stored at 4°C until further investigation.

Digestion of archaeological tooth samples

Initially microwave assisted digestion was used as default method for all types of samples addressed in this work. As a matter of fact, microwave assisted digestion strongly restricts the number of samples that can be digested in a single working day. First of all, the microwave digestion system available for this work did not allow digestion of more than 6 samples in parallel. Furthermore, table 3 can not be taken as a reliable measure for the total amount of time necessary for a defined number of samples. It was found, that it is advantageous to let the sample digests cool down for typically 1-2 h inside the digestion vessels before opening them. Opening the digestion vessels too early constitutes the risk of sample spill by overpressure. Nitrous gases resulting from digestion methods using nitric acid are released in an almost explosive manner from hot digestion vessels and can spread quickly inside the lab. Usually small amounts of sample are lost when opening the digestion vessels too soon, as the excess pressure inside the digestion vessel will result in squirting of liquid condensate adhering to the vessel's lid. This demonstrates that the use of protective goggles is imperative during all steps of sample preparation. Preferably microwave assisted digestion should be performed with control of pressure and temperature inside a reference vessel. Unfortunately a probe providing such data was not available in the lab, were digestions were performed.

Responding to the large amount of archaeological tooth samples; typically 100-200 in number; investigated during this work, a digestion method allowing a much increased sample throughput was developed. This type of digestion is not yet defined by strict specifications of temperature, pressure and time, but is based on the personal judgement of the author as to when the addressed sample is most likely fully decomposed. A dental drill was used for sampling of typically a few dozen mg of material from a tooth sample directly into a pre-cleaned and tared PFA screw cap vial. A few mL of concentrated doubly sub-boiled HNO_3 and less H_2O_2 were added as digestion reagents, to meet a final HNO_3/ H_2O_2 volume ratio of approximately 3/0.5. The amount of reagents added may vary depending on the experience of the operator. It should be kept in mind that less reagent addition means less contribution of reagent contamination. The PFA vials were closed with corresponding screw caps and placed on hot plates for digestion. The digestion temperature may vary between 80-150 °C, depending on the experience of the operator. The screw caps should not be placed too tightly on the vials to enable removal of excess pressure. It was observed that the digestion vessels showed strong deformation when placing the screw caps too tight on the vials. It should also be taken care not to overfill the digestion vessels, which may lead to explosion if screw caps are attached too tight. This was observed in one case. It is therefore inevitable to additionally use the protective glass shielding of the fume hoods in which the digestion is performed. After digestion the screw caps are removed, sample digests are evaporated to near dryness and residual sample material is dissolved in 8 mol*L^{-1} nitric acid for subsequent Sr/matrix separation.

Digestion of one sample consumes typically one hour, followed by typically another hour for evaporation. The digestion method was successfully employed for tooth meal sampled from whole teeth via a dental drill as well as tooth fragments in the size of a few mm³. Depending on the size of the hot plate, approximately 12 samples can be digested on a single hot plate simultaneously. In total 3 hot plates were available for sample digestion, resulting in a total throughput of roughly 40 samples per day with respect to sample digestion. This is a significant improvement compared to the 6-12 samples that can be processed in a single working day by using conventional microwave assisted digestion. The use of the proposed method had a very positive effect in reducing accidental contamination, as the samples did not have to be transferred from digestion vessels to evaporation vessels, as was the case for the procedure employing microwave assisted digestion. Further improvement can be expected from using larger graphite blocks with bore holes in the size of the uniform PFA screw cap vials for sample digestion and evaporation. Given the high thermal conductivity of graphite, such a block may be heated by means of a conventional hot plate from below and potentially increases the evaporation rate after digestion as well as the

speed of digestion itself by increase of the total contact area between digestion vessel and heat source.

Digestion of basalt samples

The investigated basalt samples represent the most difficult matrix that was actually dealt with during this work. The digestion procedure consisted of a sequential 2 step digestion and is described below. Samples were obtained form the Department for Geochronology on the Vienna University in milled and homogenized form.

150 mg of milled and homogenized sample were weighed into a teflon bomb for microwave assisted digestion. 0.25 mL of 40 % suprapure HF, 4 mL of sub-boiled HCl and 1.3 mL of double sub-boiled HNO_3 were added to the digestion vessel. Microwave assisted digestion was performed analogue to the program described in table 3. The sample digests had strong yellow colour and contained small quantities of a white solid, potentially insoluble CaF_2. After transfer of the samples into pre-cleaned PFA screw cap vials, the digests were evaporated to near dryness at 150°C. Subsequently 4 mL of aqua regia were added, resulting in a change of the solution colour to a deep, dark green. Lids were screwed tightly onto the PFA vials and solutions were left over night for thermal treatment at approximately 100°C on a hot plate. Over night the colour of the sample digests changed to intensive orange except for the blank, which was of pale yellow colour. Samples were again evaporated to near dryness and finally taken up in 8 mol*L^{-1} nitric acid for subsequent Sr/matrix separation.

Investigation of archaeological tooth samples

Preface

The Division for Analytical Chemistry on the BOKU Vienna has an internationally recognized reputation in archaeometry (Latkoczy et al., 2001; Prohaska et al., 2006; Simonetti et al., in press; Prohaska et al., 2002). Due to the high relative abundance variation of [87]Sr and the ubiquity of Sr in nature, Sr is one of the favourable isotopic tracers to be measured in archaeometry. Application of a high throughput digestion procedure as described in section "Sample digestion methods" combined with measurement of [87]Sr/[86]Sr isotope ratios by MC-ICPMS is currently state of the art in the Division of Analytical Chemistry and already compares favourable to more traditional approaches using TIMS with respect to total sample throughput.

Samples, materials and reagents

The investigated archaeological tooth specimens are 55 samples from an excavation site in Gars Thunau, 91 samples from Hainburg, 17 samples from Mannersdorf and 2 samples from Prellenkirchen. All places are situated in Austria. Small quantities of tooth material were sampled into PFA screw cap vials (Savillex) with an old dental drill directly at the Department for Anthropology at the Natural History Museum in Vienna. For every tooth a small quantity of enamel and dentine was sampled. For the excavation site Gars Thunau additionally soil samples and corresponding extracts, water samples and environmental samples including pheasant bone, one fish, wood, acorns, one apple and rose hips have been investigated. Samples were digested with a mixture of approximately 3 mL double sub-boiled (Milestone-MLS) HNO_3 (Merck) and 0.5 mL H_2O_2 (Merck) using either microwave assisted (Milestone – MLS) or open vessel digestion as described in section "Sample digestion methods". Samples were Sr/matrix separated employing the Sr specific resin (Eichrom) as described in section "Sample preparation – Sr/matrix separation". Sr/matrix separated samples were diluted to appropriate concentrations with 1 % (v/v) nitric acid. A 1 mol*L^{-1} NH_4NO_3 solution for soil extraction was prepared using 28% (w/w) p.a. NH_3 (Merck) and sub-boiled HNO_3. Whatman Nr. 42 (Whatman, Kent, Great Britain) filter paper was used for filtration of the soil extracts. Pre-cleaned PE ware (Ostermundigen) was used for sample storage and soil extraction. A solution of the NIST SRM 987 isotope certified $SrCO_3$ (NIST) in 1 % (v/v) HNO_3 was used for quality control of the measurements.

Soil Extraction

Soil extraction was performed in order to analyse the labile metal fraction of the soil; i.e. the fraction available to plants. A procedure according to DIN V 19730 was applied. Prior to extraction the soil was sieved using a 2 mm mesh sieve and subsequently air dried for 48 hours. The temperature should not be higher than 40 °C for drying of the soil samples. 20 g of soil were weighed into a 100 mL PE bottle and mixed with 50 mL of a 1 mol*L^{-1} NH_4NO_3 solution. Samples were shaken for 2 hours at 20 revolutions per minute using a lab shaker. Samples were taken out of the shaker and allowed to settle for 5 minutes. The samples were filtered and the first 5 mL of the filtrate were discarded. An adequate amount of sub-boiled HNO_3 was added for subsequent Sr/matrix separation of the extracts.

Measurement method

Measurements were performed using the "Nu Plasma" (Nu Instruments) with either the U/Th/Pb or the standard collector block. A desolvating membrane nebuliser "DSN 100" (Nu

Instruments) was used for introduction of the samples into the ICP. Typical instrumental parameters are summarized in table 5.

Axial mass [m/z]	86
Mass resolution [m/Δm]	300
Rf power [W]	1300
Plasma gas flow [L*min^{-1}]	13
Auxiliary gas flow [L*min^{-1}]	0.9
Nebuliser back pressure [psi]	~30
DSN 100 hot gas flow [L*min^{-1}]	~0.5
DSN 100 membrane gas flow [L*min^{-1}]	~2.7
Typical instrumental sensitivity [V*ppm^{-1}]	300-400
Dwell time [sec]	5
Measurements per block	10
Number of blocks	6
Total measurement time [min]	5

Tab. 5 Typical instrumental parameters for Sr isotope measurements

Results for Gars Thunau

Real samples

Results for tooth samples are presented as graphic in figure 3. Numerical data can be found in the Appendix. Results for determination of the recent ^{87}Sr/^{86}Sr background in Gars Thunau are presented in table 6.
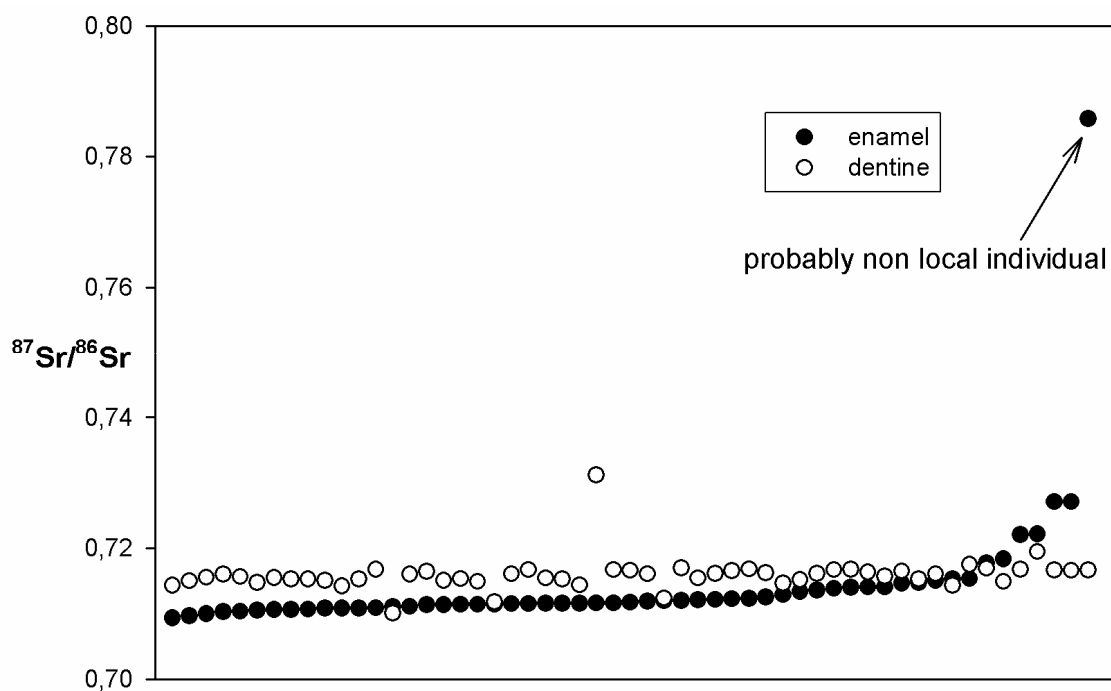
Fig. 3 ^{87}Sr/^{86}Sr isotope ratios of archaeological tooth samples from Gars Thunau

Sample	$^{87}Sr/^{86}Sr$ Isotope ratio
Water Schanze	0.71870 ± 0.00009 (1SD, n=5)
Water Kamp	0.71687 ± 0.00020 (1SD, n=7)
Rainwater	0.71639 ± 0.00004 (1SD, n=1)
Well water Nonndorf	0.71216 ± 0.00002 (1SD, n=1)
Well water Tautendorf	0.71617 ± 0.00003 (1SD, n=1)
Soil 1997, total digest	0.70604 ± 0.00055 (1SD, n=4)
Soil 2006, total digest	0.70630 ± 0.00015 (1SD, n=6)
Soil 1997, extract	0.71799 ± 0.00033 (1SD, n=3)
Soil 2006, extract	0.71840 ± 0.00073 (1SD, n=6)
Pheasant	0.71225 ± 0.00001 (1SD, n=1)
Wood	0.71703 ± 0.00001 (1SD, n=1)
Acorn	0.71709 ± 0.00001 (1SD, n=1)
Apple	0.72087 ± 0.00004 (1SD, n=1)
Rose hip	0.71801 ± 0.00002 (1SD, n=1)
Fish	0.71757 ± 0.00002 (1SD, n=1)

Tab. 6 $^{87}Sr/^{86}Sr$ background associated with Gars Thunau

Measurement results in figure 3 are sorted from left to right according to ascending $^{87}Sr/^{86}Sr$ isotope ratios of enamel. Corresponding dentine data is plotted at the same position along the x-axis of figure 3. Corresponding error bars are quoted as standard error of the mean as calculated by the "Nu Plasma" instrument software "Nu Instruments Calculation Editor" (NICE) and are smaller than the data points. Uncertainties for data in table 3 are calculated as standard deviation of the replicate investigations performed. In case only a single measurement was performed, standard deviations were calculated from the raw data using the mean of 6 blocks. $^{87}Sr/^{86}Sr$ isotope ratios for enamel scatter around a mean of 0.714 ± 0.011 (1 SD) including the outlier, and 0.7131 ± 0.0038 (1 SD) excluding the outlier marked with an arrow in figure 3. $^{87}Sr/^{86}Sr$ isotope ratios for dentine scatter around a mean of 0.7159 ± 0.0025 (1 SD). Not including the elevated value of approximately 0.73 in the middle of figure 3 will result in a mean $^{87}Sr/^{86}Sr$ isotope ratio for dentine of 0.7156 ± 0.0014 (1 SD). 2 Soil samples from the excavation site sampled during two campaigns in 1997 and 2006 and both processed in 2006 agree with respect to the $^{87}Sr/^{86}Sr$ isotope ratios found in total digests and extracts. $^{87}Sr/^{86}Sr$ isotope ratios for the soil digests are by far the lowest of the whole data set and are significantly different from $^{87}Sr/^{86}Sr$ isotope ratios of corresponding extracts. $^{87}Sr/^{86}Sr$ isotope ratios found for the soil extracts suggests no variation of the Sr isotope signature of the labile fraction from 1997 to 2006 although no intermediate data is known. On average $^{87}Sr/^{86}Sr$ isotope ratios of enamel lie deeper than $^{87}Sr/^{86}Sr$ isotope ratios of dentine. The outlier marked with an arrow in figure 3 is probably a non-local individual that migrated close to the excavation site and was finally buried there. From conversations with staff on the Department for Anthropology on the Natural History Museum Vienna it is known, that bone morphology of the respective individual is significantly different from bone morphology of the rest of the excavated individuals.

Analysis of NIST SRM 987 reference standard

In total 40 measurements of the NIST SRM 987 reference material have been performed along with measurements of the real samples. A mean $^{87}Sr/^{86}Sr$ isotope ratio of 0.71040 ± 0.00008 (1 SD) was determined for this material. This is well within the certified range of 0.71034 ± 0.00026.

Results for Hainburg, Mannersdorf and Prellenkirchen

Real samples

Samples from Hainburg, Mannersdorf and Prellenkirchen were processed in the same sample batch and are all presented in figure 4 below. Numerical data can be found in the appendix of this work.
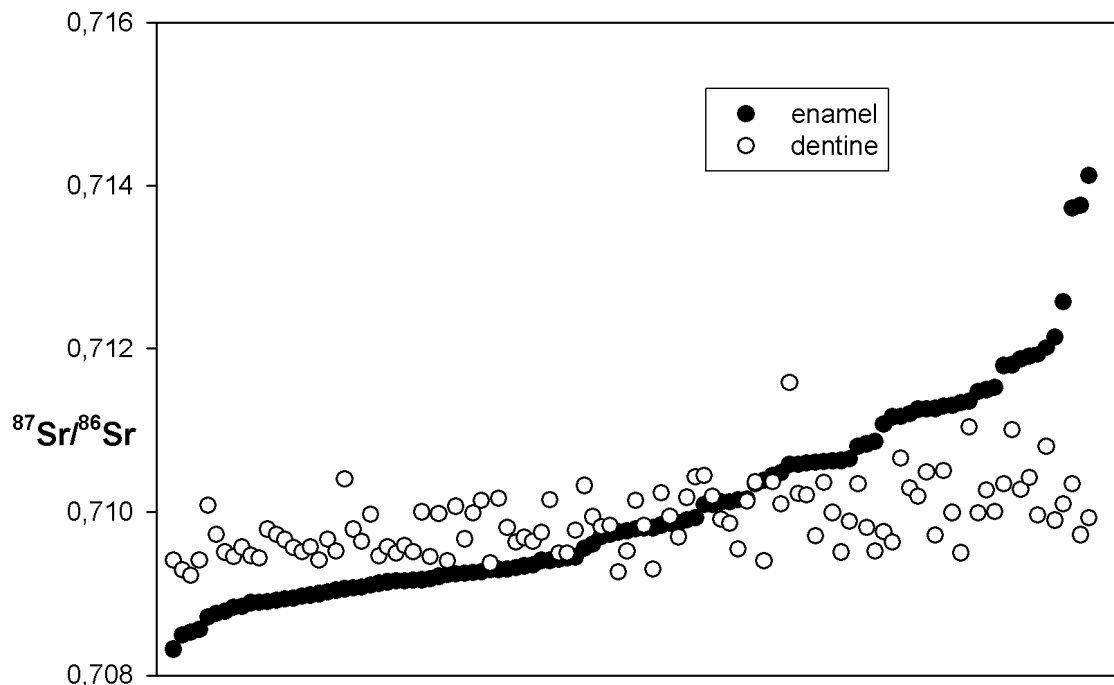
Fig. 4 $^{87}Sr/^{86}Sr$ isotope ratios of archaeological tooth samples from Hainburg, Mannersdorf and Prellenkirchen

Measurement results in figure 4 are sorted from left to right according to ascending $^{87}Sr/^{86}Sr$ isotope ratios of enamel. Corresponding dentine data is plotted at the same position along the x-axis of figure 4. Corresponding error bars are quoted as standard error of the mean as calculated by the "Nu Plasma" instrument software NICE and are smaller than the data points in the figure. $^{87}Sr/^{86}Sr$ isotope ratios yield a mean of 0.7101 ± 0.0012 (1 SD) for enamel and 0.70989 ± 0.00042 (1 SD) for dentine. The $^{87}Sr/^{86}Sr$ isotope ratios for dentine scatter very close around a mean value as they are probably more affected by diagenetic effects than enamel (Newesely, 1988; Williams 1988). Mean values for samples from

Hainburg, Mannersdorf and Prellenkirchen are summarized in table 7. The 3 ^{87}Sr/^{86}Sr isotope ratios for cow, pig and goat teeth are not included as their origin is currently unknown. The ^{87}Sr/^{86}Sr isotope ratios and corresponding uncertainties for the two samples from Prellenkirchen were calculated as arithmetic mean value and absolute distance of the two ^{87}Sr/^{86}Sr isotope ratios from the mean.

Sample origin	^{87}Sr/^{86}Sr Isotope ratio	
	Enamel	Dentine
Hainburg	0.7100 ± 0.0012 (1 SD, n=91)	0.70980 ± 0.00035 (1 SD, n=91)
Mannersdorf	0.7102 ± 0.0011 (1 SD, n=17)	0.71017 ± 0.00039 (1 SD, n=17)
Prellenkirchen	0.71121 ± 0.00004	0.71057 ± 0.00008

Tab. 7 Mean ^{87}Sr/^{86}Sr isotope ratios for investigated samples

Samples from Hainburg and Mannersdorf agree within error and do not show significant differences. No comment can be made on the samples from Prellenkirchen as the amount of data is too low.

Analysis of NIST SRM 987 reference standard

46 measurements of the NIST SRM 987 reference material have been performed along with measurements of the real samples. A mean ^{87}Sr/^{86}Sr isotope ratio of 0.71024 ± 0.00007 (1 SD) was determined for this material. This is within the certified range of 0.71034 ± 0.00026 and does agree very well with the accepted values of 0.710245 and 0.71026.

Conclusions

The investigated samples are very similar with respect to ^{87}Sr/^{86}Sr isotope ratios found in enamel, regardless of their origin. The mean ^{87}Sr/^{86}Sr isotope ratio of dentine for teeth from Gars Thunau does not even agree within 2 standard deviations with the ^{87}Sr/^{86}Sr isotope ratio found for samples from Hainburg, Mannersdorf and Prellenkirchen. This could reflect a potentially different progress with respect to diagenetic alteration of the teeth's native ^{87}Sr/^{86}Sr isotope signature. It is important to state, that a comprehensive archaeometric investigation demands well established back ground signals from water, soil, plants and animals. Mice teeth could serve in assessing recent background signatures as could snail shells

What is more interesting for high precision isotope ratio measurement applications is the fact, that in one session the mean ^{87}Sr/^{86}Sr isotope ratio determined for the NIST SRM 987 SrCO$_3$ was 0.71040 ± 0.00008 (1 SD, n=40), whereas it was 0.71024 ± 0.00007 (1 SD, n=46) in the following session. MC-ICPMS is a versatile tool for isotope tracing studies and even with the variation observed for the ^{87}Sr/^{86}Sr isotope ratio of the NIST SRM 987 SrCO$_3$

meaningful studies can be conducted. It should however be of major interest to find the reason for this variation, as this will be the only way to perform isotope ratio measurements with ultimate precision levels that MC-ICPMS can provide.

Development of an On-line Flow Injection (FI) Sr/Matrix Separation Method for MC-ICPMS Applications

Preface

The broad variety of methods available for Sr/matrix separation has been discussed in detail before. When this work was started every sample undergoing high precision Sr isotope ratio analysis was usually pre-treated with Sr/matrix separation employing the Sr specific resin commercially available from Eichrom. In some cases hundreds of samples have to be prepared using this method. On a first glance this might seem like a trivial task as the method is straight forward, does not need too many skills and has excessively been described in literature (Balcaen et al., 2005; Burton et al., 2006; Fantle and DePaolo, 2006; Horwitz et al., 1991 and 1992). When I had to separate my first batch of samples I quickly learned what the true requirements for such an operation are: endurance and patience! One of the major problems encountered was the fact, that blank levels could not be monitored until the samples were eventually measured. Simultaneous separation of large sample batches frequently led to cross-contamination of the samples if the attention span of the operator was shorter than the requested amount of time for sample preparation. Besides the frequent cross contamination, Sr/matrix separation was even more often inadequate and requiring a rerun of the complete procedure. The amount of resin was always between approximately 300-500 µL and became a quickly noticeable cost factor due to the high price of this material. Reuse of the resin is possible but bears the risk of further cross contamination. This was impressively demonstrated when a resin, formerly used for preparation of samples with an added ^{86}Sr spike, was reused by several students for preparation of their samples. Cross contamination was not noticed until the mass bias correction factors of the respective measurements suggested either extraterrestrial origin of the samples or enrichment in ^{86}Sr relative to the other Sr isotopes. It was therefore desirable to create a method that would allow automated sample preparation under more reproducible conditions, thereby avoiding cross contamination or excessively high blank levels. Ideally such a method should be compatible with the sample introduction system of an ICPMS and work completely independent from the skills of the operator. Several approaches for on-line Sr/matrix separation are currently described in literature but none of them can combine high

throughput with reasonable precision levels. Fortunately my former supervisor Andreas Limbeck and my present supervisor Thomas Prohaska had the vision of modifying off-line Sr/matrix separation using the Sr specific resin into an on-line method by means of flow injection (FI).

Materials and reagents

Materials and reagents used for development of the presented method can be found in a published article (Galler et al., 12007) as well as publication draft concerning automation of the proposed on-line Sr/matrix separation procedure, both attached in the appendix of this work. Instrumentation needed for assembly of the automated on-line FI Sr/matrix separation manifold includes an "AS 93 plus" auto sampler (Perkin Elmer, Massachusetts, USA), a "Cheminert" 10-port valve combined with PEEK fittings (Valco Instruments Co. Inc., Houston, USA), a 2 position actuator control module (Valco Instruments Co. Inc.), a "FIMS 400" mercury analyser (Perkin Elmer) and a peristaltic pump "Minipuls 3" (Gilson, Middleton, USA). The operating software of the "Elan DRC-e" was used for control of the FI assembly. The "WinLab 32 for AA" software was used for off-line optimisation of the method. PVC pump tubing (Spetec, Eferding, Germany) and PTFE capillary tubing (Burde Co., Vienna, Austria) was used for the conduits of the FI device. PVC pump tubing (Spetec) was used also as jacket material for the Sr/matrix separation columns. A desolvating membrane nebuliser "DSN 100" (Nu Instruments) is used for sample introduction. What was never discussed in detail in the article or publication draft is, how the separation columns are actually produced. Therefore the following section includes a detailed description of the materials and procedures involved. The modified hypodermic needle used as puncher or the water jet pump used for suction of the resin slurry can both not be assigned to any producer as these are things that were readily available for more than 10 year or so in the lab where columns were made. The modified hypodermic needle used as puncher was "home made" by a person that was already retired when it was applied for production of the Sr/matrix separation columns for the first time. It is hoped, that this essential tool will survive a few more generations of chemists until the proposed on-line Sr/matrix separation method is commercially available and globally widespread.

Preparation of the separation columns

The column preparation outline is summarized in figure 5 on the following page.
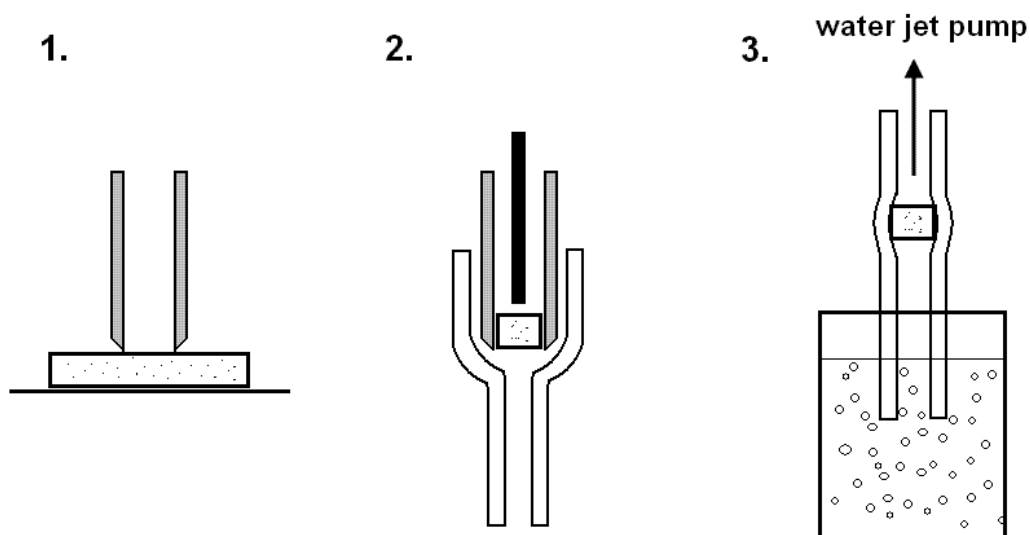
Fig. 5 Outline of column preparation

In the first step a modified hypodermic needle is used as puncher for frits. Frits for the Sr/matrix separation column are prepared from abandoned SPE cartridges that can probably be found in most routine laboratories. Note, that the hypodermic needle is not used in its original form, but that the tip is symmetrically sharpened. To support the punching process it helps to twist or rotate the needle a bit clock- and counter-clockwise between the fingertips, according to the needles only rotation symmetry axis. When punching the frits it is recommended to use a soft support in order not to damage the needle when the frit source material is fully penetrated by the needle. After the frit source material has been fully penetrated a smaller frit is retained inside the needle. The needle including the frit is gently pushed into a flexible PVC tubing of convenient diameter. The diameter chosen depends on the desired bed volume and aspect ratio of the column. The frit is inserted into the PVC tubing by pushing it out from behind using a long piece of wire that fits into the hypodermic needle. Note that the PVC tubing covering the needle will later on be needed to connect the separation column to the conduits of the FI manifold and should therefore be long enough. The frit can also be gently pushed a bit further into the PVC tubing to a desired position using the employed wire. In the third step, the part of the PVC tubing serving for connection to the conduits of the FI manifold is connected to a water jet pump using an adapter in the form of tubing of a convenient diameter. The water jet pump is turned on and the other end of the PVC tubing is held into a suspension of Sr resin particles. It can be observed that the column bed is building up as Sr resin particles will be sucked into the PVC tubing and retained by the frit. Care should be taken not to overfill the columns with Sr resin as it is difficult to remove excess Sr resin. The speed of the building up process of the column bed can easily be controlled by the number of particles suspended. If the desired column bed volume is

reached, the column can be sealed from the other end with a frit. The prepared columns are filled with water or dilute nitric acid and connected to a circle using some tubing available. It is recommended that the columns are kept wet during storage as it is unknown what effect a drying and reconditioning of the Sr resin has on retention capacity. The columns should occasionally be controlled for liquid content and additional liquid should be added if a loss is observed. Potential shelf life of Sr resin of a few months should be considered as well (Charlier et al., 2006). The advantage of this procedure is hat columns can be prepared rather quickly. At first the quantity of desired columns are equipped with frits on one side. Further it is recommended that all columns are filled with the Sr resin before sealing of the other column end as this will significantly increase the throughput rate. A prepared column should look somewhat like presented in figure 6.
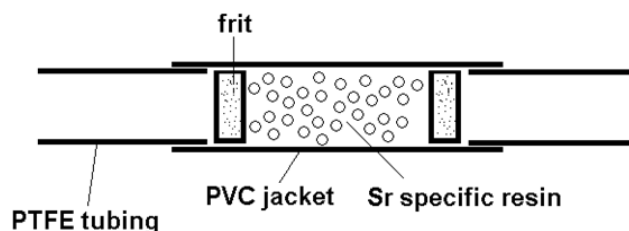
Fig. 6 Sr/matrix separation column design

PVC pump tubing proved to be best suited so far for column preparation as resulting columns can easily be connected to the conduits of the FI manifold using a push fit approach. Less flexible PTFE jacket material was tried in the beginning but it was found that it was very difficult to connect these columns to PTFE conduits of the FI manifold without permanently leaking. PVC columns were also found to occasionally leak but these leaks can efficiently be dealt with (figure 7).
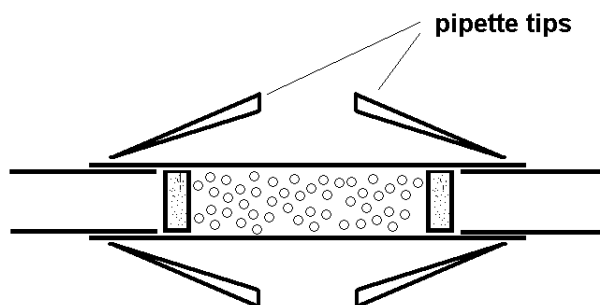
Fig. 7 Leak proof Sr/matrix separation column design

In figure 7 a simple method is proposed for making the column – conduit interface leak proof. For this purpose it is recommended to take 1 mL pipette tips and cut or grind as much of the

narrow end of, as is necessary to fit the columns' PVC jacket through. The narrow end shall be fixed on a part of the column jacket that already harbours part of the FI conduit tubing. It was found favourable to make the hole in the narrow end of the pipette small enough, that it significantly and symmetrically indents the PVC jacketing material along its complete circumference. As much of the wider end of the pipette tip is removed as is necessary to fit one pipette tip at each end of the separation column.

A short reference to column performance

A detailed investigation of the influence of the nitric acid concentration of the carrier, the carrier flow rate, Sr concentration in the sample, injected sample volume and Ca content of the sample on Sr retention was performed (Galler et al., 2007). The method was subsequently applied to a small selection of real samples including bone ash (NIST SRM 1400), bone (NIST SRM 1486), 5 basalts and one mica sample which represented the worst case with respect to the Rb/Sr concentration ratio of the sample (Galler et al., 2007). In a first experiment 3 different columns possessing aspect ratios of 5, 12.5 and 30 were tested. Experimental results indicate only limited influence of column geometry on the elution characteristics. The elution profile and corresponding length of the transient signal can significantly be influenced by changing the flow rate of the eluent H_2O. The results of first, principle investigations were published in 2007 in the scientific journal Analytical Chemistry (Galler et al., 2007).

A short reference to baseline correction

Baseline correction ca be performed via measuring a procedural blank, overlapping the blank elution maximum with the elution maximum of a sample elution and perform point by point baseline subtraction. This operation can for example be conducted in an excel spread sheet. Blank correction can alternatively be performed by subtracting a water baseline blank recorded before the actual elution. Provided procedural blanks can be kept low, both methods deliver equivalent results.

A short reference to fractionation processes along the elution profile from a Sr/matrix separation column

What was observed during measurement of all elution profiles was a fractionation of the baseline corrected $^{87}Sr/^{86}Sr$ isotope ratio along the elution profile according to figure 8. The fractionation of the blank corrected $^{87}Sr/^{86}Sr$ isotope ratio (brown curve) in figure 8 can effectively be corrected for by application of the measured $^{86}Sr/^{88}Sr$ isotope ratio in equations 2 and 3 in the section "Data reduction – mass bias correction". The corresponding $^{86}Sr/^{88}Sr$ isotope ratio for figure 8 is reproduced in figure 9.
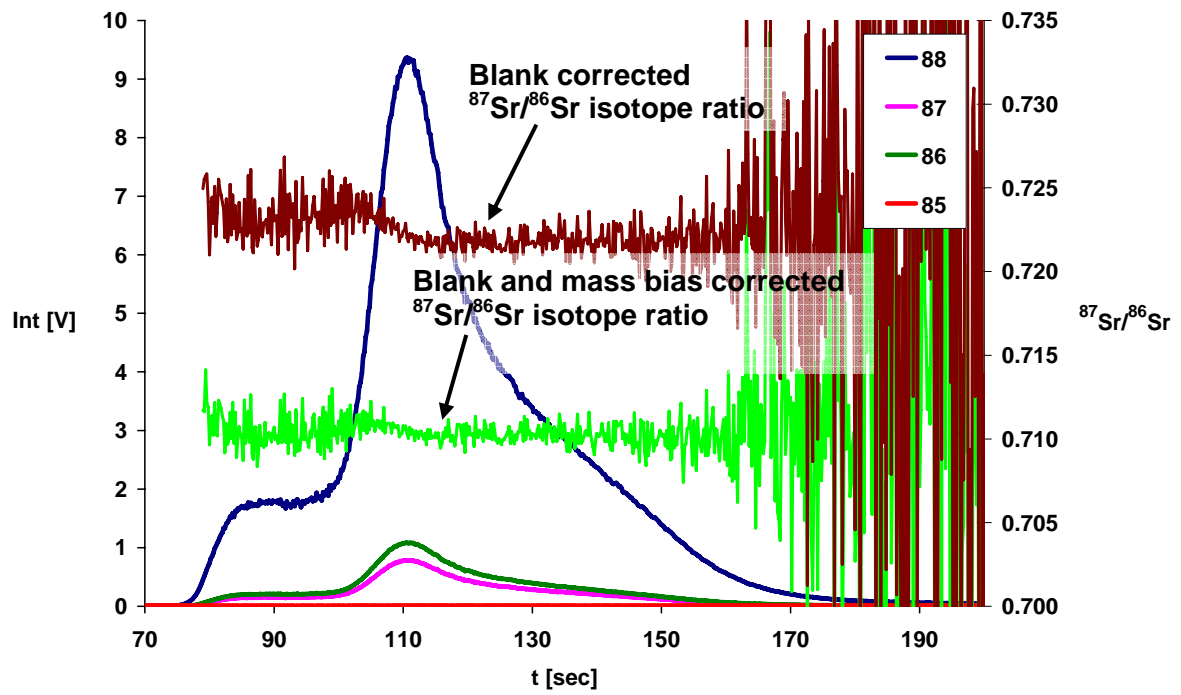
Fig. 8 Isotopic fractionation effects along Sr elution profile (I)
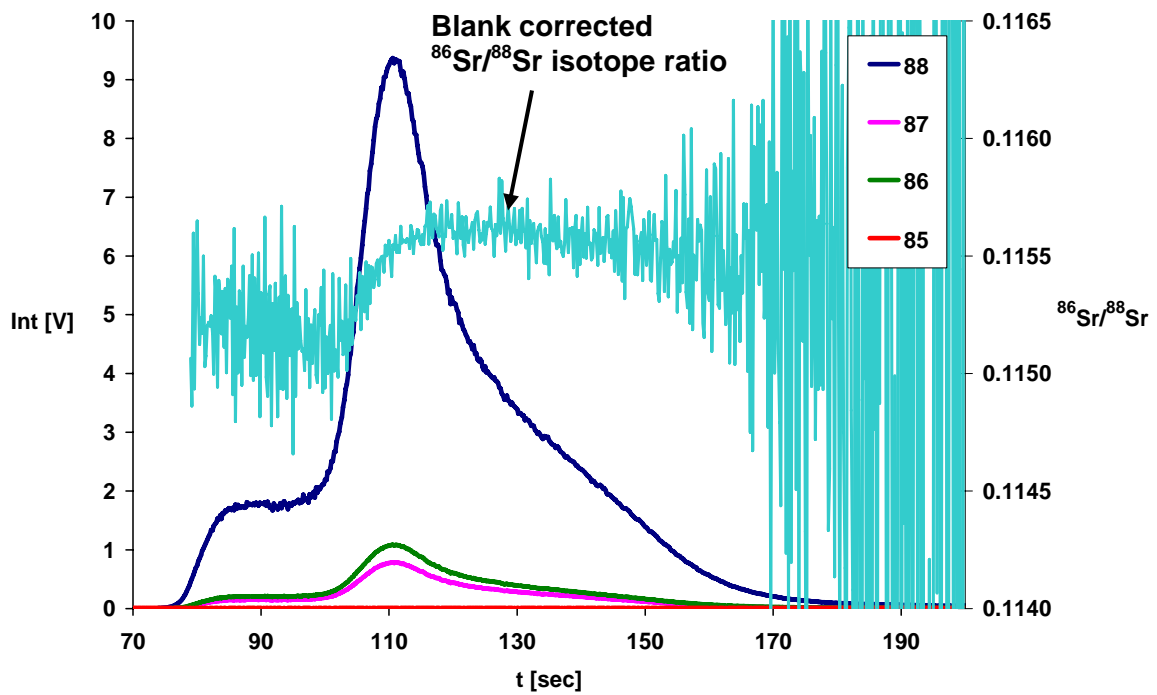
Fig. 9 Isotopic fractionation effects along Sr elution profile (II)

It is worth considering that the fractionation observed in figures 8 and 9 exhibits two distinct regions. The blank corrected $^{87}Sr/^{86}Sr$ and $^{86}Sr/^{88}Sr$ isotope ratios in figures 8 and 9 are more or less constant during the first 20-25 seconds of elution, represented by the almost constant ^{88}Sr signal intensity of approximately 2 V from approximately 80 to 100 seconds. With approaching the maximum signal intensity of the elution profile, the blank corrected $^{87}Sr/^{86}Sr$ and $^{86}Sr/^{88}Sr$ isotope ratios change to a significantly different value. The area at the beginning of the elution profile represented by the plateau of approximately 2 V signal intensity for ^{88}Sr correlates very well with the volume of the FI conduits before and after the separation column. As described in the corresponding publication (Galler et al., 2007) a small amount of nitric acid carrier will be trapped between the employed valves before elution with water, presumably leading to the documented observation of a constant signal intensity plateau before the maximum at approximately 110 seconds in figures 8 and 9. It is therefore assumed, that the observed difference in mass bias along elution is a result of the different matrices between the first plateau (nitric acid) and maximum signal intensity (water). At the end of the elution profile scattering of the measured isotope ratios increases due to the unfavourable signal/background ratio.

Assembly of an automated on-line FI Sr/matrix separation manifold

Automation of on-line Sr/matrix separation was achieved by combining an "AS 93 plus" auto sampler, a "Cheminert" 10-port valve combined with PEEK fittings, a 2 position actuator control module, a "FIMS 400" mercury analyser and a peristaltic pump "Minipuls 3". A schematic of the final experimental arrangement is depicted in figure 10.
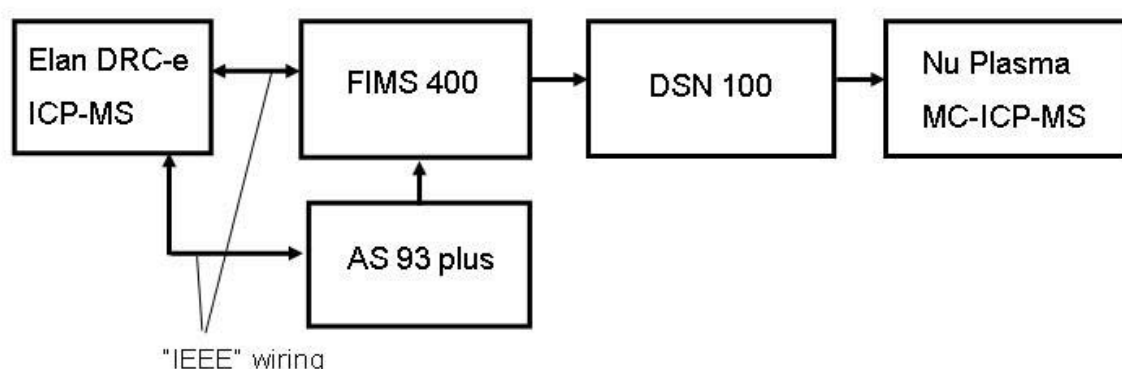
Fig. 10 Experimental arrangement of automated on-line FI Sr/matrix separation

It has to be taken care, that correct DIP switch settings as quoted in the manuals of the devices are used. This enables proper control and interaction of the "FIMS 400" and "AS 93 plus". A detailed schematic explaining the actual connection of employed valves and pumps

with capillary PTFE tubing is displayed in figure 11 below and can also be found in an attached publication draft dealing with automation and miniaturisation of on-line Sr/matrix separation.
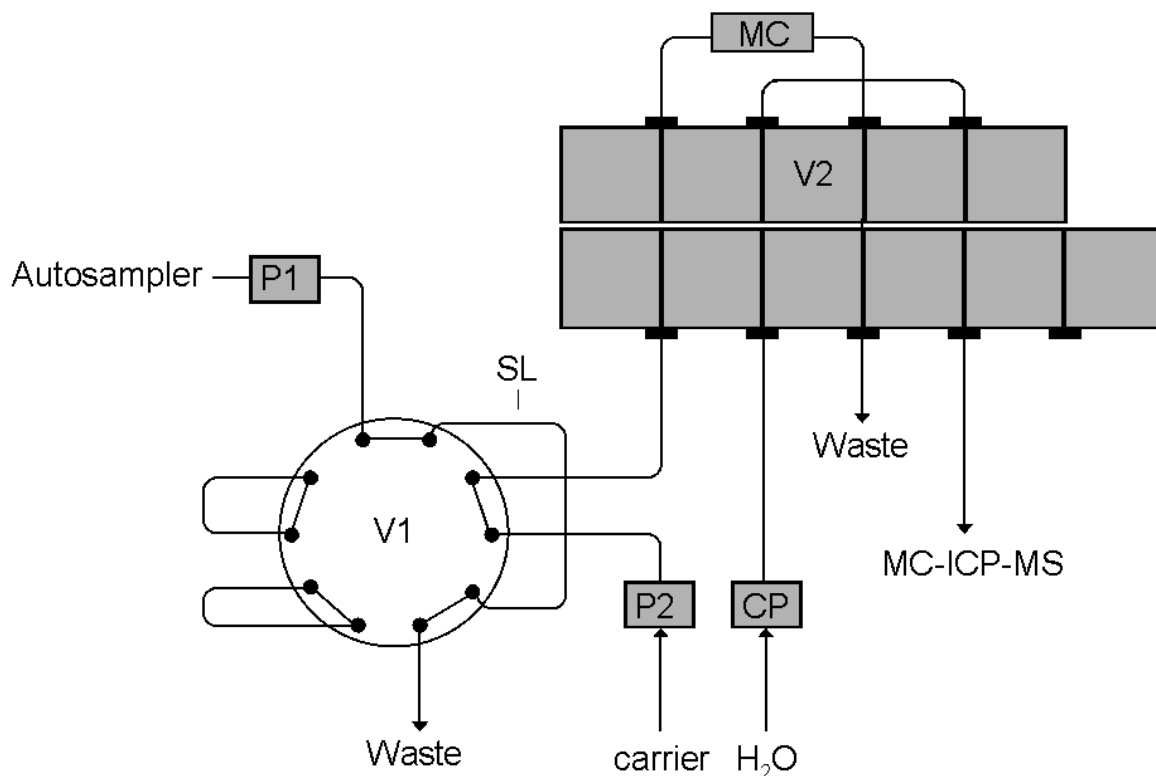
Fig. 11 Automated FI manifold for on-line Sr/matrix separation

The sample loop is represented by "SL" in figure 11. It is attached to two ports of the external 10 port valve "V1". In fact it is sufficient to use a 6 port instead of a 10 port valve. The 10 port valve was nevertheless employed as it was the only automatic valve, within the lab were this work was performed. "P1" and "P2" are two programmable peristaltic pumps attached to the "FIMS 400", as is the 5 port valve "V2". Pumps "P1" and "P2" are used solely for transferring sample solution from the auto sampler to the sample loop and loading of the sample solution from the sample loop onto the micro-separation column "MC". Peristaltic pump "CP" is continuously working and delivering a flow rate of 100 µL*min^{-1} of water to the MC-ICPMS. Below all steps necessary for establishment of the automated FI manifold are described. It is described how the FI manifold can be assembled for off-line method optimisation purposes and how it can finally be used for real on-line investigations.

How to set up the automated Sr/matrix separation FI manifold for off-line investigations

- An IEEE GPIB interface card has to be inserted into an empty cartridge slot of a PC.

- Connect the "FIMS 400" with its IEEE GPIB cable to the corresponding socket on the interface card inserted into the PC in the previous step. The following DIP switch settings have to be used on the "FIMS 400": on = 1, 3, 8; off = 2, 4, 5, 6, 7.
  Note: Whenever changing the DIP switch setting the device addressed has to be turned off for 1 -2 minutes before changing the DIP switch settings and turning it on again. Reason can be found in a buffer capacitor that keeps supplying the device internally with power for a short time. The device will not recognize new DIP switch settings until the buffer capacitor is empty and the system subsequently restarted with new DIP switch settings. Do also make notes of all DIP switch settings before changing them.
- The "AS 93 plus" auto sampler's IEEE GPIB interface cable has to be connected to the female backside of the IEEE GPIB connector directly on the "FIMS 400". If the auto sampler's IEEE GPIB interface cable is connected to the socket on the PC, the set up may not work. The following DIP switch settings have to be used on the "AS 93 plus" auto sampler: on = 2, 3, 4, 8; off = 1, 5, 6, 7.
- The CD ROM containing the installation package of the "WinLab 32 for AA" software (version used for this work: 6.0.0.0065) has to be inserted into the corresponding CD ROM drive on the PC for installation of the software. The "FIMS 400" and "AS 93 plus" may remain turned on during installation.
- The option "Install WinLab 32" is chosen and installation is performed accordingly. In case the software is configured incorrectly it may be reconfigured choosing the following pop-up menu: Start → Programme → PerkinElmer WinLab for AA → Reconfigure. It is favourable to restart the PC after reconfiguration.
- The "WinLab 32 for AA" software is selected from the Windows Explorer folder menu.
- The option "Install IEEE-488 driver" is chosen by double clicking.
- The PC is restarted
- The "WinLab 32 for AA" software is finally opened and it has to be controlled whether all components are properly initialised. These are: "FIMS 400" spectrometer, "AS 93 plus" auto sampler and "FIMS 400" flow injection.
- Within the "WinLab 32 for AA" software the "Diagnostics" window is opened by clicking on the corresponding "Diagnostics" button. The tab "Auto sampler" is chosen and firmware is loaded to the auto sampler by clicking "download firmware".
- In order to be able to run an FI sequence the "FIMS 400" has usually to be connected to a gas line delivering a pressure between 3.2 and 4 bar. This is currently avoided via bypassing two contacts associated with a pressure triggered switch inside the "FIMS 400". In case the easily identifiable bypass inside the "FIMS 400" is removed a connection to a gas line has to be established.

- The two position actuator control module has a flat cable and a round cable attached. The round cable is usually connected to the 10 position valve. The flat cable shows two bared wires that are connected to a TTL plug that fits into the plug receptacle "Instrument Interface S1 – S5" at the back of the "FIMS 400".
- The TTL plug connected to the two position actuator control module is plugged into the plug receptacle "Instrument Interface S1 – S5" at the back of the "FIMS 400". A random position of the plug in the plug receptacle may be chosen.
- The button "FIAS" is pushed in the "WinLab 32 for AA" software. The corresponding "Remote" button 1 – 5 is pressed and it is controlled whether or not the 10 port valve reacts correspondingly.

How to set up the automated Sr/matrix separation FI manifold for on-line investigations
- All original DIP switch settings have to be restored.
- The "AS 93 plus" auto sampler is connected to the "Elan DRC e" directly at the female IEEE GPIB socket on the instrument. This is a default setting used for routine analysis and probably already available.
- The "FIMS 400" is connected to the same socket. Corresponding DIP switch settings have to be adjusted according to the manual for this device.
- All instruments building up the automated FI manifold can be controlled via the option "Devices" in the method editor of the "Elan DRC e".
- For every operational step of the automated FI procedure a method of corresponding length has to be written. For example if the time for filling the sample loop; the very first step of the automated sample preparation sequence; is 80 seconds, peristaltic pump "P1" (fig. 11) has to run for 80 seconds. Therefore it is necessary to create a method on the "Elan DRC e" actually measuring for 80 seconds and simultaneously using pump "P1" while the method is running.
- In order to have a fully automated sample preparation procedure it is necessary to write a sequence of methods running sequentially on the "Elan DRC e". The ICP of the "Elan DRC e" does not need to be running while the sequence of measurements is performed. This is only to make the "FIMS 400" operate without interruption.
- Transient signals are recorded on the "Nu Plasma" MC-ICPMS in a time resolved manner using integration times between 0.2 and 1 seconds. Note, that transient signals on the "Nu Plasma" can only be recorded for 30 minutes before recording is terminated automatically. It is therefore necessary to restart the process of signal recording approximately every 30 minutes between two elutions.

Future perspectives

The first step should definitely deal with reduction of the infrastructure needed for operating the automated FI assembly. The use of the "Elan DRC-e" operating software did not allow any work to be performed simultaneously on this instrument which is naturally a cost factor. Ideally the FI manifold should be operated via the same PC that is used for operating the employed detector, the "Nu Plasma". Additionally, triggering between the automated FI manifold and the "Nu Plasma" has to be established, making presence of an operator during measurement sequences dispensable.

It was already discussed, that a naturally invariant $^{86}Sr/^{88}Sr$ isotope ratio for internal mass bias correction is an ideal image that is not necessarily true (Cavazzini, 2005; Ohno et al., in press). Various mass dependent fractionation effects between stable isotopes may occur in nature and demand methods capable of delivering appropriate precisions for detecting those. Of course the measured $^{87}Sr/^{86}Sr$ isotope ratio will change depending on the assumed $^{86}Sr/^{88}Sr$ isotope ratio for correction. Therefore it is desirable to make mass bias correction independent of Sr as target analyte itself, and subject all of the Sr isotopes to isotope ratio and abundance analysis rather than a priori assuming constant ratios in nature. It is therefore proposed to use isotope pairs of a different element for mass bias monitoring and correction. Zr, consisting of the isotopes ^{90}Zr, ^{91}Zr, ^{92}Zr, ^{94}Zr and ^{96}Zr (De Bievre and Taylor, 1993), can potentially be used for this purpose. None of the Zr isotopes interferes with any of the natural Sr isotopes and both elements are comparable with respect to their masses and first ionisation potentials which are 5.6949 eV for Sr (Rubbmark and Borgström 1978) and 6.6339 eV for Zr (Hackett et al., 1986). The experimental set up may be realised according to figure 12.
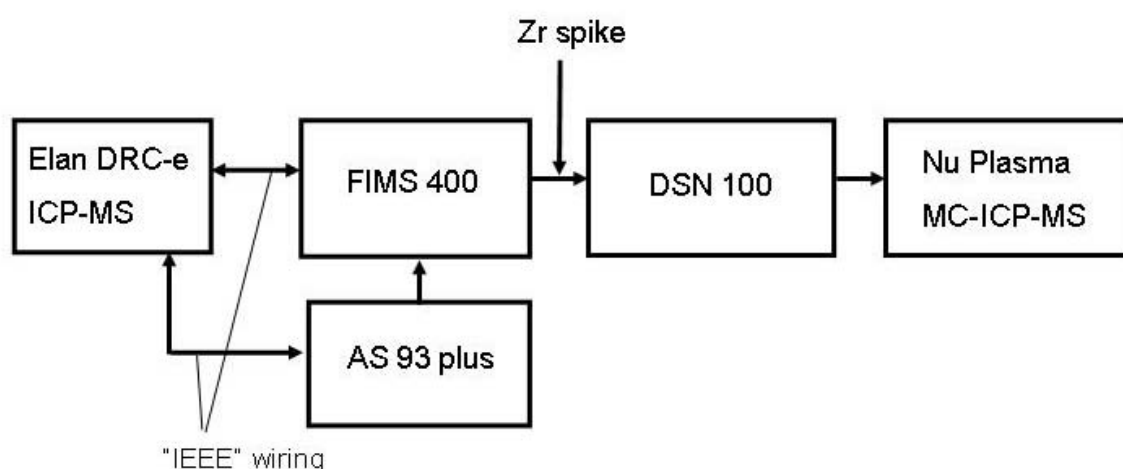
Fig. 12 On-line Addition of Zr spike for Sr isotope analysis

Basically the Zr spike can be added in solution form after the Sr/matrix separation column and provide a constant mass bias monitor. This way, potential drifts of the mass bias will be permanently covered by monitoring of a stable Zr signal. Until now this has only been possible by investigation of $^{86}Sr/^{88}Sr$ isotope ratios of consecutive elution profiles. Introducing Zr as internal standard, it is furthermore possible to differentiate between column degradation and drift of instrumental sensitivity which is not possible now. Absolute $^{86}Sr/^{88}Sr$ isotope ratios can only be determined by employing Zr isotope ratios for mass bias correction if the correlation between Zr and Sr with respect to mass bias is known. Nevertheless it is possible to determine values relative to an arbitrary reference ratio. Another potential lying within application of on-line Zr spike addition is the possible differentiation between matrix- and column-induced isotopic fractionation of the eluting Sr fraction. Illustration is provided in figures 8 and 9 where data was recorded using a 100 µL separation column with the set up as described in literature (Galler et al., 2007). Here it can be seen, that the blank corrected $^{87}Sr/^{86}Sr$ isotope ratio shows significant fractionation behaviour along the Sr elution profile. From seconds 80 to approximately 105 the blank corrected $^{87}Sr/^{86}Sr$ isotope ratio remains constant and is changing to a lower value with the maximum of the elution profile. On closer inspection there seems to be some residual fractionation of the blank and mass bias corrected $^{87}Sr/^{86}Sr$ isotope ratio in figure 8 that can obviously not fully be corrected for.

Development of a LA-MC-ICPMS method for determination of $^{87}Sr/^{86}Sr$ isotope ratios in archaeological human dental material

Preface

Usually samples are prepared accordingly and subsequently analysed using a conventional solution nebulisation MC-ICPMS approach. However preparation of samples for measurement is a very critical point of the whole analytical scheme. Sample preparation currently constitutes the major limitation concerning sample throughput and always bears the risk of sample contamination. As pointed out earlier, the quality of sample preparation can depend on the performance of the operator, which can become an intolerable risk if samples investigated are very valuable from a scientific point of view. This was the case for a sub set of samples from the Mladeč findings, which was received for Sr isotope analysis from the Natural History Museum in Vienna (Prohaska et al., 2006). Archaeological human remains found in Mladeč in the Czech Republic are, at this time, believed to play a key role in assessment of modern human emergence within Europe (Prohaska et al., 2006). Mechanical sampling of a tooth fraction and subsequent digestion are considered as the worst case with

respect to sample preservation. Preferably the samples should be analysed in a non-invasive manner, leaving behind enough sample material for repetitive future investigations. Considering this, laser ablation (LA) represents an attractive approach with respect to sample preservation, as only a small amount of sample material will be ablated by a small focussed laser beam and subsequently be introduced into the MC-ICPMS. This way the whole sample preparation procedure; employing wet chemistry susceptible to contamination; can be eliminated. This will also have a favourable effect on sample throughput of the applied analytical scheme.

It was stated before, that analyte/matrix separation is a prerequisite for accurate, high precision isotope ratio analysis (Albarède et al., 2004; Andrén et al., 2004; Leya et al., 2007). Employment of LA for in-situ sample analysis does currently not allow on-line Sr/matrix separation. When ablating any sample essentially all of the analyte and the matrix will be introduced into the ICP, potentially resulting in atomic and molecular ionic interferences overlapping with all of the natural Sr isotopes. The following experimental data is an attempt in developing an analytical method that employs LA-MC-ICPMS for reliable estimation of $^{87}Sr/^{86}Sr$ isotope ratios in human dental material. For the first time such an analytical protocol has partly successfully been employed for assessment of $^{87}Sr/^{86}Sr$ isotope ratios in human dental material.

Instrumentation, materials and reagents

An "LSX 200" LA system (CETAC Technologies, Omaha, USA) was used for sample ablation under He and Ar atmosphere. Laser ablation (LA) aerosol delivered from the ablation chamber was introduced into the spray chamber of an ultrasonic nebuliser (USN) "U-6000AT$^+$" (CETAC Technologies). From there, the aerosol was transferred into the ICP of the "Nu Plasma" MC-ICPMS (Nu Instruments Ltd., Wrexham, UK), via the membrane dissolvation unit of the USN. A schematic of the experimental set up is reproduced in figure 13. A "DSN 100" desolvating membrane nebuliser (DSN) (Nu Instruments Ltd.) was employed for solution nebulisation based determination of the $^{87}Sr/^{86}Sr$ isotope ratio of the Sr impurity in the purchased hydroxyl-apatite (Aldrich, St. Louis, USA) and of Sr in the NIST SRM 987 doped hydroxyl-apatite. A study for investigation of potential isobaric interferences on natural Sr masses (^{84}Sr, ^{86}Sr, ^{87}Sr, ^{88}Sr) has been performed on a single collector, high resolution ICPMS "Element 2" (Thermo Fisher Scientific, Bremen, Germany). A peltier cooled cinnabar spray chamber "PC³" (Elemental Scientific Inc., Omaha, USA) was used for sample introduction to the "Element 2". Typical instrumental parameters applied for the presented studies are summarized in table 8.

A tooth retrieved from a local Viennese Dentist was used for first steps of method development. NIST SRM 987 SrCO$_3$ with a certified isotopic composition of $^{87}Sr/^{86}Sr$ =

0.71034 ± 0.00026, NIST SRM 1400 bone ash and NIST SRM 1486 bone meal (National Institute of Standards and Technology, Gaithersburg, USA) with certified Sr concentrations of 249±7 μg^*g^{-1} and 264±7 μg^*g^{-1} respectively, have been used for quality control of the presented measurements. Commercially available poly-ethylene (PE) (Sigma Aldrich, St.Louis, USA) and hydroxyl-apatite [$Ca_{10}(PO_4)_6(OH)_2$] (Sigma Aldrich) have been used for preparation of the quality control samples. HNO_3; prepared by double sub-boiling distillation (Milestone-MLS GmbH, Leutkirch, Germany) of analytical reagent grade acid (Merck KGaA, Darmstadt, Germany); and water; pre-treated by reverse osmosis, further purified by a laboratory-reagent grade water system (F+L GmbH, Vienna, Austria) and final sub-boiling distillation (Milestone-MLS GmbH); have been used for dissolvation and the procedure of Sr extraction from hydroxyl-apatite. Sr traces have been extracted from hydroxyl-apatite employing Sr specific resin (Eichrom, Bruz, France). A similar procedure was applied for extracting back the Sr from the hydroxyl-apatite doped with NIST SRM 987 $SrCO_3$, as well as for analysing Sr isotope abundances of the NIST SRM 1400 and 1486 bone materials and the recent tooth retrieved from a local Viennese Dentist.

A set of archaeological samples from the Mladeč excavation site was finally investigated by the proposed LA-MC-ICPMS approach. The investigated tooth and bone samples have been excavated in the early 1880s by Josef Szombathy, and are believed to play a key role in assessment of modern human emergence within Central Europe. Detailed information on approximate age and context of these archaeological discoveries can be found elsewhere (Prohaska et al., 2006; Wild et al., 2005). The tooth samples were sonicated for approximately 5 minutes in 1% nitric acid followed by a rinsing step with 18 mΩ water and final sonication in iso-propanol. The samples were dried at room temperature. The fossilized bone samples were not pre-treated in any way and analysed as received from the Natural Historic Museum in Vienna.

All sample preparation steps have been performed in a class 10000 clean room laboratory on the BOKU Vienna.
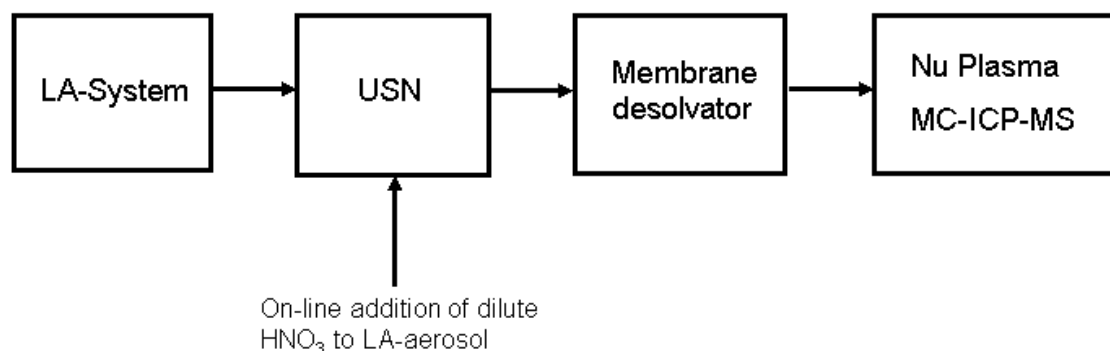
Fig. 13 LA-MC-ICPMS setup employing a USN and membrane desolvator for particle separation

(LA)-MC-ICPMS Parameters "Nu Plasma"	
Axial mass [m/z]	86
Mass resolution [m/Δm]	~ 300
Rf power [W]	1300
Plasma gas flow [L*min^{-1}]	13
Auxiliary gas flow [L*min^{-1}]	0.9
Cones	Ni
Data acquisition mode	Time resolved analysis (TRA)
Dwell time [sec]	1
LA Parameters "LSX 200"	
Ablation mode	static point ablation
Laser wavelength [nm]	266
Ablation gas	He, Ar
LA gas flow [L*min^{-1}]	1.6-1.8
Repetition rate [Hz]	10-20
Ablation duration [sec]	60
Laser spot size [µm]	200-300
Laser energy per pulse/energy level	3/20 (maximum)
USN membrane unit parameters "U-6000AT+"	
Sweep gas	Ar
Sweep gas flow [L*min^{-1}]	2-2.3
Desolvating membrane nebuliser parameters "DSN 100"	
Nebuliser	µ-flow PFA
Nebuliser back pressure [psi]	~ 30
Hot gas flow [L*min^{-1}]	~ 0.5
Membrane gas flow [L*min^{-1}]	~ 2.7
High resolution ICPMS parameters "Element 2"	
Nebuliser	µ-flow PFA
Spray chamber	ESI PC³
Masses monitored [m/z]	84, 86, 87, 88
Mass resolution	~ 4000
Cones	Ni
Oxide formation rate [%]	~ 10
Sample time [ms]	20
Samples per peak	20
Runs*passes	1*280
Total measurement time [min]	~ 60

Tab. 8 Typical instrumental parameters employed for LA studies

Interferences

Using the "ICP Interference Determination Utility" software provided by Nu Instruments approximately 250 interferences for each of the Sr and Rb isotopes can be identified, including all possible atomic, bi-atomic and tri-atomic interferences as well as doubly charged species. Doubly charged molecular interferences are not considered in the software, probably due to their thermodynamic instability. Among these approximately 250 interferences only Kr, Rb, Er, Yb, Lu and Hf account for singly or doubly charged atomic

isobars. The vast majority of interferences are of a molecular nature. Considering the fact that the ablated target material mainly consists of hydroxyl-apatite possessing the chemical formula of $Ca_{10}(PO_4)_6(OH)_2$, especially molecular interferences consisting of matrix elements should be taken care of. A list of all potential interferences is far too long to be quoted. It should however be clear, that contribution of an isobaric interference on any of the Sr isotopes puts the validity of the whole concept of blank and subsequent mass bias correction at stake. Especially as it is very difficult to retrieve a blank measurement from a Sr free tooth, which is somewhat hampered by the ubiquity of Sr in nature.

In order to identify potential interferences resulting from the hydroxyl-apatite matrix, the following experiment was designed. First of all a hydroxyl-apatite solution was purified from Sr, using the Sr specific resin from Eichrom. A detailed description on how the separation was actually performed is stated in the section below. Subsequently a 1% nitric acid solution of the presumably Sr free hydroxyl-apatite was prepared at a Ca concentration of approximately 2 µg*g^{-1}. This solution was measured for Sr isotopes ^{84}Sr, ^{86}Sr, ^{87}Sr and ^{88}Sr for approximately one hour in medium mass resolution (m/Δm ≈ 4000) on an "Element 2" single collector, high resolution ICPMS. A conventional solution nebulisation set up consisting of a low flow PFA nebuliser and a cooled cinnabar spray chamber was used for sample aspiration. Spectra recorded over one hour were averaged and compared to spectra recorded for a 1% nitric acid blank and a 1 ppb Sr solution. Recorded spectra are reproduced herein in figure 14.
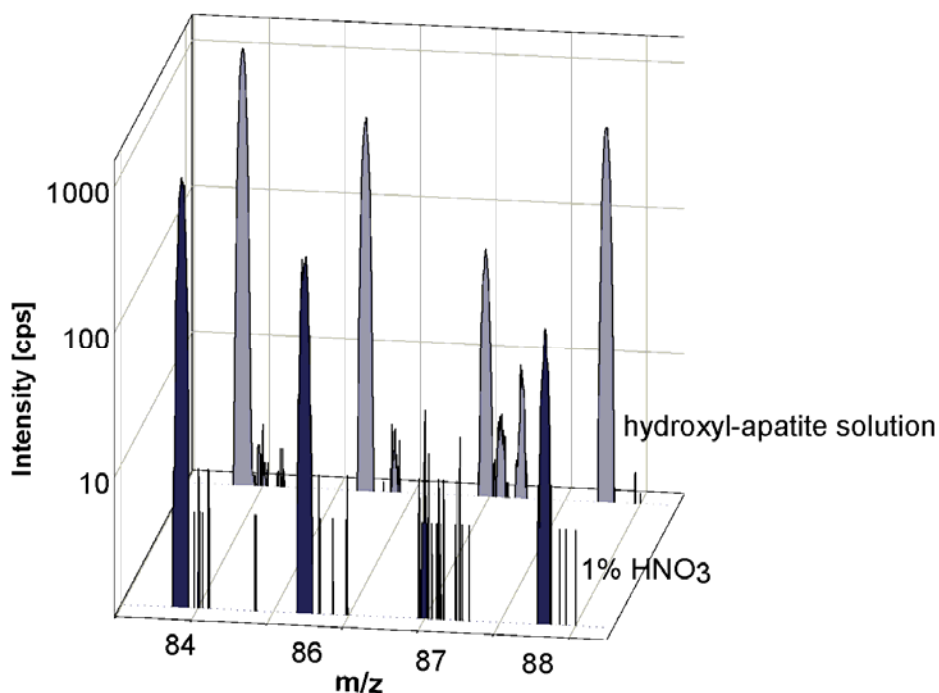
Fig. 14 Interference spectra recorded for a hydroxyl-apatite solution and 1% nitric acid

55

Intensities for a 1 ppb Sr solution under identical experimental conditions are approximately 1000, 4000, 2800 and 33000 cps for masses 84, 86, 87 and 88 respectively. It is clear that spectra recorded with a liquid nebulisation set up under wet plasma conditions can not directly be compared to the plasma conditions during laser ablation. Nonetheless mass 87 is notably found to be most affected by interferences. Three distinct peaks are found for the hydroxyl-apatite solution at mass 87. The signal on mass 88 is increasing from 120 to 490 cps going from the 1% nitric acid blank to the hydroxyl-apatite solution. It is interesting to see, that at all masses except at mass 88, small additional peaks can be found on the high mass side of the highest intensities when measuring the hydroxyl-apatite solution. These peaks are typically only a few cps in their intensities and they were not found when the total measurement time was only about 15 minutes. In this case only spiky signals that did not possess peak like shapes were found on the high mass sides. In order to identify these small intensities as peaks it is necessary to collect signal intensities sufficiently long, which was roughly one hour for the above presented spectra. Similar spectra may be obtained using a shorter total integration time of 30 minutes. However the peak shapes were found to be better identifiable employing longer integration times. When operating the "Element 2" in high resolution these additional signals could not be found, likely due to the insufficiently small ion transmission through the slit system of the ion optics.

There are two remarkable observations made that demand discussion within this section. The first is that additional peaks are much more pronounced when a conventional peltier cooled cinnabar spray chamber is used for sample aspiration instead of a membrane desolvating nebuliser. The initial idea was, to match ICP conditions for recording of these spectra as closely as possible to dry plasma conditions during laser ablation. The second observation is, that similar peak patterns will be found when a mixture of a Ca and P solutions is aspirated, despite the Sr impurities recorded for the Ca solution. From these spectra it can also be concluded that the main intensity at mass 87 for the hydroxyl-apatite spectrum presented in figure 14 is; in fact; ^{87}Sr or ^{87}Rb. Unfortunately it is unknown what spectra pure Ca and P solutions would yield, using the same experimental set up.

All of the Sr masses are potentially interfered by 1-3 Ca dimers. These represent isobars that can not be resolved in medium mass resolution as the minimum mass spectrometric resolution necessary to resolve e.g. ^{48}Ca^{40}Ca from the ^{88}Sr peak is approximately m/Δm ≈ 9000. All other Ca dimers can only be resolved by mass spectrometric resolutions better than m/Δm = 10 000 which is impossible to achieve with the "Element 2".

The interferences found on mass 87 correlate well with the experience, that ^{87}Sr/^{86}Sr isotope ratios measured by LA-MC-ICPMS in hydroxyl-apatite matrices are systematically always higher than ^{87}Sr/^{86}Sr isotope ratios measured of the same material in solution after Sr/matrix separation. The same observation has already been described in literature and it is

assumed that formation of $(^{40}Ca\text{-}^{31}P\text{-}^{16}O)^+$ molecular ions is responsible (Simonetti et al., in press, Vroon et al., 2008). In the same work it was tried correlating the difference between $^{87}Sr/^{86}Sr$ isotope ratios determined by laser ablation- and solution nebulisation-MC-ICPMS with the P, Ca and Sr content of the samples investigated. Due to the very poor correlation expressed by a correlation coefficient of $R^2 = 0.53$ it is suggested that not only $(^{40}Ca\text{-}^{31}P\text{-}^{16}O)^+$ molecular ions are responsible for the off-set between LA and solution nebulisation based data. Taking into consideration that commercial ICPMS instrumentation is based on an Ar plasma as ionisation source it is likely that next to $(^{40}Ca\text{-}^{31}P\text{-}^{16}O)^+$ molecular ions also $(^{40}Ar\text{-}^{31}P\text{-}^{16}O)^+$ molecular ions are formed which could explain the poor correlation found.

It is known however, that particles being generated by laser ablation are not fully evaporated in the ICP if they are too large (Fliegel and Günther 2006; Aeschlimann et al., 2003). Contribution of particles not being fully evaporated to elemental fractionation in laser ablation is considered significant (Fliegel and Günther 2006; Aeschlimann et al., 2003). It is probably also valid to assume, that not only elemental species can evaporate from a solid particles surface within an ICP. Assuming that the energy transfer between ICP and evaporating particle is insufficient for full evaporation it is possible, that the same can be the case for evaporated clusters of atoms. It is therefore a somewhat logical conclusion to suspect particles not being fully evaporated in the ICP, of being a potential source of molecular interferences.

Interference of ^{87}Rb and doubly charged rare earth elements (REEs) was not considered significant for these studies. ^{85}Rb intensities are commonly too low in these matrices to be able to explain the difference between solution nebulisation- and laser ablation based $^{87}Sr/^{86}Sr$ isotope ratios measured by MC-ICPMS. REEs were excluded from interference considerations due to results found later on by application of the developed method. Excellent correlation of $^{87}Sr/^{86}Sr$ isotope ratios for dentine with the cave water sampled at the excavation site did not suggest significant influence of REEs on the measurements.

Preparation of potential reference matrices

The in situ investigation of $^{87}Sr/^{86}Sr$ isotope ratios by LA-MC-ICPMS demands a suitable reference material in order to control the quality of the measurement results. Unfortunately there is no hydroxyl-apatite matrix with a defined Sr isotope composition available. In order to overcome this limitation it was decided to produce such a material in house. As previously stated in section "Interferences", commercially available hydroxyl-apatite was purified from Sr traces by employing Sr extraction with the Sr specific resin from Eichrom. 3.1311 g of the purchased hydroxyl-apatite were dissolved in 16 g of 6 mol*L^{-1} nitric acid. The prepared solution was loaded onto a solid phase extraction column containing approximately 2.5 mL of

pre-conditioned Sr specific resin. The column loaded with the hydroxyl-apatite solution was rinsed with 2-3 mL of 6 mol*L^{-1} nitric acid. The percolating fraction was collected and loaded onto a new column. This procedure was repeated 4 times. We found an ^{87}Sr/^{86}Sr isotope ratio of 0.70644 ± 0.00006 for the Sr impurity in the hydroxyl-apatite which correlated well with our expectations. In fact the ^{87}Sr/^{86}Sr isotope ratio of the Sr extracted from the hydroxyl-apatite was predicted pretty much accurately from preceding work on the on-line FI Sr/matrix separation, were the same hydroxyl-apatite was used for simulation of a bone matrix and was found to significantly bias the measurement results due to Sr impurities. After the hydroxyl-apatite solution was considered acceptably free of Sr traces it was split in two equally sized portions. One half was spiked with the NIST SRM 987 material and the other half remained as it was. NIST SRM 987 SrCO$_3$ was added in a quantity, that the final Sr concentration was approximately 250 µg per g hydroxyl-apatite which is similar to Sr concentrations found in human bone and teeth and expected for the investigation of archaeological human remains (Tandon et al., 1998; Losee et al., 1974; Grupe et al., 1997). Both hydroxyl-apatite solutions, the spiked and the Sr free one, were evaporated on a hot plate to total dryness and yielded pure white, sponge like, highly porous, solid materials. Retrospectively it could not be experimentally verified, that the produced material was really hydroxyl-apatite. It is therefore suggested to use a different procedure for synthesising hydroxyl-apatite such as the Tiselius method (Hirano et al., 1985). Another potential way to generate hydroxyl-apatite as a solid bulk material rather than particulate matter may be found in welding, which can in some variations provide temperatures significantly above the melting point of hydroxyl-apatite (≈ 1650°C). Nonetheless the above mentioned spongy material could successfully be applied for reference purposes in LA-MC-ICPMS.

In order to have a sufficiently large number of reference materials a second approach was followed. The NIST SRM 1400 bone ash and NIST SRM 1486 bone meal are two bone materials provided by the National Institute of Standards and Technology in the USA. These materials are not certified for their Sr isotopic composition but for a wide range of trace elements. So far only the NIST SRM 1400 bone ash has been investigated for its Sr isotope composition by another research group as reported in Galler et al. 2007. Reported ^{87}Sr/^{86}Sr isotope ratios do agree very well with our findings for the NIST SRM 1400 bone ash. Additionally we investigated the NIST SRM 1486 bone meal for its ^{87}Sr/^{86}Sr isotope signature over long periods using conventional solution nebulisation MC-ICPMS. Having a very good indication of the Sr isotope signatures of these materials, they were pressed into pellets using a conventional laboratory press equipped with stainless steel plungers and pre-cleaned granulate PE as binder material. The PE/bone material weight ratio was approximately 1/5. The resulting pellets proved to be very homogeneous and provided constant signal intensities during the ablation procedure. Ablation profiles of the prepared reference targets

using the 266 nm LA-system together with the USN for signal stabilisation can be found later on within this section.

Investigation of experimental parameters

Choice of LA system

A 193 nm, 213 nm and 266 nm wavelength laser ablation system are available in the VIRIS laboratory facility for LA-MC-ICPMS applications. Shorter wavelengths typically show better performance for ablation of most matrices than longer wavelengths. This effect has been studied in detail for ablation of hydroxyl-apatite (Nakata et al., 2007). In order to efficiently destroy the chemical bonds within the hydroxyl-apatite short wavelengths are necessary and will furthermore lead to development of a more defined laser ablation crater geometry. 266 nm laser ablation systems are know to produce to a larger degree coarse primary particles which are; in contrary to laser ablation performed at 193 nm; not very much influenced by the laser ablation carrier gas (Horn and Günther, 2003; Horn et al., 2001). In order to reduce interferences potentially resulting from incomplete evaporation of particles in the ICP, it is favourable to use a laser ablation system operating at a low wavelength and use He as ablation carrier gas. Nonetheless a 266 nm laser ablation system "LSX 200" from Cetac Technologies (Omaha, USA) was used for this work, as the 193 nm laser ablation system was unable to deliver sufficiently high signal intensities, adequate for precise isotope ratio measurements. This can be accredited to the fact that ablation rate, laser fluence and spot size are more restricted for the 193 nm LA-system than they are for the 266 nm LA-system in our laboratory.

Particle separation

When doing the first steps in method development for investigation of $^{87}Sr/^{86}Sr$ isotope ratios in human dental material, a procedure of trial and error was applied. Recent human tooth samples were retrieved from a local dentist, broken into pieces, analysed by laser ablation- and subsequently by solution nebulisation-MC-ICPMS. Several experiments were performed using different lasers and ablation gases but no correlation between $^{87}Sr/^{86}Sr$ isotope ratios acquired by laser ablation- and solution nebulisation-MC-ICPMS was found. Provided that incomplete evaporation of LA particles in the ICP is responsible for molecular interferences biasing the measurement results, use of a particle separation device seems worth a try for improving data correlation between LA and solution nebulisation based $^{87}Sr/^{86}Sr$ isotope ratios. Furthermore it can be expected, that signal smoothing due to particle separation has a favourable effect on data quality (Tunheng and Hirata, 2004; Hirata et al., 2003).

Parameters for modification of the particle size distribution eventually entering the ICP include the employed laser ablation carrier gas (Horn and Günther, 2003; Hirata, 2003), low pressure ablation (Hirata, 2007; Fliegel and Günther, 2006), laser wavelength, laser irradiance, laser pulse length, ablation crater depth, ablation cell geometry (Hirata and Miyazaki, 2007) and particle separation devices (Tunheng and Hirata, 2004; Russo et al., 2004; Schultheis et al., 2004; Guillong and Günther, 2002; Aeschlimann et al., 2003). Being restricted to the 266 nm LA-system and given default ablation cell geometry, particle separation is suggested to be a feasible path to reduce particle related interferences on Sr isotope masses. Use of a glass wool filter plug as frequently recommended in literature (Russo et al., 2004; Schultheis et al., 2004; Guillong and Günther, 2002) should be omitted. Application of large spot-sizes combined with high ablation rates can lead to clogging of the glass wool plug and subsequent intolerable losses of sensitivity. Furthermore does unpredictable release of particles from the glass wool plug, put data quality at stake. Particle separation without excessive loss of sensitivity is possible by using a large flow through diameter incorporated in the sample transfer tubing between laser ablation cell and ICP (Tunheng and Hirata, 2004; Aeschliman et al., 2003). For this purpose the spray chamber integrated into an ultra sonic nebuliser (USN) "U-6000AT$^+$" from Cetac Technologies was used. LA aerosol delivered from the ablation cell was introduced into the spray chamber via the carrier gas port. From there the aerosol was transported through the membrane unit of the "U-6000AT$^+$" and finally directed from the sample outlet of the membrane unit to the ICP. The sweep gas flow adjustment of the membrane unit may also be used for addition of Ar gas to the ablation gas flow in order to optimize the operating conditions of the ICP. Resulting transient signals from LA were observed to be very stable when employing this kind of particle separator. It can be expected, that this will significantly improve the quality of the data with respect to precision. In this specific case it was even possible to finally achieve correlation between solution nebulisation and laser ablation based MC-ICPMS data. An impressive demonstration of the effect of introduction of the USN including the membrane unit as particle separation device and signal stabiliser is presented in figure 15.
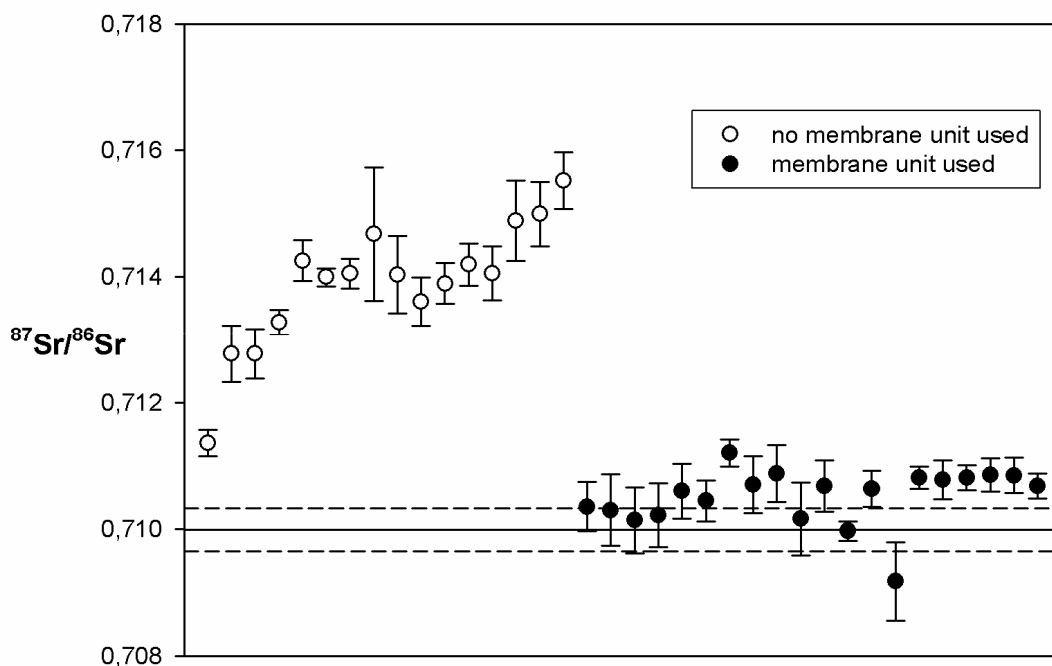
Fig. 15 Effect of USN and membrane for particle separation on measured ^{87}Sr/^{86}Sr isotope ratio

Data contained in figure 15 was generated by ablation of a fragment of a recent tooth sample from a local dentist. Foregoing solution nebulisation based MC-ICPMS analysis of 5 fragments of this tooth yielded an average ^{87}Sr/^{86}Sr isotope ratio of 0.70999 ± 0.00017 1 SD (n = 5). This mean value and two corresponding standard deviations are represented by the solid and dashed black lines in figure 15. LA-MC-ICPMS investigations using the USN plus the membrane device for signal stabilisation yielded an average ^{87}Sr/^{86}Sr isotope ratio of 0.71052 ± 0.00044 1 SD (n = 20). Error bars for data points generated using LA-MC-ICPMS correspond to a single standard deviation. Interestingly use of the USN spray chamber without the membrane unit yielded results comparable to the conventional LA-MC-ICPMS set up without any signal stabilisation device. ^{87}Sr/^{86}Sr Isotope ratios measured without USN and membrane unit are neither as accurate nor as precise as data generated using proper signal stabilisation devices. Nonetheless it has to be commented on the fact, that one time a large particle was found adhering to the tip of the skimmer cone of the "Nu Plasma". From this single observation it may concluded that despite the quality improvement observed for measurement data, some large particles still are not fully separated from the LA aerosol.

Choice of ablation gas

It is widely recognized, that the ambient gas under which laser ablation is performed may have significant influence on the final particle size distribution of the aerosol that enters the ICP (Horn and Günther, 2003; Hirata, 2003). For this specific application differences resulting from the use of He and Ar as ablation gases were evaluated from two experiments. A NIST

1400 bone ash – PE pellet and the hydroxyl-apatite spiked with the NIST SRM 987 $SrCO_3$ were chosen as target materials. Results of $^{87}Sr/^{86}Sr$ isotope ratio measurements by LA-MC-ICPMS are compared to the published $^{87}Sr/^{86}Sr$ isotope ratio of this material (Galler et al., 2007). Results are summarized in figures 16 and 17.

Fig. 16 Effect of use of Ar and He as ablation gases for NIST 1400 bone ash - PE pellet

Fig. 17 Effect of use of Ar and He as ablation gases for hydroxyl-apatite spiked with NIST SRM 987 $SrCO_3$

The published ^{87}Sr/^{86}Sr isotope ratio of 0.71314 ± 0.00028 for the NIST SRM 1400 bone meal is represented by the solid and dashed black lines in figure 16 (Galler et al., 2007). Error bars for LA data correspond to a single standard deviation in both figures. Ablation using Ar as carrier gas yielded an ^{87}Sr/^{86}Sr isotope ratio of 0.71363 ± 0.00034 (1 SD, n = 10), whereas ablation using He as carrier gas yielded an ^{87}Sr/^{86}Sr isotope ratio of 0.71553 ± 0.00033 (1 SD, n = 10) for the NIST SRM 1400 – PE pellet. The certified ^{87}Sr/^{86}Sr isotope ratio of 0.71034 ± 0.00026 for the NIST SRM 987 SrCO$_3$ is represented by corresponding solid and dashed lines in figure 17. Ablation using Ar as carrier gas resulted in an ^{87}Sr/^{86}Sr isotope ratio of 0.71066 ± 0.00046 (1 SD, n = 10), ablation using He resulted in an ^{87}Sr/^{86}Sr isotope ratio of 0.7176 ± 0.0091 (1 SD, n = 9). In both cases ablation using Ar as carrier gas for LA-MC-ICPMS yielded results agreeing with results obtained from solution nebulisation based MC-ICPMS measurements after Sr/matrix separation. Using He as ablation gas consistently yields results higher than ^{87}Sr/^{86}Sr isotope ratios measured using Ar as ablation gas. ^{88}Sr signal intensities for ablation of the NIST SRM 1400 bone meal – PE pellet are approximately 0.3 V when using Ar and 0.7 V when using He as ablation gas. In the case of ablation of the hydroxyl-apatite spiked with the NIST SRM 987 SrCO$_3$ ^{88}Sr signal intensities for ablation using He and Ar as ablation gases are both around 0.35 V. Increase of sensitivity when employing He as LA carrier gas could only be observed when ablating bone material – PE targets.

Variation of basic LA-MC-ICPMS parameters

Repetition rate, laser ablation spot-size and position of the sample inside the laser ablation cell were found to have no influence on the final measurement result. It is suggested in literature that use of conventional liquid nebulisation spray chambers is not an effective means for separation of coarse particles from the LA aerosol, unless solution is simultaneously aspirated and mixed with the LA aerosol inside the spray chamber (Aeschliman et al., 2003). However no difference was found between the finally determined ^{87}Sr/^{86}Sr isotope ratios depending on the fact whether or not dilute nitric acid is aspirated and mixed with LA aerosol in the USN spray chamber employed for signal stabilisation. As the initial idea was to let the LA aerosol interact with the nebulised nitric acid in order to shift the particle size distribution to smaller particle diameters, also different nitric acid concentrations from 1-10 % (v/v) have been investigated but did not influence the measurement result. Use of He as ablation gas was omitted. In a preliminary experiment using He as ablation carrier gas it was found, that ^{87}Sr/^{86}Sr isotope ratios measured using He as ablation gas are consistently higher than ^{87}Sr/^{86}Sr isotope ratios measured using Ar as ablation gas. Furthermore no difference in sensitivity was found between use of Ar and He as ablation gas for ablation of human dental material.

Variation of the LA gas flow and corresponding signal intensity during laser ablation were found to have very strong influence on the measurement result as is also documented in figure 18. For this experiment recent human dental enamel was ablated.
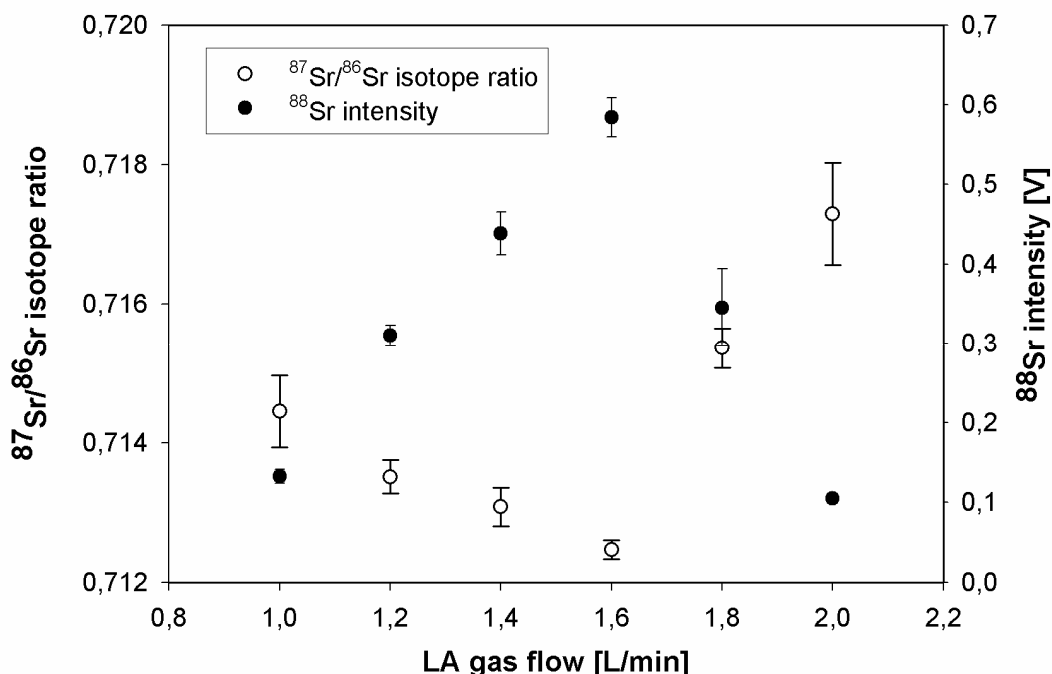
Fig. 18 Influence of LA gas flow on signal intensity and final measurement result

In fact little is known on behaviour of interferences during LA, but it is recommended to keep the ^{88}Sr signal intensity as high as possible for Sr isotope ratio measurements by LA-MC-ICPMS.

Reproducibility of laser ablation signal profiles

Several experiments investigating the reproducibility of laser ablation signal profiles have been performed. A recent tooth was ablated 20 times on 3 days, the hydroxyl-apatite spiked with NIST SRM 987 SrCO$_3$ was ablated 20 times on two days and each of the bone material - PE targets was ablated 10 times on a single day. Ablations were performed for 1 minute using Ar or He. Ablations on tooth were performed on dentine. Peak areas of the transient signals for corresponding experiments conducted on one day have been calculated in Microsoft Excel and are summarized including their respective reproducibilities in table 9 below.

Sample	Ablation gas	Ablation events	Avg. area ^{88}Sr signal [V*s]
Tooth	Ar	20	46.1 ± 3.3 (1 SD)
Tooth	Ar	20	36.5 ± 1.7 (1 SD)
Tooth	He	20	53.4 ± 5.1 (1 SD)

Hydroxyl-apatite	Ar	20	22.4 ± 6.5 (1 SD)
Hydroxyl-apatite	He	20	29.8 ± 6.8 (1 SD)
NIST SRM 1486 - PE	He	10	225 ± 15 (1 SD)
NIST SRM 1400 - PE	He	10	126 ± 10 (1 SD)

Tab. 9 Reproducibility of laser ablation signal profiles

From the results summarized in table 8 it may be concluded, that the PE - bone material ratio is approximately by a factor of 2 different for the NIST SRM 1400 - and 1486-PE pellets.

Variation of the $^{87}Sr/^{86}Sr$ isotope ratio during LA-MC-ICPMS

It is a known fact that laser ablation crater geometry significantly changes during LA as does the particle size distribution of the ablated aerosol (Saetveit et al., 2008; Guillong and Günther, 2002; Borisov et al., 2000). It is also well understood, that particle size is correlated with elemental fractionation processes observed in LA-ICPMS (Horn and Blanckenburg, 2007; Kuhn and Günther, 2003; Liu et al., 2005). Not surprisingly it has been reported that also isotopic fractionation does occur during LA-MC-ICPMS measurements when using nanosecond-LA systems like the one employed for this work (Horn and Blanckenburg, 2007). Reports state that isotope ratios preferentially change to heavier isotopic compositions of ablated matter during the ablation process (Norman et al., 2006; Jackson and Günther, 2003; Košler et al., 2005). However it was found, that Sr isotope ratios can exhibit quite different behaviour than what is reported in literature.

Ablation was performed for 1 minute at a repetition rate of 20 Hz and signals were recorded with a dwell time of 1 second. The first 5 seconds of the ablation profile were rejected from data evaluation. Raw signal intensities were on peak baseline corrected by subtracting a corresponding gas blank. The ablation profiles were divided into 3-5 blocks covering identical time spans of a few seconds. In the case of the hydroxyl-apatite spiked with the NIST SRM 987 $SrCO_3$ the signal decay after the maximum signal intensity with beginning ablation is so pronounced, that only approximately 30 seconds of the respective signals were used for evaluation. For each block average $^{86}Sr/^{88}Sr$ and $^{87}Sr/^{86}Sr$ isotope ratios were calculated and averaged for corresponding blocks from all ablation events. Calculating the means of such corresponding blocks for 10-20 measurements provides a better estimation of isotopic fractionation along a laser ablation signal profiles than can be observed from a single ablation. In fact it is extremely difficult to determine isotopic fractionation from a single ablation event using the proposed experimental set up. The averaged isotope ratios for equal blocks were plotted against the time axis and linear regressions were fitted through the data points to reveal isotopic fractionation trends. Regression curve slopes and corresponding correlation coefficients of blank corrected (blankcorr.) $^{86}Sr/^{88}Sr$, blank-, Rb interference- and mass bias corrected (fully corr.) $^{87}Sr/^{86}Sr$

and blank and Rb interference-corrected (Rb corr.) ^{87}Sr/^{86}Sr isotope ratios have been considered. Data are divided according to individual analytical sessions. Corresponding data are compiled in table 10. Slopes of regression curves are quoted in scientific notation.

Sample	Isotope ratio	Ablation gas	Ablation events	Slope, R²
Tooth	^{86}Sr/^{88}Sr blankcorr.	Ar	20	4.58e-6, 0.90
	^{87}Sr/^{86}Sr fully corr.	Ar	20	-3.43e-5, 0.98
	^{87}Sr/^{86}Sr Rb corr.	Ar	20	-4.73e-5, 0.97
Tooth	^{86}Sr/^{88}Sr blankcorr.	Ar	20	6.53e-7, 0.52
	^{87}Sr/^{86}Sr fully corr.	Ar	20	-1.95e-5, 0.98
	^{87}Sr/^{86}Sr Rb corr.	Ar	20	-1.94e-5, 0.38
Tooth	^{86}Sr/^{88}Sr blankcorr.	He	20	3.15e-7, 0.48
	^{87}Sr/^{86}Sr fully corr.	He	20	-1.64e-5, 0.92
	^{87}Sr/^{86}Sr Rb corr.	He	20	-1.78e-5, 0.93
Hydroxyl-apatite	^{86}Sr/^{88}Sr blankcorr.	Ar	20	1.32e-5, 0.61
	^{87}Sr/^{86}Sr fully corr.	Ar	20	6.45e-5, 0.93
	^{87}Sr/^{86}Sr Rb corr.	Ar	20	2.62e-5, 0.71
Hydroxyl-apatite	^{86}Sr/^{88}Sr blankcorr.	He	20	-2.62e-6, 0.20
	^{87}Sr/^{86}Sr fully corr.	He	20	-2.83e-5, 0.89
	^{87}Sr/^{86}Sr Rb corr.	He	20	-2.54e-5, 0.82
NIST SRM 1486 - PE	^{86}Sr/^{88}Sr blankcorr.	He	10	-3.42e-7, 0.31
	^{87}Sr/^{86}Sr fully corr.	He	10	-1.07e-5, 0.77
	^{87}Sr/^{86}Sr Rb corr.	He	10	-9.90e-6, 0.80
NIST SRM 1400 - PE	^{86}Sr/^{88}Sr blankcorr.	He	10	1.46e-6, 0.89
	^{87}Sr/^{86}Sr fully corr.	He	10	-1.01e-5, 0.74
	^{87}Sr/^{86}Sr Rb corr.	He	10	-1.47e-5, 0.84

Tab. 10 Fractionation of Sr isotope ratios along transient signal; blankcorr = on peak baseline corrected; fully corr. = on peak baseline, Rb interference and mass bias corrected; Rb corr. = on peak baseline and Rb interference corrected

Typically the ^{86}Sr/^{88}Sr isotope ratio is getting lighter at a rate of approximately 4e-6/sec, excluding findings for the doped hydroxyl-apatite and NIST SRM 1486 bone meal pellet ablated under He were it is getting heavier during ablation. The ^{87}Sr/^{86}Sr isotope ratio is getting lighter at a typical rate of -2.12e-5/sec, except for the ablation of doped hydroxyl-apatite using Ar as ablation gas were ^{87}Sr/^{86}Sr isotope ratios are getting heavier. The rate at which the ^{87}S/^{86}Sr isotope ratio is changing is approximately the same for blank-, Rb- and mass bias as well as exclusively blank- and Rb interference-corrected ^{87}Sr/^{86}Sr isotope ratios. This means, that the finally determined ^{87}Sr/^{86}Sr isotope ratio changes by an absolute value of approximately 0.0013 during a 60 second ablation. This drift is however only that clearly empirically observable when averaging 10-20 measurements. It was also observed, that during some of the experiments the ^{87}Sr/^{86}Sr isotope ratio starts levelling of to a more or less constant value at the end of ablation. Yet corresponding experiments ablating for longer than 60 seconds are missing to verify this impression. Furthermore the reproducibility of the slopes of the regression curves through the measured isotope ratios have to be investigated

as well as the exact reason for their variation. For example it can currently not be explained why the isotope fractionation does not consistently lead to heavier or lighter isotopic compositions in the course of a static point ablation. The fact that blank-, Rb interference- and mass bias as well as only blank- and Rb interference-corrected $^{87}Sr/^{86}Sr$ isotope ratios change at the same rate is remarkable. It may be assumed that this is the result of a particle related interference that contributes to different extents during an ablation process, being most pronounced at the beginning and least pronounced at the end of a static point ablation. This is only an assumption tough!

Experiments involving half masses

Measurements of half masses when investigating Sr isotope signature in situ can be important for interference monitoring. For example the signal recorded at mass 86.5 will be representative for $^{173}Yb^{2+}$, which can than be used to estimate the contribution of $^{176}Yb^{2+}$ to the ^{88}Sr signal. In order to reveal potential differences between the ablated matrices; including the hydroxyl-apatite doped with NIST SRM $SrCO_3$, bone material – PE pellets and human tooth samples; all of the available faraday detectors have been used to record signals on masses 90.5, 89, 88.5, 88, 87.5, 87, 86.5, 86, 85.5, 85, 82.5 and 81.5. The experiments have been performed using He as ablation gas which is not representative for experimental conditions under which investigation of real samples has been performed. The observations made will therefore be only shortly described. It is recommended to re-investigate half masses under "default" experimental conditions using Ar as ablation gas.

For ablation of a recent tooth, no signals on concerned half masses were observed. Only a drop in signal intensity by approximately 0.1 mV was observed for mass 88.5 with beginning sample ablation. When ablating the doped hydroxyl-apatite signal spikes at mass 89 of roughly 0.1-0.2 mV were observed. There is no correlation between maximum signal intensities at mass 89 and Sr masses. The same effect for mass 88.5 was observed as was observed for ablation of tooth. Significant signals in the order of 5 mV can be measured on mass 89 for ablation of bone material – PE targets. The effect described for measurements of mass 88.5 when ablating doped hydroxyl-apatite and human tooth is more pronounced when ablating bone material – PE targets. The corresponding drop in signal intensity is approximately 0.2 mV. A similar effect is observed for mass 87.5 and 82.5, being least pronounced for mass 82.5. The results potentially demonstrate fundamental differences between the matrices investigated.

Ablation profiles

The appearance of a laser ablation signal profile is a reflection of relevant physical processes during the ablation process. Highest reliability of reference measurements is provided if all

materials; including samples and reference materials; exhibit the same physical properties. In this section appearance of the laser ablation signal profiles of the different matrices involved will be presented. It will briefly be discussed what leads to the appearance of different ablation profiles of the materials involved. Laser ablation signal profiles for involved reference materials are reproduced in figure 19, laser ablation signal profiles for investigated archaeological tooth samples are reproduced in figure 20. All ablation profiles have been recorded under comparable experimental conditions.
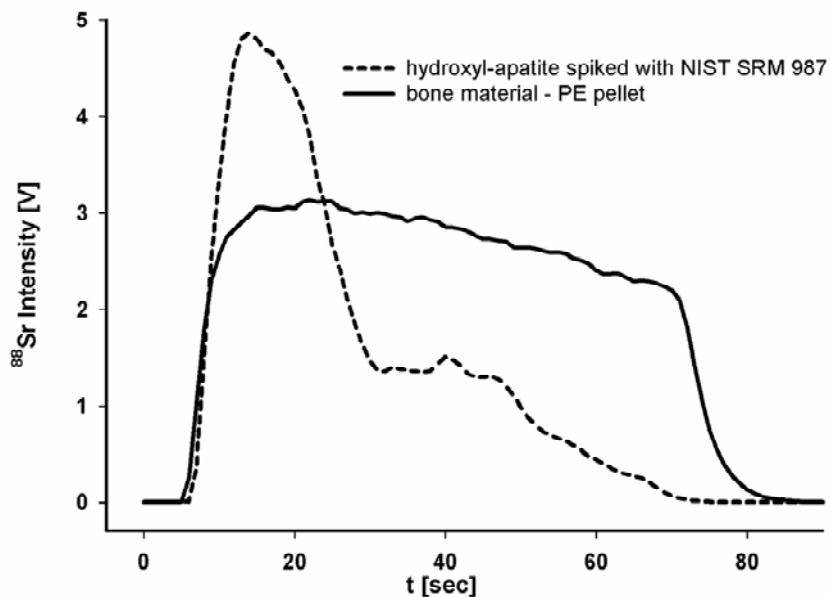
Fig. 19 Laser ablation signal profiles of reference targets

The laser ablation signal profile for bone material – PE targets provides nearly constant signal intensity during the ablation process. It is therefore assumed that the ablation rate for this material is only subjected to minor changes or even a drift during ablation of sample. Ablations of hydroxyl-apatite doped with NIST SRM 987 $SrCO_3$ are typically characterised by high intensities at the beginning of an ablation. The signal intensity drops much faster though than for bone material – PE pellet ablation. Furthermore the laser ablation profiles for doped hydroxyl-apatite are only poorly reproducible as already documented in table 8. It is assumed that observed laser ablation signal profiles for this material are a result of the porous structure of this material. This may lead to significant particle trapping effects as the focussed laser beam penetrates into the material and uncovers various cavities present in this material. Resulting signal intensities for laser ablation of doped hydroxyl-apatite were observed to vary by a factor of up to 3 depending on the location of the ablation event on this material.
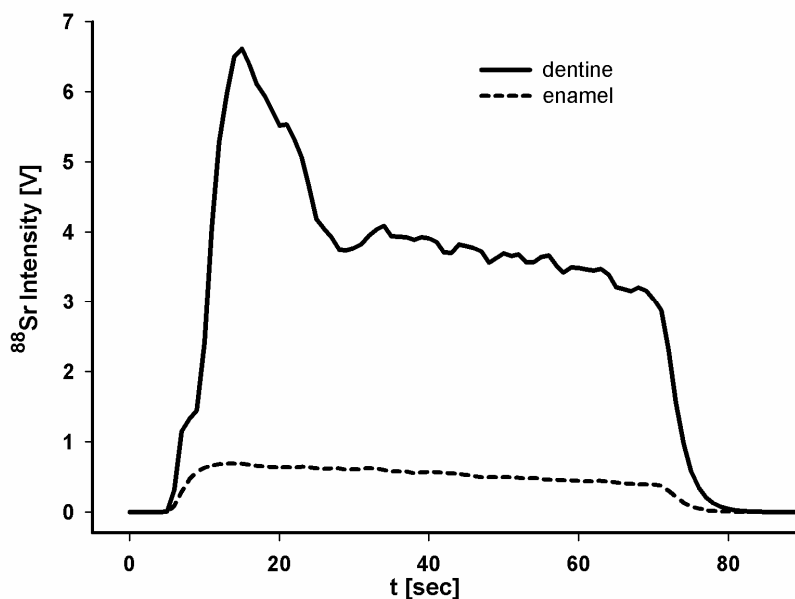
Fig. 20 Laser ablation signal profiles of archaeological tooth samples

Observed laser ablation signal intensities for dentine are significantly higher than they are for enamel. Laser ablation of dentine of archaeological tooth samples is usually characterised by a significant signal spike at the beginning of an ablation event that levels of to almost constant signal intensity thereafter. This spike is not observed for laser ablation of recent tooth samples, which is likely a result of superficial contamination of archaeological teeth. Porous structures like dentine are certainly more susceptible to such effects than enamel (Camargo et al., 2008). Laser ablation of enamel typically yields much less signal intensity for Sr, owing to the mechanical hardness of this matrix (He et al., 2006; Zaslansky et al., 2006). The resulting laser ablation signal profile is very stable though. The fact that archaeological dentine is usually of a dark brown colour whereas enamel is usually close to being of a pure white colour plays an additional role with respect to absorption of laser radiation and resulting ablation efficiency (Mao et al., 1998). Reasonable signal intensities for laser ablation of dentine can already be achieved using smaller spot sizes of approximately 200 μm and a laser ablation repetition frequency of 10 Hz. It is advised to use the largest available spot size for the ablation of enamel as well as the highest available ablation rate of 20 Hz in order to achieve reasonable measurement precisions when employing the proposed experimental LA-MC-ICPMS set up.

Long term investigations of reference targets by LA-MC-ICPMS

This section covers results for $^{87}Sr/^{86}Sr$ isotope ratio measurements by LA-MC-ICPMS for the NIST SRM 1400 and 1486 – PE targets as well as for the hydroxyl-apatite spiked with the NIST SRM 987 $SrCO_3$ reference material. Results are summarized in table 11.

69

Hydroxyl-apatite spike with NIST SRM 987 SrCO$_3$		
Date	mean ^{87}Sr/^{86}Sr isotope ratio	typical precision of single ablation
4th of April 07	0.71037 ± 0.00045 (n=19)	0.10
5th of April 07	0.71066 ± 0.00070 (n=21)	0.11
6th of April 07	0.71111 ± 0.00069 (n=12)	0.11
10th of April 07	0.71066 ± 0.00046 (n=10)	0.08
15th of May 07	0.71127 ± 0.00050 (n=36)	0.09
14th of August 07	0.71042 ± 0.00010 (n=39)	0.03
mean value	0.71075 ± 0.00037 (1 SD)	
conventional solution nebulisation based data		
Sr/matrix separated	0.71044 ± 0.00004 (n=1)	
no Sr/matrix	0.71023 ± 0.00004 (n=1)	
certified value	0.71034 ± 0.00026	
accepted value 1	0.71026	
accepted value 2	0.710245	
NIST SRM 1400 bone ash – PE pellet		
4th of April 07	0.71350 ± 0.00020 (n=6)	0.06
5th of April 07	0.71419 ± 0.00021 (n=24)	0.04
6th of April 07	0.71377 ± 0.00014 (n=6)	0.03
10th of April 07	0.71363 ± 0.00034 (n=10)	0.09
14th of August 07	0.71370 ± 0.00014 (n=24)	0.03
mean value	0.71376 ± 0.00026 (1 SD)	
published value	0.71314 ± 0.00028	
NIST SRM 1486 bone meal – PE pellet		
4th of April 07	0.70962 ± 0.00013 (n=6)	0.05
5th of April 07	0.70978 ± 0.00008 (n=12)	0.02
6th of April 07	0.70975 ± 0.00009 (n=18)	0.02
11th of April 07	0.70895 ± 0.00044 (n=39)	0.03
mean value	0.70953 ± 0.00039 (1 SD)	
published value	0.70931 ± 0.00012	

Tab. 11 Long term investigations of reference targets

As documented in table 10, measurement results determined by LA-MC-ICPMS are typically higher than ^{87}Sr/^{86}Sr isotope ratios determined by conventional solution nebulisation MC-ICPMS. Typically ^{87}Sr/^{86}Sr isotope ratios start deviating in the fourth digit after the comma. Given the similarity of measurement results of conventional solution nebulisation and LA-based MC-ICPMS measurements it can be assumed that it is indeed possible to give a fair estimation of ^{87}Sr/^{86}Sr isotope ratios in human bone like materials by LA-MC-ICPMS. It should however be taken well care to provide a reasonable number of replicate measurements by LA-MC-ICPMS as single ablations are not a reliable measure due to occurrence of outliers. The hydroxyl-apatite spiked with the NIST SRM 987 SrCO$_3$ was additionally investigated by conventional solution nebulisation MC-ICPMS with and without preceding Sr/matrix separation. Measurements have been performed only one time and respective uncertainties are quoted as instrumental precisions. Note that the measured ^{87}Sr/^{86}Sr isotope ratio for this material is higher without than it is with preceding Sr/matrix separation. Based on figure 2 within this work it is proposed, that Rb levels present in the

bone material targets (Galler et al., 2007) are not responsible for elevated $^{87}Sr/^{86}Sr$ isotope ratios determined for these matrices via LA-MC-ICPMS.

Precision levels for bone material PE pellets are generally better than precision levels for the hydroxyl-apatite spiked with the NIST SRM 987 $SrCO_3$. This can be accredited to the fact, that signal profiles resulting from laser ablation of the bone material – PE pellets are far more stable and better reproducible than ablation profiles of the spiked hydroxyl-apatite. This is probably a result of the different physical properties of these materials. Whereas the bone material – PE pellets are very compact and homogeneous, the doped hydroxyl-apatite is very porous. Signal intensities resulting from ablation of the doped hydroxyl-apatite may vary by a factor of up to 3, depending on the location of ablation on one and the same target.

In total 137 measurements of the hydroxyl-apatite spiked with the NIST SRM 987 $SrCO_3$ have been performed under comparable experimental conditions (tab. 10). A plot of measured $^{87}Sr/^{86}Sr$ isotope ratios for this material versus the average ^{88}Sr signal intensity of the concerned ablation is reproduced in figure 21.
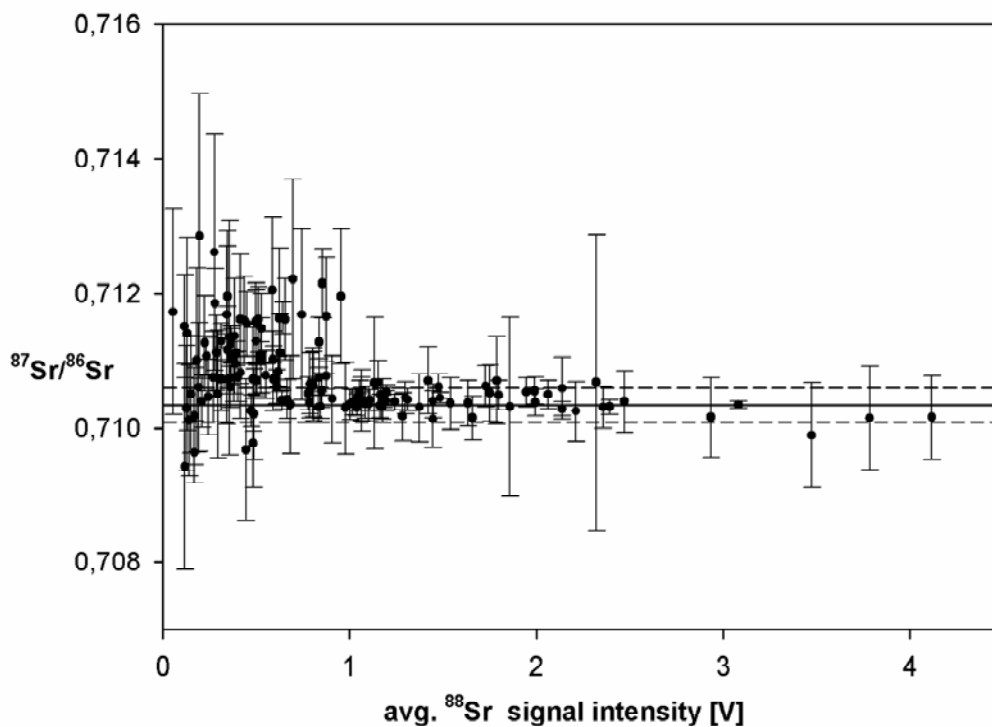
Fig. 21 Measured $^{87}Sr/^{86}Sr$ isotope ratio plotted versus average ^{88}Sr signal intensities during ablation; straight lines correspond to certified value

As deducible from figure 21 it is preferable to maintain the signal intensity during ablation as high as possible in order to generate data that provide a reliable estimation of the true $^{87}Sr/^{86}Sr$ isotope ratio within the hydroxyl-apatite matrix. As the poor reproducibility of ablation profiles may lead to comparably low signal intensities for the hydroxyl-apatite spiked

with the NIST SRM 987 $SrCO_3$, measurements should be repeated in case of too low signal intensities. It is yet unclear, what the reason for locally varying signal intensities is. The porosity of the generated material may be one, local enrichment of Sr within the material may be another. It is also assumed that the employed ablation cell is not tightly closed, leading to strongly drifting optimum LA gas flows during measurement session. Typically the optimum LA gas flow has to be increased, sometimes even to the maximum which can naturally not be further optimized.

Error bars in figure 21 correspond to a single standard deviation of the respective determination. These standard deviations were plotted against the average [88]Sr signal intensity during measurement as well. A corresponding scatter plot is provided in figure 22.
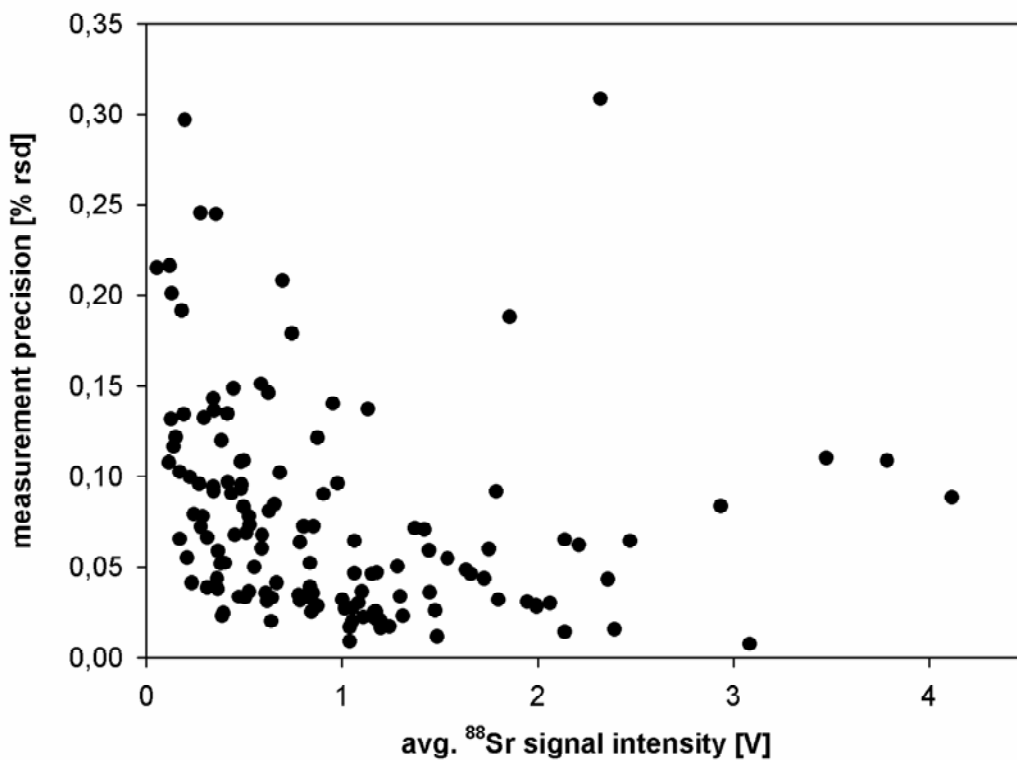
Fig. 22 Precision of single ablation events plotted versus average [88]Sr signal intensities during ablation

The correlation between measurement precision and observed [88]Sr signal intensity is very poor. Nonetheless it may be concluded from figure 21, that high signal intensities are favourable with respect to reliability of a series of repetitive measurements.

Strategy for setting up LA-MC-ICPMS measurements for in-situ Sr isotope investigations of archaeological tooth samples

In order to conduct reliable $^{87}Sr/^{86}Sr$ isotope ratio measurements the following strategy is proposed:

- Assembly of the LA set-up including the USN as particle separation device.
- Tuning of MC-ICPMS parameters such as torch position, lens voltages, peak alignment and peak shape with a Sr solution of convenient concentration introduced via the USN.
- Tuning of LA parameters by ablation of a convenient LA target. It is recommended to use bone material - PE pellets with a known $^{87}Sr/^{86}Sr$ isotope ratio or a solid hydroxyl-apatite spiked with the NIST SRM 987 $SrCO_3$ isotope reference material.
- Performance of a few test measurements and recording of the data.
- Evaluation of the test measurements and control whether or not the generated $^{87}Sr/^{86}Sr$ isotope data agrees with expected values.
- Investigation of real samples with a sufficient number of reference measurements and consequent standard sample bracketing. It is advised to conduct at least as many reference measurements as real sample investigations.

Investigation of archaeological tooth samples

The proposed LA-MC-ICPMS set up was used for investigation of a set of archaeological tooth and bone samples from the Mladeč excavation site (Prohaska et al., 2006; Wild et al., 2005). For measurement, cleaned samples were affixed with play dough on glass slides and placed into the LA cell as received from the Natural History Museum Vienna. Tooth samples were received either as whole tooth or fragment of a tooth. Fossilized bone samples were received in fragmentary form only. All investigated samples and control standards as well as corresponding results of their investigations are summarized in table 12. Results for LA-MC-ICPMS of the archaeological samples are quoted as mean and standard deviation of typically 6 measurements. For each mean value, corresponding ablations have been arranged in a dense 2x3 lattice on the sample surface. Ablation craters observed through the focusing optics of the LA system were of spheric geometry, without perceptible irregular features. Whenever a whole tooth instead of a fragment was received for measurement, a comment is made on where approximately on the tooth sample ablation was performed. Usually it was tried to investigate the 'youngest' (crown base or close to the root), compared to the 'oldest' (apex of the crown) part of the enamel of a single tooth. $^{87}Sr/^{86}Sr$ isotope ratios of the control samples are quoted as overall mean and standard deviation of all performed measurements.

Solution based, certified and 'accepted' data of the control samples are quoted for comparison. Results obtained for the archaeological samples are compared to the Sr isotope signature of 2 cave water samples from the Mladeč excavation site. Water samples have been investigated by thermal ionisation mass spectrometry (TIMS) at the Department for Geology on the University of Vienna. Finally enamel and dentine of sample "Mladeč 1" have been digested, Sr/matrix separated and investigated by conventional solution nebulisation MC-ICPMS. Uncertainties of these measurements were calculated as standard deviation of 6 measurement blocks extracted from a single 10 minute measurement using 10 seconds of dwell time. Results are quoted beneath LA data.

Sample (species)	Tooth	Tissue	Approx. ablation region	Set up	$^{87}Sr/^{86}Sr \pm 1$ SD
Mladeč 1 (human)	right M² (fragment)	enamel	-	LA-MC-ICPMS	0.71306±0.00037 (n=6)
				MC-ICPMS	0.71113±0.00034 (n=6)
	left P³ (fragment)	dentine	-	LA-MC-ICPMS	0.71103±0.00007 (n=6)
				MC-ICPMS	0.71062±0.00008 (n=6)
Mladeč 2 (human)	left M³ (fragment)	enamel	-	LA-MC-ICPMS	0.71157±0.00037 (n=6)
	left M³ (fragment)	dentine	-	LA-MC-ICPMS	0.71069±0.00006 (n=6)
Mladeč 8 (human)	probably left M² (fragment)	enamel	-	LA-MC-ICPMS	0.71108±0.00007 (n=6)
	left I² (fragment)	dentine	-	LA-MC-ICPMS	0.71025±0.00006 (n=6)
	left M² (fragment)	dentine	-	LA-MC-ICPMS	0.71034±0.00005 (n=6)
Mladeč 9a (human)	right C	enamel	crown apex	LA-MC-ICPMS	0.71165±0.00017 (n=7)
	right C	enamel	crown base	LA-MC-ICPMS	0.71181±0.00019 (n=6)
	right C	dentine	6 spots at center, 2 spots at root end	LA-MC-ICPMS	0.71027±0.00007 (n=8)
Mladeč 9b (human)	right P³	enamel	crown apex	LA-MC-ICPMS	0.71303±0.00025 (n=6)
	right P³	enamel	crown base	LA-MC-ICPMS	0.71354±0.00024 (n=6)
	right P³	dentine	close to dentine-enamel boundary	LA-MC-ICPMS	0.71080±0.00004 (n=6)
Mladeč 10 (human)	right M³	enamel	crown apex	LA-MC-ICPMS	0.71164±0.00006 (n=6)
	right M³	enamel	crown base	LA-MC-ICPMS	0.71128±0.00005 (n=6)
	right M³	dentine	6 spots at center	LA-MC-ICPMS	0.71050±0.00006 (n=6)
	right M³	dentine	3 spots at root end	LA-MC-ICPMS	0.71049±0.00005 (n=3)
72.205 (fox)	unknown tooth (fragment)	enamel	-	LA-MC-ICPMS	0.71259±0.00028 (n=6)
	unknown tooth (fragment)	dentine	-	LA-MC-ICPMS	0.71077±0.00007 (n=5)

Sample (species)	Bone fragment	Comments	Set up	$^{87}Sr/^{86}Sr \pm 1$ SD
72.205 (fox)	mandible	-	LA-MC-ICPMS	0.71119±0.00068 (n=3)
72.204 (fox)	humerus	-	LA-MC-ICPMS	0.71105±0.00005 (n=4)
72.203 (fox)	femur	-	LA-MC-ICPMS	0.71088±0.00008 (n=4)
72.202 (fox)	tibia	-	LA-MC-ICPMS	0.71109±0.00017 (n=4)
72.192 (lion)	t.r. 3, t.r. 4, t.l. 4	average of 2-3 spots per fragment	LA-MC-ICPMS	0.71075±0.00026 (n=8)

Water sample	Sampling site	Comments	Set up	$^{87}Sr/^{86}Sr \pm 1$ SD
Mladeč W01	Witch cave	uncertainty quoted as instrumental precision ,sampled in spring 2006	TIMS	0.710545±0.000003
Mladeč W02	Virgin cave	see above	TIMS	0.71056±0.00008

Control sample	Sample matrix	Comments	Set up	$^{87}Sr/^{86}Sr \pm 1$ SD
Hydroxyl-apatite doped with NIST SRM 987 $SrCO_3$	Hydroxyl-apatite (?)	-	LA-MC-ICPMS	0.71042±0.00010 (n=39)
	Hydroxyl-apatite (?)	uncertainty quoted as instrumental precision, sample not Sr/matrix separated	MC-ICPMS	0.71044±0.00004
	approx. 1% HNO_3	uncertainty quoted as instrumental precision, sample Sr/matrix separated	MC-ICPMS	0.71023±0.00002
NIST SRM 987 $SrCO_3$	-	certified value	-	0.71034±0.00026
	-	'accepted values', no uncertainties available	-	0.710245 and 0.71026
NIST SRM 1400 bone ash	PE– bone ash pellet	-	LA-MC-ICPMS	0.71372±0.00014 (n=30)
	approx. 1% HNO_3	sample Sr/matrix separated	MC-ICPMS	0.71315±0.00016
NIST SRM 1486 bone meal	PE– bone ash pellet	-	LA-MC-ICPMS	0.70975±0.00009 (n=18)
	approx. 1% HNO_3	sample Sr/matrix separated	MC-ICPMS	0.70931±0.00006

Tab. 12 Results of investigation of archaeological samples by LA-MC-ICPMS

As demonstrated by the data in table 12, LA-MC-ICPMS measurements give a good indication of $^{87}Sr/^{86}Sr$ isotope ratios in the applied reference LA targets and dentine of the samples investigated. The $^{87}Sr/^{86}Sr$ isotope ratio measured in enamel of sample Mladeč 1 by LA-MC-ICPMS is significantly elevated compared to data generated by conventional solution nebulisation based MC-ICPMS. It is possible that part of this observation can be explained by Sr isotope heterogeneity within enamel. The enamel sample of Mladeč 1 however consisted of only a few mm³ of material. In figure 18 of this work it is shown, that signal intensity is of crucial importance with respect to the developed LA-MC-ICPMS method. LA-MC-ICPMS measurements of enamel are generally characterized by comparably low signal intensities. It therefore needs to be urgently clarified, if the developed LA-MC-ICPMS method can be applied for reliable estimation of $^{87}Sr/^{86}Sr$ isotope ratios in human dental enamel.

The ^{87}Sr/^{86}Sr isotope ratios found for samples Mladeč 2 and 8 do correlate well with recently published values (Prohaska et al., 2006). The ^{87}Sr/^{86}Sr isotope ratio for enamel of Mladeč 1 in the same study is approximately 0.16 % below the ^{87}Sr/^{86}Sr isotope ratio found in this work. ^{87}Sr/^{86}Sr isotope ratios of dentine of Mladeč 1 correlate well between these two investigation campaigns as well as with conventional solution nebulisation based MC-ICPMS data in table 11. The mean value of all ^{87}Sr/^{86}Sr isotope ratios in dentine measured by LA-MC-ICPMS is 0.71057 ± 0.00027 and therefore suggesting Sr isotope equilibrium with the cave water. A further observation consists of significantly different ^{87}Sr/^{86}Sr isotope ratios for Mladeč 9a and Mladeč 9b. It needs to be clarified whether this observation consists of a measurement artefact or whether these samples; supposedly stemming from the same individual; are really that much different. If they are significantly different with respect to their Sr isotope composition, this is a potential indicator for change of nutrition sources, potentially correlated with a migration event. Albeit Sr isotope data generated by LA-MC-ICPMS does not seem to correlate with conventional solution nebulisation base MC-ICPMS data, the solution nebulisation based data of enamel of Mladeč 1 still is higher than the Sr isotope signature found for the cave water at the excavation site.

The investigated bone samples were selected due to their low Rb content, as Rb is known to seriously affect measurement accuracy of ^{87}Sr/^{86}Sr isotope ratio determinations. In some of the samples measured ^{87}Sr/^{86}Sr isotope ratios were rather heterogeneous, which explains the low reproducibility for fox bone sample "72.205". Generally these samples exhibit ^{87}Sr/^{86}Sr isotope ratios close to the Sr isotope signature of the cave water. The ^{87}Sr/^{86}Sr isotope ratios of the control samples measured by LA and solution based MC-ICPMS procedures show consistent deviation in the fourth digit after the comma. Data generated by LA-MC-ICPMS is in all cases higher than data generated by solution based MC-ICPMS. The contribution of interfering ^{87}Rb; calculated from the measured signal intensity at m/z = 85; for the presented measurements is assumed to cause a shift of the measured ^{87}Sr/^{86}Sr isotope ratios of < 0.00001 (Galler et al., 2007), and is therefore considered insignificant with respect to the levels of precision and accuracy achieved in this work.

Conclusive remarks concerning investigation of archaeological tooth samples

It is demonstrated, that ^{87}Sr/^{86}Sr isotope ratios in archaeological human dentine can be estimated from LA-MC-ICPMS measurements without tedious sample preparation. It is evident from our data, that reasonable assumptions about the Sr isotope signature in this type of samples can be made.

Sadly however the developed LA-MC-ICPMS method did not deliver results that would allow reliable estimation of $^{87}Sr/^{86}Sr$ isotope ratios in enamel. Sadly, because enamel is the potentially most interesting matrix due to presumably least pronounced diagenetic alteration of the native Sr isotope signature that could potentially serve as migration tracer. It is therefore recommended that future efforts focus on the investigation of enamel as well as synthesis of a reference target physically and chemically comparable to enamel.

Future perspectives

The work done so far covers first approximative investigations of certain relevant parameters such as the effect of a signal stabilisation device or effects resulting from application of He and Ar as ablation gases. Clearly the proposed experimental set up is far away from being optimum as is for example demonstrated by the gas-tightness and unfavourable default geometry of the ablation cell or the wavelength of the employed laser system. Hereafter a bulleted list of investigations and optimizations that urgently need to be performed is quoted.

- Optimization of the laser ablation cell geometry.
- Investigation of different particle separation devices and their effects on particle size distributions that may enter the ICP.
- Repeated investigations of the effect of different ablation gases.
- Investigation of isotope ratio fractionation along the transient signal of an ablation event.
- Investigation of contribution of Ca and P to spectral interferences and their impact on the final measurement result.
- Investigation of contribution of rare earth elements (REE) to spectral interferences and their impact on the final measurement result.
- Generation of a reference matrix with defined Sr isotope composition that physically and chemically matches the human bone and/or tooth matrix.
- Influence of the organic phase of dentine and bone material – PE pellets to the measurement result.
- Influence of reactive components added via the USN spray chamber to the LA-aerosol on the measurement result.
- Influence of the employed magnet mass on the measurement result.
- Investigations concerning separation of molecular interferences from analyte signals, using the instrumental MC-ICPMS parameters relevant for mass resolution.

Summary

Summing up it can be said that a lot of time has been invested in setting up a working laboratory infrastructure and learning of basic principles applied in MC-ICPMS. From the authors point of view the installation of a MC-ICPMS laboratory in Vienna is a big step for the Austrian community of analytical chemistry. Considering the number of publications, the VIRIS project can already be considered a big success.

The developed FI method for automated on-line Sr/matrix separation proved to be highly rugged and superior in terms of sample throughput, compared to conventional analytical procedures employing manual sample preparation. Considering levels of precision and accuracy achieved using the proposed automated set-up, further application of this analytical method is highly recommended. The total amount of solvents consumed for on-line Sr/matrix separation combined with re-usable µ-columns suggests significant economic savings potential. The absence of high tech equipment such as liquid-chromatographic pumps has additional impact on the economy of the proposed method. Additionally, the fact that Sr may be extracted from virtually any sample on a fully automated basis, can effectively eliminate irreproducible human performance. Given the number of recent publications dealing with Sr isotope analysis, dispersion of the developed method; if necessary even on a commercial basis; should be seriously considered. Taking into account that the scientific community now starts realizing mass dependent isotopic fractionation in nature, it is advised to fathom the potential of this method for stable Sr isotope analysis using an external post-column spike for mass bias correction. An element potentially useful for this type of mass bias correction is Zr, as it is very similar to Sr with respect to its mass. It should also be considered that the "Sr resin" employed for the separation columns does not only retain Sr from nitric acid solutions, but even stronger Pb. For Pb exhibiting significant natural isotopic variation, this element could additionally be used for tracer studies in combination with Sr, ideally eluting sequentially from the same column.

The strong performance exhibited by the developed on-line FI method for Sr/matrix separation with respect to sample throughput may be surpassed by LA-MC-ICPMS methodology. $^{87}Sr/^{86}Sr$ isotope ratios determined for powdered, homogenized and pressed pellets using poly-ethylene as binder are promising. LA-MC-ICPMS measurements of dentine too gave a good indication of the sample's $^{87}Sr/^{86}Sr$ isotope ratio. However, the method did not deliver satisfactory results for $^{87}Sr/^{86}Sr$ isotope ratio measurements of enamel. Sample heterogeneity may play one role and spectral interferences resulting from the matrix ablated may play another. It therefore needs to be clarified whether or not organic material such as poly-ethylene (PE) in the bone meal – PE pellets or collagen in dentine have an effect on the measurement result and how isotopically homogeneous Sr actually is within the samples addressed. Although enamel and dentine are, apart from their relative

organic content, very similar concerning their inorganic chemistry, they exhibit significantly different physical features with respect to porosity, colour, hardness, piezo- and pyro-electricity. In order to control any influence of interference contribution it seems inevitable to establish reference materials of defined Sr concentration and Sr isotope composition, matched to the physical properties of bone, dentine and enamel. Before such materials are available it seems more than worthwhile to attempt in separating spectral interferences from the analytes of interest employing the mass resolution features of the "Nu Plasma" MC-ICPMS.

Literature references

Aeschliman D.B., Bajic S.J., Baldwin D.P., Houk R.S., High-s6peed digital photographic study of an inductively coupled plasma during laser ablation6: Comparison of dried solution aerosols from a micro concentric nebuliser and solid particles from laser ablation, *J. Anal. At. Spectrom.*, 2003, **18**, 1008-14.

Albarède F. Telouk P., Blichert-Toft J., Boyet M., Agranier A., Nelson B., *Geochim. Cosmochim. Acta*, Precise and accurate isotopic measurements using multiple-collector ICPMS, 2004, **68**, 2725-44.

Almeida C.M., M.T.S.D. Vasconcelos, ICP-MS determination of strontium isotope ratio in wine in order to be used as a fingerprint of its regional origin, *J. Anal. At. Spectrom.*, 2001, **16**, 607-11.

Andrén H., Rodushkin I., Stenberg A., Malinovsky D., Baxter D.C., Sources of mass bias and isotope ratio variation in multi collector ICP-MS: optimization of instrumental parameters based on experimental observations, *J. Anal. At. Spectrom.*, 2004, **19**, 1217-24.

Archer C., Vance D, Mass discrimination in multiple-collector plasma source mass spectrometry: an example using Cu and Zn isotopes, *J. Anal. At. Spectrom.*, 2004, **19**, 656-66.

Arriens P.A., Compston W., A method for isotopic ratio measurement by voltage peak switching, and its application with digital output, *Int. J. Mass Spectrom.*, 1968, **1**, 471-81.

Åberg G., Fosse G., Stray H., Man, nutrition and mobility: A comparison of teeth and bone from the Medieval era and the present from Pb and Sr isotopes, *Sci. Total Environ.*, 1998, **224**, 109-19.

Balcaen L., De Schrijver I., Moens L., Vanhaecke F., Determination of the [87]Sr/[86]Sr isotope ratio in USGS silicate reference materials by multi-collector ICP-mass spectrometry, *Int. J. Mass Spectrom.*, 2005, **242**, 251-5.

Barker S.L.L., Cox S.F., Eggins S.M., Gagan M.K., Microchemical evidence for episodic growth of antitaxial veins during fracture-controlled fluid flow, *Earth Planet. Sci. Lett.*, 2006, **250**, 331-44.

Belshaw N.S., Freedman P.A., O'Nions R.K., Frank M., Guo Y., A new variable dispersion double-focusing plasma mass spectrometer with performance illustrated for Pb isotopes, *Int. J. Mass Spectrom.*, 1998, **181**, 51-8.

Benson L.V., Taylor H.E., Peterson K.A., Shattuck B.D., Ramotnik C.A., Stein J.R., Development and evaluation of geochemical methods for the sourcing of archaeological maize, *J. Archaeol. Sci.*, Article in press (doi: 10.1016/j.jas.2007.06.018).

Bentaleb I., Langlois C., Martin C., Iacumin P., Carré M., Antoine P.O., Duranthon F., Moussa I., Jaeger J.J., Barrett N., Kandorp R., Rhinocerotid tooth enamel ^{18}O/^{16}O variability between 23 and 12 Ma in southwestern France, *C. R. Geosci.*, 2006, **338**, 172-9.

Bentley R.A., Strontium isotopes from the earth to the archaeological skeleton: A review, *J. Archaeol. Method. Th.*, 2006, **13**, 135-87.

Berkovitz B.K.B., Boyde A., Frank R.M., Höhling H.J., Moxham B.J., Nalbandian J., Tonge C.H., *Teeth*, 1st edition, Springer: Berlin, Heidelberg, New York 1989.

Bizzarro M., Simonetti A., Stevenson R.K., Kurszlaukis S., In situ [87]Sr/[86]Sr investigation of igneous apatites and carbonates using laser-ablation MC-ICP-MS, *Geochim. Cosmochim. Acta*, 2003, **67**, 289-302.

Borisov O.V., Mao X., Russo R.E., Effects of crater development on fractionation and signal intensity during laser ablation inductively coupled plasma mass spectrometry, *Spectrochim. Acta Part B*, 2000, **55**, 1693-1704.

Boulyga S.F., Heumann K.G., Direct determination of halogens in powdered geological and environmental samples using isotope dilution laser ablation ICP-MS, *Int. J. Mass Spectrom.*, 2005, **242**, 291-6.

Brenot A., Baran N., Petelet-Giraud E., Négrel P., Interaction between different water bodies in a small catchment in the Paris basin (Brévilles, France): Tracing of multiple Sr sources through Sr isotopes coupled with Mg/Sr and Ca/Sr ratios, *Appl. Geochem.*, 2008, **23**, 58-75.

Budd P., Montgomery J., Barreiro B., Thomas R.G., Differential diagenesis of strontium in archaeological human dental tissues, *Appl. Geochem.*, 2000, **15**, 687-94.

Budd P., Montgomery J., Evans J., Trickett M., Human lead exposure in England from approximately 5500 BP to the 16th century AD, *Sci. Total Environ.*, 2004, **318**, 45-58.

Burton G.R., Rosman K.J.R., Van den Velde K.P., Boutron C.F., A two century record of strontium isotopes from an ice core drilled at Mt Blanc, France, *Earth Planet. Sci. Lett.*, 2006, **248**, 217-26.

Camargo M.A., Marques M.M., de Cara A.A., Morphological analysis of human and bovine dentine by scanning electron microscope investigation, *Arch. Oral Biol.*, 2008, **53**, 105-8.

Capo R.C., Stewart B.W., Chadwick O.A., Strontium isotopes as tracers of ecosystem processes: theory and methods, *Geoderma*, 1998, **82**, 197-225.

Cavazzini G., A method for determining isotopic composition of elements by thermal ionization source mass spectrometry – Application to Sr, *Int. J. Mass Spectrom.*, 2005, **240**, 17-26.

Charlier B.L.A., Ginibre C., Morgan D., Nowell G.M., Pearson D.G., Davidson J.P., Ottley C.J., Methods for the microsampling and high-precision analysis of strontium and rubidium isotopes at single crystal scale for petrological and geochronological applications, *Chem. Geol.*, 2006, **232**, 114-33.

Chavagnac V., Lair M., Milton J.A., Lloyd A., Croudace I.W., Palmer M.R., Green D.R.H., Cherkashev G.A., Tracing dust input to the Mid-Atlantic Ridge between 14°45'N and 36°14'N: Geochemical and Sr isotope study, *Mar. Geol.*, 2008, **247**, 208-25.

Chen J., Li G., Yang J., Rao W., Lu H., Balsam W., Sun Y., Ji J., Nd and Sr isotopic characteristics of Chinese deserts: Implications for the provenances of Asian dust *Geochim. Cosmochim. Acta*, 2007, **71**, 3094-14.

Choi S.H., Mukasa S.B., Zhou X.H., Xian X.H., Andronikov A.V., Mantle dynamics beneath East Asia constrained by Sr, Nd, Pb and Hf isotopic systematics of ultramafic xenoliths and their host basalts from Hannuoba, North China, *Chem. Geol.*, 2008, **248**, 40-61.

Clough R., Evans P., Catterick T., Evans E.H., $\delta^{34}S$ Measurements of sulphur by multicollector inductively coupled plasma mass spectrometry, *Anal. Chem.,* 2006, **78**, 6126-32.

De Bievre P., Taylor P.D.P., Table of the isotopic composition of the elements, *Int. J. Mass. Spectrom. Ion. Phys.*, 1993, **123**, 149-66.

Douthitt C.B., The evolution and applications of multicollector ICPMS (MC-ICPMS), *Anal. Bioanal. Chem.*, 2008, **390**, 437-40.

Eis C., Watkins M., Prohaska T., Nidetzky B., Fungal trehalose phosphorylase: kinetic mechanism, pH-dependence of the reaction and some structural properties of the enzyme from *Schizophyllum commune*, *Biochem. J.*, 2001, **356**, 757-67.

Evans J., Chenery C.A., Fitzpatrick A.P., Bronze age childhood migration of individuals near Stonehenge, revealed by strontium and oxygen isotope tooth enamel analysis, *Archaeometry*, 2006, **48**, 309-21.

Fantle M.S., DePaolo D.J., Sr isotopes and pore fluid chemistry in carbonate sediment of the Ontong Java Plateau: Calcite recrystallization rates and evidence for a rapid rise in seawater Mg over the last 10 million years, *Geochim. Cosmochim. Acta*, 2006, **70**, 3883-904.

Faure G., Mensing T., in: *Isotopes: Principles and Applications*, 3rd ed., Wiley: Hoboken, NJ, USA, 2005.

Fliegel D., Günther D., Low pressure laser ablation coupled to inductively coupled plasma mass spectrometry, *Spectrochim. Acta Part B*, 2006, **61**, 841-9.

Font L., Nowell G.M., Pearson D.G., Ottley C.J., Willis S.G., Sr isotope analysis of bird feathers by TIMS: a tool to trace bird migration paths and breeding sites, *J. Anal. At. Spectrom.*, 2007, **22**, 513-22.

Fortunato G., Mumic K., Wunderli S., Pillonel L., Bosset J.O., Gremaud G., Application of strontium isotope abundance ratios measured by MC-ICP-MS for food authentication, *J. Anal. At. Spectrom.*, 2004, **19**, 227-34.

Gale N.H., A new method for extracting and purifying lead from difficult matrices for isotopic analysis, *Anal. Chim. Acta*, 1996, **332**, 15-21.

Galler P., Limbeck A., Boulyga S.F., Stingeder G., Hirata T., Prohaska T., Development of an on-line flow injection Sr/matrix separation method for accurate, high-throughput determination of Sr isotope ratios by multiple collector-inductively coupled plasma-mass spectrometry, *Anal. Chem.*, 2007, **79**, 5023-9.

García-Ruiz S., Moldovan M., García Alonso J.I., Large volume injection in ion chromatography separation of rubidium and strontium for on-line inductively coupled plasma mass spectrometry determination of strontium isotope ratios, *J. Chromatogr. A.*, 2007, **1149**, 275-281.

García-Ruiz S., Moldovan M., García Alonso J.I., Measurement of strontium isotope ratios by MC-ICP-MS after on-line Rb-Sr ion chromatography separation, *J. Anal. At. Spectrom.*, 2008, **23**, 84-93.

Grousset F.E., Biscaye P.E., Tracing dust sources and transport patterns using Sr, Nd and Pb isotopes, *Chem. Geol.*, 2005, **222**, 149-67.

Grupe G., Price T.D., Schröter P., Söllner F., Johnson C.M., Beard B.L., Mobility of Bell Beaker people revealed by strontium isotope ratios of tooth and bone: a study of southern Bavaria skeletal remains, *Appl. Geochem.*, 1997, **12**, 517-25.

Guillong M., Günther D., Effect of particle size distribution on ICP-induced elemental fractionation in laser ablation-inductively coupled plasma-mass spectrometry, *J. Anal. At. Spectrom.*, 2002, **17**, 831-7.

Guillong M., Kuhn H.R., Günther D., Application of a particle separation device to reduce inductively coupled plasma-enhanced elemental fractionation in laser ablation-inductively coupled plasma-mass spectrometry, *Spectrochim. Acta Part B*, 2003, **58**, 211-20.

Hackett P.A., M.R. Humphries, Mitchell S.A., Rayner D.M., The first ionization potential of zirconium atoms determined by two laser, field-ionization spectroscopy of high lying Rydberg series, *J. Chem. Phys.*, 1986, **85**, 3194-7.

Hattendorf B., Latkoczy C., Günther D., Laser ablation-ICPMS, *Anal. Chem. A pages*, 2003, **75**, 341A-7A.

He L.H., Fujisawa N., Swain M.V., Elastic modulus and stress-strain response of human enamel by nano-indentation, *Biomaterials*, 2006, **27**, 4388-98.

Heumann K.G., Gallus S.M., Rädlinger G., Vogl J., Precision and accuracy in isotope ratio measurements by plasma source mass spectrometry, *J. Anal. At. Spectrom.*, 1998, **13**, 1001-8.

Hirano H., Nishimura T., Iwamura T., High-flow-rate hydroxylapatites, *Anal. Biochem.*, 1985, **150**, 228-34.

Hirata T., Lead isotopic analyses of NIST standard reference materials using multiple collector inductively coupled plasma mass spectrometry coupled with a modified external correction method for mass discrimination effect, *Analyst*, 1996, **121**, 1407-11.

Hirata T., Chemically assisted laser ablation ICP mass spectrometry, *Anal. Chem.*, 2003, **75**, 228-33.

Hirata T., Development of an on-line low gas pressure cell for laser ablation-ICP-mass spectrometry, *Anal. Sci.*, 2007, **23**, 1195-1201.

Hirata T., Hayano Y., Ohno T., Improvements in precision of isotopic ratio measurements using laser ablation-multiple collector-ICP-mass spectrometry: Reduction of changes in measured isotopic ratio, *J. Anal. At. Spectrom.*, 2003, **18**, 1283-8.

Hirata T., Miyazaki Z., High-speed camera imaging for laser ablation process: For further reliable analysis using inductively couple plasma mass spectrometry, *Anal. Chem.*, 2007, **79**, 147-52.

Hoffmann D.L., Richards D.A., Elliott T.R., Smart P.L., Coath C.D., Hawkesworth C.J., Characterisation of secondary electron multiplier nonlinearity using MC-ICPMS, *Int. J. Mass Spectrom.*, 2005, **244**, 97-108.

Holden N.E., Total half-lives for selected nuclides, *Pure Appl. Chem.*, 1990, **62**, 941-58.

Horn I., Blanckenburg F., Investigation on elemental and isotopic fractionation during 196 nm femtosecond laser ablation multiple collector inductively coupled plasma mass spectrometry, Spectrochim. Acta Part B, 2007, **62**, 410-22.

Horn I., Guillong M., Günther D., Wavelength dependant ablation rates for metals and silicate glasses using homogenized laser beam profiles – implications for LA-ICP-MS, *Appl. Surf. Sci.*, 2001, **182**, 91-102.

Horn I., Günther D., The influence of ablation carrier gasses Ar, He and Ne on the particle size distribution and transport efficiencies of laser ablation-induced aerosols, *Appl. Surf. Sci.*, 2003, **207**, 144-57.

Horwitz E.P., Chiariza R., Dietz M.L., A novel strontium-selective extraction chromatographic resin, *Solvent Extr. Ion Exc.*, 1992, **10**, 313-41.

Horwitz E.P., Dietz M.L., Fisher D.E., Separation and preconcentration of strontium from biological, environmental, and nuclear waste samples by extraction chromatography using a crown ether, *Anal. Chem.*, 1991, **63**, 522-5.

Hosono T., Nakano T., Igeta A., Tayasu I., Tanaka T., Yachi S., Impact of fertilizer on a small watershed of Lake Biwa: Use of sulphur and strontium isotopes in environmental diagnosis, *Sci. Total Environ.*, 2007, **384**, 342-54.

Ingle C.P., Sharp B.L., Horstwood M.S.A., Parrish R.R., Lewis D.J., Instrument response functions, mass bias and matrix effects in isotope ratio measurements and semi-quantitative analysis by single and multi-collector ICP-MS, *J. Anal. At. Spectrom.*, 2003, **18**, 219-29.

Irisawa K., Hirata T., Tungsten isotopic analysis on six geochemical reference materials using multiple collector-ICP-mass spectrometry coupled with a rhenium-external correction technique. *J. Anal. At. Spectrom.*, 2006, **21**, 1387-95.

Ishikawa H., Ohba T., Fujimaki H., Sr isotope diversity of hot spring and volcanic lake waters from Zao volcano, Japan, *J. Volcanol. Geoth. Res.*, 2007, **166**, 7-16.

Jackson S., Günther D., The nature and sources of laser induced isotopic fractionation in laser ablation-multicollector-inductively coupled plasma-mass spectrometry, *J. Anal. At. Spectrom.*, 2003, **18**, 205-12.

Jarvis K.E., Gray A.L., Houk R.S., *Handbook of Inductively Coupled Plasma Mass Spectrometry*, 1st edition, Blackie: Glasgow and London, Great Britain, 1993.

Jeong G.Y., Cheong C.S., Kim J., Rb-Sr and K-Ar systems of biotite in surface environments regulated by weathering processes with implications for isotopic dating and hydrological cycles of Sr isotopes, *Geochim. Cosmochim. Acta*, 2006, **70**, 4734-49.

Jørgensen N.O., Andersen M.S., Engesgaard P., Investigation of a dynamic seawater intrusion event using strontium isotopes (^{87}Sr/^{86}Sr), *J. Hydrol.*, 2008, **348**. 257-69.

Klingbeil P., Vogl J., Pritzkow W., Riebe G., Müller J., Comparative studies on the certification of reference materials by ICPMS and TIMS using isotope dilution procedures, *Anal. Chem.*, 2001, **73**, 1881-8.

Knudson K.J., Tung T.A., Nystrom K.C., Price T.D., Fullagar P.D., The origin of the Juch'uypampa Cave mummies: strontium isotope analysis of archaeological human remains from Bolivia, *J. Archaeol. Sci.*, 2005, **32**, 903-13.

Kohn M.J., Schoeninger M.J., Barker W.W., Altered states: Effects of diagenesis on fossil tooth chemistry, *Geochim. Cosmochim. Acta*, 1999, **63**, 2737-47.

Komiya T., Suga A., Ohno T., Han J., Guo J., Yamamoto S., Hirata T., Li Y., Ca isotopic compositions of dolomite, phosphorite and the oldest animal embryo fossils from the Neoproterozoic in Weng'an, South China, *Gondwana Res.*, Article in press (doi: 10.1016/j.gr.2007.10.004).

Korte C., Jasper T., Kozur H.W., Veizer J., ^{87}Sr/^{86}Sr record of Permian seawater, *Palaeogeogr. Palaeocl.*, 2006, **240**, 89-107.

Košler J., Fonneland H., Sylvester P., Tubrett M., Pederson R.B., U-Pb dating of detrital zircons for sediment provenance studies – a comparison of laser ablation ICPMS and SIMS techniques, *Chem. Geol.*, 2002, **182**, 605-18.

Košler J., Pedersen R., Kruber C., Sylvester P., Analysis of Fe isotopes in sulfides and iron meteorites by laser ablation high-mass resolution multi-collector ICP mass spectrometry, *J. Anal. At. Spectrom.*, 2005, **20**, 192-9.

Krupp E.M., Donard O.F.X., Isotope ratios on transient signals with GC-MC-ICP-MS, *Int. J. Mass Spectrom.*, 2005, **242**, 233-42.

Kuhn H.R., Günther D., Elemental fractionation studies in laser ablation inductively coupled plasma mass spectrometry on laser-induced brass aerosols, *Anal. Chem.*, 2003, **75**, 747-53.

Latkoczy C., Prohaska T., Watkins M., Teschler-Nicola M., Stingeder G., Strontium isotope ratio determination in soil and bone samples after on-line matrix separation by coupling ion chromatography (HPIC) to an inductively coupled plasma sector field mass spectrometer (ICP—SFMS), *J. Anal. At. Spectrom.*, 2001, **16**, 806-11.

Lee-Thorp J., Sponheimer M., Three case studies used to reassess the reliability of fossil bone and enamel isotope signals for paleodietary studies, *J. Anthropol. Archaeol.*, 2003, **22**, 208-16.

Leya I., Schönbächler M., Wiechert U., Krähenbühl U., Halliday A.N., High precision titanium isotope measurements on geological samples by high resolution MC-ICPMS, *Int. J. Mass Spectrom.*, 2007, **262**, 247-55.

Liu C., Mao X., Mao S.S., Greif R., Russo R.E., Particle size dependent chemistry from laser ablation of brass, *Anal. Chem.*, 2005, **77**, 6687-91.

Losee F.L., Cutress T.W., Brown R., Natural elements of the periodic table in human dental material, *Caries Res.*, 1974, **8**, 123-34.

Makishima A., Nakamura E., Calibration of faraday cup efficiency in a multicollector mass spectrometer, *Chem. Geol.*, 1991, **94**, 105-10.

Mao X.L., Borisov O.V., Russo R.E., Enhancements in laser ablation inductively coupled plasma-atomic emission spectrometry based on laser properties and ambient environment, *Spectrochim. Acta. Part B*, 1998, **53**, 731-9.

Martin R.B., Burr D.B., Sharkey N.A., *Skeletal Tissue Mechanics*, 1st edition, Springer: New York, 1998.

Mason P.R.D., Košler J., de Hoog J.C.M., Sylvester P.J., Meffan-Main S., In situ determination of sulphur isotopes in sulphur-rich materials by laser ablation multiple-collector inductively coupled plasma mass spectrometry, *J. Anal. At. Spectrom.*, 2006, **21**, 177-86.

Meija J., Mester Z., Signal correlation in isotope ratio measurements with mass spectrometry: Effects on uncertainty propagation, *Spectrochim. Acta Part B*, 2007, **62**, 1278-84.

Melgunov M.S., Bobrov V.A., Zolotarev K.V., The determination of Rb, Sr, Y, Zr and Nb in reference samples using SRXFA, *Nucl. Instrum. Methods Phys. Res., Sect. A,* 1995, **359**, 331-3.

Milton D., Halliday I., Sellin M., Marsh R., Staunton-Smith J., Woodhead J., The effect of habitat and environmental history on otolith chemistry of barramundi Lates calcarifer in estuarine populations of a regulated tropical river, *Estuar. Coast. Shelf Sci.*, Article in press (doi: 10.1016/j.ecss.2007.12.009).

Moens L.J., Vanhaecke F.F., Bandura D.R., Baranov V.I., Tanner S.D., Elimination of isobaric interferences in ICP-MS, using ion-molecule reaction chemistry: Rb/Sr age determination of magmatic rocks, a case study, *J. Anal. At. Spectrom.*, 2001, **16**, 991-4.

Montgomery J., Evans J.A., Wildmann G., ^{87}Sr/^{86}Sr isotope composition of bottled British mineral waters for environmental and forensic purposes, *Appl. Geochem.*, 2006, **21**, 1626-34.

Müller W., Strengthening the link between geochronology, textures and petrology, *Earth Planet. Sci. Lett.*, 2003, **206**, 237-51.

Müller W., Fricke H., Halliday A.N., McCulloch M.T., Wartho J.A., Origin and migration of the alpine iceman, *Science (within supporting online material)*, 302, 2003, 862-6.

Nakano T., Tayasu I., Yamada Y., Hosono T., Igeta A., Hyodo F., Ando A., Saitoh Y., Tanaka T., Wada E., Yachi S., Effect of agriculture on water quality of Lake Biwa tributaries, Japan, *Sci. Total Environ.*, 2008, **389**, 132-48.

Nakata K., Umehara M., Tsumura T., Excimer laser ablation of sintered hydroxyapatite, *Surf. Coat. Tech.*, 2007, **201**, 4943-7.

Nebel O., Mezger K., Reassessment of the NBS SRM-607 K-feldspar as a high precision Rb/Sr and Sr isotope reference, *Chem. Geol.*, 2006, **233**, 337-45.

Nebel. O., Mezger K., Scherer E.E., Münker C., High precision determinations of $^{87}Rb/^{85}Rb$ in geologic materials by MC-ICP-MS, *Int. J. Mass Spectrom.*, 2005, **246**, 10-8.

Négrel P., Petelet-Giraud E., Strontium isotopes as tracers of groundwater-induced floods: the Somme case study (France), *J. Hydrol.*, 2005, **305**, 99-119.

Newesely H., *Chemical stability of Hydroxyapatite under different conditions* in *Trace elements in environmental history*, ed. Grupe G. and Herrmann B., Springer Verlag, Berlin, 1988, 1-16.

Nielsen S.P., The biological role of Strontium, *Bone*, 2004, **35**, 583-8.

Niu H., Houk R.S., Fundamental aspects of ion extraction in inductively coupled plasma mass spectrometry, *Spectrochim. Acta Part B*, 1996, **51**, 779-815.

Norman M., McCulloch M., O'Neill H., Yaxley G., Magnesium isotopic analysis of olivine by laser-ablation multi-collector ICP-MS: composition dependent matrix effect and a comparison of the earth and moon, *J. Anal. At. Spectrom.*, 2006, **21**, 50-4.

Ntaflos T., Richter W., Geochemical constraints on the origin of the Continental Flood Basalt magmatism in Franz Josef Land, Arctic Russia, *Eur. J. Mineral.*, 2003, **15**, 649-63.

Ohno T., Komiya T., Ueno Y., Hirata T., Maruyama S., Determination of $^{88}Sr/^{86}Sr$ mass-dependent fractionation and radiogenic isotope variation of $^{87}Sr/^{86}Sr$ in the Neoproterozoic Doushantuo Formation, *Gondwana Res.*, Article in press (doi: 10.1016/j.gr.2007.10.007).

Petelet-Giraud E., Negrel P., Geochemical flood deconvolution in a Mediterranean catchment (Hérault, France) by Sr isotopes, major and trace elements, *J. Hydrol.*, 2007, **337**, 224-41.

Pinson W.H., Herzog L.F., Faierairn H.W., Cormier R.F., Sr/Rb age studies of tektites, *Geochim. Cosmochim. Acta*, 1958, **14**, 331-9.

Ponzevera E., Quétel C.R, Berglund M., Taylor P.D.P, Evans P., Loss R.D., Fortunato G., Mass discrimination during MC-ICPMS isotopic ratio measurements: investigation by means of synthetic isotopic mixtures (IRMM-007 series) and application to the calibration of natural-like zinc materials (including IRMM-3702 and IRMM-651), *J. Am. Soc. Mass Spectrom.*, 2006, **17**, 1412-27.

Potter D., A commercial perspective on the growth and development of the quadrupole ICP-MS market, *J. Anal. At. Spectrom.*, 2008, article in press (doi: 10.1039/b717322a).

Price T.D., Manzanilla L., Middleton W.D., Immigration and the ancient city of Teotihuacan in Mexico: A study using Strontium isotope ratios in human bone and teeth, *J. Archaeol. Sci*, 2000, **27**, 903-13.

Prohaska T., Latkoczy C., Schultheis G., Teschler-Nicola M., Stingeder G., Investigation of Sr isotope ratios in prehistoric human bones and teeth using laser ablation ICP-MS and ICP-MS after Rb/Sr separation, *J. Anal. At. Spectrom.*, 2002, **17**, 887-91.

Prohaska T., Teschler-Nicola M., Galler P., Přichystal A., Stingeder G., Jelenc M., Klötzli U., *Non-destructive determination of $^{87}Sr/^{86}Sr$ isotope ratios in early Upper Palaeolithic human teeth from the Mladeč Caves – preliminary results* in *Early Modern Humans at the Moravian Gate*, ed. Teschler-Nicola M., Springer-Verlag, Vienna, 2006, 505-14.

Prohaska T., Stadlbauer C., Wimmer R., Stingeder G., Latkoczy C., Hoffmann E., Stephanowitz H., Investigation of element variability in tree rings of young Norway spruce by laser ablation-ICP-MS, *Sci. Total Environ.*, 1998, **219**, 29-39.

Prohaska T., Wenzel W.W., Stingeder G., ICP-MS-based tracing of metal sources and mobility in a soil depth profile via the isotopic variation of Sr and Pb, *Int. J. Mass Spectrom.*, 2005, **242**, 243-50.

Ramos F.C., Wolff J.A., Tollstrup D.L., Measuring $^{87}Sr/^{86}Sr$ variations in minerals and groundmass from basalts using LA-MC-ICPMS, *Chem. Geol.*, 2004, **211**, 135-58.

Rauch E., Rumel S., Lehn C., Büttner A., Origin assignment of unidentified corpses by use of stable isotope ratios of light (bio-) and heavy (geo-) elements – A case report, *Forensic Sci. Int.*, 2007, **168**, 215-8.

Reimann C., Arnoldussen A., Boyd R., Finne T.E., Koller F., Nordgulen Ø., Englmaier P., Element contents in leaves of four plant species (birch, mountain ash, fern ad spruce) along anthropogenic and geogenic concentration gradients, *Sci. Total Environ.*, 2007, **377**, 416-33.

Revel-Rolland M., De Deckker P., Delmonte B., Hesse P.P., Magee J.W., Basile-Dolesch I., Grousset F., Bosch D., Eastern Australia: A possible source of dust in East Antarctica interglacial ice, *Earth Planet. Sci. Lett.*, 2006, **249**, 1-13.

Richter S., Goldberg S.A., Mason P.B., Traina A.J., Schwieters J.B., Linearity tests for secondary electron multipliers used in isotope ratio mass spectrometry, *Int. J. Mass Spectrom.*, 2001, **206**, 105-27.

Rodushkin I., Bergman T., Douglas G., Engström E., Sörlin D., Baxter D.C., Authentication of Kalix (N.E. Sweden) vendace caviar using inductively coupled plasma-based analytical techniques: Evaluation of different approaches, *Anal. Chim. Acta*, 2007, **583**, 310-8.

Rowland A., Housh T.B., Holcombe J.A., Use of electrothermal vaporisation for volatility-based separation of Rb-Sr isobars for determination of isotopic ratios by ICP-MS, *J. Anal. At. Spectrom.*, 2008, **23**, 167-72.

Rubbmark J.R., Borgström S.A., Rydberg series in strontium found in absorption by selectively laser-excited atoms, *Phys. Scripta*, 1978, **18**, 196-208.

Russell W.A., Papanastassiou D.A., Tombrello T.A., Ca isotope fractionation on the Earth and other solar system materials, *Geochim. Cosmochim. Acta*, 1970, **42**, 1075-90.

Russo R.E., Mao X.L., Liu C., Gonzalez J., Laser assisted plasma spectrochemistry: laser ablation, *J. Anal. At. Spectrom.*, 2004, **19**, 1084-9.

Saetveit N.J., Bajic S.J., Baldwin D.P., Houk R.S., Influence of particle size on fractionation with nanosecond and femtosecond laser ablation in brass by online differential mobility

analysis and inductively coupled plasma mass spectrometry, *J. Anal. At. Spectrom.*, 2008, **23**, 54-61.

Schmitz B., Ingram S.L., Dockery T.D., Åberg G., Testing $^{87}Sr/^{86}Sr$ as a palaeosalinity indicator on mixed marine, brackish-water and terrestrial vertebrate skeletal apatite in late Paleocene-early Eocene near-costal sediments, Mississippi, *Chem. Geol.*, 1997, **140**, 275-87.

Schultheis G., Prohaska T., Stingeder G., Dietrich K., Jembrih-Simbürger D., Schreiner M., Characterisation of ancient and art nouveau glass samples by Pb isotopic analysis using laser ablation coupled to a magnetic sector filed inductively coupled plasma mass spectrometer (LA-ICP-SF-MS), *J. Anal. At. Spectrom.*, 2004, **19**, 838-43.

Schumacher G.H., Schmidt H., *Anatomie und Biochemie der Zähne*, 1st edition, Gustav Fischer Verlag: Stuttgart, 1983.

Sealy J.C., Armstrong R., Schrire C., Beyond lifetime averages: Tracing life histories through isotopic analysis of different calcified tissues from archaeological human skeletons. *Antiquity*, 1995, **69**, 290-300.

Serapinas P., Venskutonis P.R., Aninkevičius V., Ežerinskis Ž., Galdikas A., Juzikienė V., Step by step approach to multi-element data analysis in testing the provenance of wines, *Food Chem.*, 2008, **107**, 1652-60.

Simon J.I., Reid M.R., Yound E.D., Lead isotopes by LA-MC-ICPMS: Tracking the emergence of mantle signatures in an evolving silicic magma system, *Geochim. Cosmochim. Acta*, 2007, **71**, 2014-35.

Simonetti A., Buzon M.R., Creaser R.A., In-situ elemental and Sr isotope investigations of human tooth enamel by laser ablation-(MC)-ICP-MS: successes and pitfalls, *Archaeometry*, Article in press (doi: 10.1111/j.1475-4754.2007.00351.x).

Smith T.M., Incremental dental development: Methods and applications in hominoid evolutionary studies, *J. Hum. Evol.*, 2007, Article in press (doi: 10.1016/j.hevol.2007.09.020).

Smith D.R., Woolard D., Luck M.L., Laughlin N.K., Succimer and the reduction of tissue lead in juvenile monkeys, *Toxicol. Appl. Pharmacol.*, 2000, **166**, 230-40.

Steiger R.H., Jäger E., Subcomission on geochronology: Convention on the use of decay constants in geo- and cosmochronology, *Earth Planet. Sci. Lett.*, 1977, **36**, 359-62.

Stein M., Starinsky A., Katz ., Goldstein S.L., Machlus M., Schramm A., Strontium isotopic, chemical, and sedimentological evidence for the evolution of Lake Lisan and the Dead Sea, *Geochim. Cosmochim. Acta*, 1997, **61**, 3975-92.

Stewart B.W., Capo R.C., Chadwick O.A., Effects of rainfall on weathering rate, base action provenance, and Sr isotope composition of Hawaiian soils, *Geochim. Cosmochim. Acta*, 2001, **65**, 1087-99.

Swoboda S., Brunner M., Boulyga S.F., Galler P., Horacek M., Prohaska T., Identification of Marchfeld asparagus using Sr isotope ratio measurements by MC-ICP-MS, *Anal. Bioanal. Chem.*, 2007, **390**, 487-94.

Tanaka K., Takahashi Y., Shimizu H., Determination of rare earth element in carbonate using laser-ablation inductively-coupled plasma mass spectrometry: An examination of the

influence of the matrix on laser-ablation inductively-coupled plasma mass spectrometry analysis, *Anal. Chim. Acta.*, 2007, **583**, 303-9.

Tandon L., Iyengar G.V., Parr R.M., A review of radiologically important trace elements in human bones, *Appl. Radiat. Isotopes*, 1998, **49**, 903-10.

Thirlwall M.F., Long-term reproducibility of multicollector Sr and Nd isotope ratio analysis, *Chem. Geol. Isotope Geoscience section*, 1991, **94**, 85-104.

Tunheng A., Hirata T., Development of signal smoothing device for precise elemental analysis using laser ablation-ICP-mass spectrometry, *J. Anal. At. Spectrom.*, 2004, **19**, 932-4.

Van Geldern R., Joachimski M.M., Day J., Jansen U., Alvarez F., Yolkin E.A., Ma X.P., Carbon, oxygen and strontium isotope records of Devonian brachiopod shell calcite, *Palaeogeogr. Palaeocl.*, 2006, **240**, 47-67.

Vonderheide A.P., Zoriy M.V., Izmer A.V., Pickhardt C., Caruso J.A., Ostapczuk P., Hille R., Becker J.S., Determination of ^{90}Sr at ultratrace levels in urine by ICP-MS, *J. Anal. At. Spectrom.*, 2004, **19**, 675-80.

Vroon P.Z., van der Wagt B., Koorneef J.M., Davies G.R., Problems in obtaining precise and accurate Sr isotope analysis from geologic materials using laser ablation MC-ICPMS, *Anal. Bioanal. Chem.*, 2008, **390**, 465-76.

Waight T., Baker J., Peate D., Sr isotope measurements by double-focusing MC-ICPMS: Techniques, observations, pitfalls, *Int. J. Mass Spectrom.*, 2002a, **221**, 229-44.

Waight T., Baker J., Willigers B., Rb isotope dilution analyses by MC-ICPMS using Zr to correct for mass fractionation: Towards improved Rb-Sr geochronology?, *Chem. Geol.*, 2002b, **186**, 99-116.

Walczyk T., von Blanckenburg F., Natural iron isotope variations in human blood, *Science*, 2002, **295**, 2065-5.

Walder A.J., Freedman P.A., Communication. Isotopic ratio measurement using a double focusing magnetic sector mass analyser with an inductively coupled plasma as ion source, *J. Anal. At. Spectrom.*, 1992, **7**, 571-5.

Wang J., Hansen E.H., On-line sample-pre-treatment schemes for trace-level determinations of metals by coupling flow injection or sequential injection with ICP-MS, *Trends Anal. Chem.*, 2003, **22**, 836-46.

Wang Z.L., Zhang J., Liu C.Q., Strontium isotopic compositions of dissolved and suspended loads from the main channel of the Yangtze River, *Chemosphere*, 2007, **69**, 1081-8.

Weber P.K., Bacon C.R., Hutcheon I.D., Ingram B.L., Wooden J.L., Ion microprobe measurement of strontium isotopes in calcium carbonate with application to salmon otoliths, *Geochim. Cosmochim Acta*, 2005, **69**, 1225-39.

Weiss D., Boyle E.A., Chavagnac V., Herwegh M., Wu J., Determination of lead isotope ratios in seawater by quadrupole inductively coupled plasma mass spectrometry after $Mg(OH)_2$ co-precipitation, *Spectrochim. Acta Part B*, 2000, **55**, 363-74.

Weiss D.J., Kober B., Dolgopolova A., Gallagher K., Spiro B., Le Roux G., Mason T.F.D., Kylander M., Coles B.J., Accurate and precise Pb isotope ratio measurements in environmental samples by MC-ICP-MS, *Int. J. Mass Spectrom.*, 2004, **232**, 205-15.

White T.D, Folkens P.A., *The Human Bone Manual*, 1st edition, Elsevier, 2005.

Wild E.M., Teschler-Nicola M., Kutschera W., Steier P., Trinkaus E., Wanek W., Direct dating of Early Upper Palaeolithic human remains from Mladeč, *Nature*, 2005, **435**, 332-5.

Williams C.T., *Alteration of Chemical Composition of Fossil Bones by Soil Processes and Groundwater* in *Trace Elements in Environmental History*, ed. Grupe G. and Herrmann B., Springer Verlag, Berlin, 1988, 27-40.

Woodhead J., Swearer S., Hergt J., Maas R., In—situ Sr-isotope analysis of carbonates by LA-MC-ICP-MS: interference corrections, high spatial resolution and an example from otolith studies, *J. Anal. At. Spectrom.*, 2005, **20**, 22-7.

Wright L.E., Identifying immigrants to Tikal, Guatemala: Defining local variability in strontium isotope ratios of human tooth enamel, *J. Archaeol. Sci*, 2005, **32**, 555-66.

Zaslansky P., Friesem A.A., Weiner S., Structure and mechanical properties of the soft zone separating bulk dentine and enamel in crowns of human teeth: Insight into tooth function, *J. Struct. Biol.*, 2006, **153**, 188-99.

Appendix

Data concerning the comparions of the "Neptun" and "Nu Plasma" MC-ICPMS

Standard solutions and samples used for investigation of instrument performance

Standard/Sample material	Conc. [ppb]
Sr	
NIST SRM 987	1.1
NIST SRM 987	11.4
NIST SRM 987	98.6
NIST SRM 987 + hydroxyl-apatite	$1/3.6*10^3$
NIST SRM 987 + hydroxyl-apatite	$9,9/36.7*10^3$
NIST SRM 987 + hydroxyl-apatite	$97.5/361.2*10^3$
NIST bone meal 1486	1 (Sr)
NIST bone meal 1486	10,2 (Sr)
NIST bone meal 1486	102 (Sr)
Pb	
NIST SRM 981	1.1
NIST SRM 981	11.9
NIST SRM 981	110.3
Fe	
Mix 1 ($^{56}Fe/^{57}Fe\approx1$)	
Mix 1 ($^{56}Fe/^{57}Fe\approx1$)	
Mix 5 ($^{56}Fe/^{57}Fe\approx5$)	
Mix 5 ($^{56}Fe/^{57}Fe\approx5$)	
S	999
Mladeč samples	
Individual 1 (female) enamel/dentine	
Individual 2 (female) enamel/dentine	
Individual 8 (male) enamel/dentine	

Tab. 13 Standard and sample solutions for MC-ICPMS testing

Experimental parameters

Experimental parameters for Sr isotope measurements by solution nebulisation MC-ICPMS

Parameter	Neptun			Nu Plasma		
Cup configuration	^{82}Kr:L4,	^{83}Kr:L3,	^{84}Sr:L2,	^{82}Kr:L5,	^{83}Kr:L4,	^{84}Sr:L3,
	^{85}Rb:L1,	^{86}Sr:C,	^{87}Sr:H1,	^{85}Rb:L2,	^{86}Sr:Ax,	^{87}Sr:H2,
	^{88}Sr:H2,	^{89}SrH:H3		^{88}Sr:H4,	^{89}SrH:H5	
RF Power	1200 W			1300 W		
Cool gas flow	15 L/min			13 L/min		
Auxiliary gas flow	0.6-0.7 L/min			0.75 L/min		
Sample gas flow/back pressure	0.98-1.02 L/min			33.3 psi		

Cones	Ni	Ni
Sample uptake rate	50 µL/min self aspirating	200 µL/min pumped
Integration time per datapoint	4 seconds	4 seconds
Number of datapoints per measurement	50	50

Tab. 14 MC-ICPMS Parameters for Sr isotope measurements by solution nebulisation

Experimental parameters for Sr isotope measurements by LA-MC-ICPMS

Parameter	Neptun			Nu Plasma		
Cup configuration	^{82}Kr:L4, ^{83}Kr:L3, ^{84}Sr:L2, ^{85}Rb:L1, ^{86}Sr:C, ^{87}Sr:H1, ^{88}Sr:H2, ^{89}Sr:H3			^{82}Kr:L5, ^{83}Kr:L4, ^{84}Sr:L3, ^{85}Rb:L2, ^{86}Sr:Ax, ^{87}Sr:H2, ^{88}Sr:H4, ^{89}Sr:H5		
RF Power	1200 W			1300 W		
Cool gas flow	15 L/min			13 L/min		
Auxiliary gas flow	0.7 L/min			0.75 L/min		
Sample gas flow/ mixing gas 2	0.339 L/min			0.5 L/min		
He gas flow ablation cell/ mixing gas 1	0.59 L/min			0.7 L/min		
Cones	Ni			Ni		
Integration time per datapoint	1 second			0.2 seconds		

Tab. 15 MC-ICPMS Parameters for Sr isotope measurements by laser ablation

Experimental parameters for Pb isotope measurements

Parameter	Neptun			Nu Plasma		
Cup configuration	^{201}Hg:L3, ^{202}Hg:L2, ^{203}Tl:L1, ^{204}Pb:C, ^{206}Pb:H1, ^{207}Pb:H2, ^{208}Pb:H3			^{200}Hg:L3, ^{202}Hg:L2, ^{203}Tl:L1, ^{204}Pb:Ax, ^{205}Tl:H1, ^{206}Pb:H2, ^{207}Pb:H3, ^{208}Pb:H4		
RF Power	1200 W			1300 W		
Cool gas flow	15 L/min			13 L/min		
Auxiliary gas flow	0.6-0.7 L/min			0.75 L/min		
Sample gas flow/back pressure	0.98-1.02 L/min			32.5 psi		
Cones	Ni			Ni		
Sample uptake rate	50 µL/min self aspirating			200 µL/min pumped		
Integration time per datapoint	8 seconds			8 seconds		
Number of datapoints per measurement	50			50		

Tab. 16 MC-ICPMS Parameters for Pb isotope measurements

Experimental Parameters for Fe isotope measurements

Parameter	Neptun			Nu Plasma		
Cup configuration	^{53}Cr:L4, ^{54}Fe:L2, ^{56}Fe:L1, ^{57}Fe:H1, ^{58}Fe:H2, ^{60}Ni:H3			^{53}Cr:L5, ^{54}Fe:L3, ^{56}Fe:H4, ^{57}Fe:H6		
RF Power	1200 W			1300 W		
Cool gas flow	15 L/min			13 L/min		
Auxiliary gas flow	0.6-0.7 L/min			0.75 L/min		
Sample gas flow/back pressure	0.98-1.02 L/min			33.3 psi		
Cones	Ni			Ni		
Sample uptake rate	50 µL/min self aspirating			100 µL/min pumped, DSN 100		
Integration time per datapoint	4 seconds			4 seconds		
Number of datapoints per measurement	50			50		

Tab. 17 MC-ICPMS Parameters for Fe isotope measurements

Experimental Parameters for S isotope measurements

Parameter	Neptun	Nu Plasma
Cup configuration	^{32}S:L2, ^{33}S:C, ^{34}S:H2	^{32}S:L4, ^{33}S:Ax, ^{34}S:H5
RF Power	1200 W	1300 W
Cool gas flow	15 L/min	13 L/min
Auxiliary gas flow	0.6-0.7 L/min	0.75 L/min
Sample gas flow/back pressure	0.98-1.02 L/min	33.3 psi
Cones	Ni	Ni
Sample uptake rate	50 µL/min self aspirating	200 µL/min pumped
Integration time per datapoint	8 seconds	8 seconds
Number of datapoints per measurement	50	50

Tab. 18 MC-ICPMS Parameters for S isotope measurements

Results

Sr isotope measurements of NIST SRM 987

	Ratio	Neptun	rsd [%]	Nu Plasma	rsd [%]	certified	rsd [%]
1 ppb	^{88}Sr/^{86}Sr	8.37861	0.51	8.37861	0.32	8.37861	0.04
	^{87}Sr/^{86}Sr	0.71123	0.23	0.70832	0.55	0.71034	0.04
	^{84}Sr/^{86}Sr	0.05697	3.35	0.05611	4.49	0.05655	0.25
10 ppb	^{88}Sr/^{86}Sr	8.37861	0.04	8.37861	0.02	8.37861	0.04
	^{87}Sr/^{86}Sr	0.71058	0.02	0.71052	0.06	0.71034	0.04
	^{84}Sr/^{86}Sr	0.05650	0,.31	0.05651	0.26	0.05655	0.25
100 ppb	^{88}Sr/^{86}Sr	8.37861	0.014	8.37861	0.007	8.37861	0.04
	^{87}Sr/^{86}Sr	0.71050	0.007	0.71050	0.004	0.71034	0.04
	^{84}Sr/^{86}Sr	0.05641	0.025	0.05642	0.025	0.05655	0.25

Tab. 19 Results for NIST SRM 987 (all results normalized to ^{86}Sr/^{88}Sr = 0.1194)

	Neptun				Nu Plasma			
Signal stability [% rsd]	^{88}Sr	^{87}Sr	^{86}Sr	^{84}Sr	^{88}Sr	^{87}Sr	^{86}Sr	^{84}Sr
1 ppb	0.7	1.8	3.0	5.8	1.5	1.8	1. 8	4.7
10 ppb	0.8	0.8	0.8	1.4	1.3	1.3	1.3	1.7
100 ppb	0.6	0.6	0.6	0.6	1.3	1.3	1.3	1.3
Sensitivity [V/ppb]	0.0339	0.0332	0.0325	0.0312	0.0215	0.0211	0.0207	0.0199
rsd [%]	4.4	4.4	4.4	3.8	5.1	5.3	5.2	5.3

Tab. 20 Signal stabilities and sensitivities for Sr measurements

Concentration	Neptun	Nu Plasma
1 ppb	0.96112	0.96320
10 ppb	0.96101	0.96588
100 ppb	0.96121	0.96551
average	0.96111	0.96486
rsd [%]	0.01	0.15

Tab. 20 Mass bias correction factors derived from ^{86}Sr/^{88}Sr

Pb isotope measurements of NIST SRM 981

	Ratio	Neptun	rsd [%]	Nu Plasma	rsd [%]	certified	rsd [%]
1 ppb	$^{208}Pb/^{206}Pb$	2.16810	0.009	2.16810	0.046	2.16810	0.004
	$^{207}Pb/^{206}Pb$	0.91477	0.036	0,91444	0.018	0.91464	0.004
	$^{204}Pb/^{206}Pb$	0.05924	2.56	0.05891	0.30	0.059042	0.006
10 ppb	$^{208}Pb/^{206}Pb$	2.16810	0.004	2.16810	0.012	2.16810	0.004
	$^{207}Pb/^{206}Pb$	0.91503	0.004	0.91500	0.012	0.91464	0.004
	$^{204}Pb/^{206}Pb$	0.05903	0.10	0.05898	0.19	0.059042	0.006
100 ppb	$^{208}Pb/^{206}Pb$	2.16810	0.004	2.16810	0.013	2.16810	0.004
	$^{207}Pb/^{206}Pb$	0.91494	0.002	0.91504	0.004	0.91464	0.004
	$^{204}Pb/^{206}Pb$	0.05900	0.020	0.05898	0.009	0.059042	0.006

Tab. 21 Results for NIST SRM 981 (all results normalize to certified $^{206}Pb/^{208}Pb$ ratio)

	Neptun				Nu Plasma			
Signal stability [%]	^{208}Pb	^{207}Pb	^{206}Pb	^{204}Pb	^{208}Pb	^{207}Pb	^{206}Pb	^{204}Pb
1 ppb	1.3	1.3	1.3	1.2	1.4	1.4	1.5	4.2
10 ppb	1.0	1.0	1.0	1.2	1.1	1.1	1.1	1.1
100 ppb	1.3	1.3	1.3	1.3	1.0	1.0	1.0	1.0
Sensitivity [V/ppb]	0.0556	0.0552	0.0548	0.0541	0.0324	0.0322	0.0321	0.0317
rsd [%]	1.2	1.2	1.2	1.3	5.4	5.4	5.5	5.8

Tab. 22 Signal stabilities and sensitivities for Pb measurements

Concentration	Neptun	Nu Plasma
1 ppb	0.98906	0.99056
10 ppb	0.98573	0.98866
100 ppb	0.98574	0.98846
average	0.98923	0.98684
rsd [%]	0.12	0.19

Tab. 23 Mass bias correction factors derived from $^{206}Pb/^{208}Pb$

Fe isotope measurements

	Ratio	Neptun	rsd [%]	Nu Plasma	rsd [%]	expected	rsd [%]
mix 1/100 ppb	$^{57}Fe/^{56}Fe$	0.983043	0.007	0.979963	0.027	-	-
	$^{54}Fe/^{56}Fe$	0.062209	0.010	0.062234	0.066	-	-
mix 1/1 ppm	$^{57}Fe/^{56}Fe$	0.982176	0.034	0.980579	0.006	-	-
	$^{54}Fe/^{56}Fe$	0.062262	0.006	0.062310	0.012	-	-
mix 5/100 ppb	$^{57}Fe/^{56}Fe$	0.199766	0.013	0.199746	0.140	-	-
	$^{54}Fe/^{56}Fe$	0.063422	0.031	0.063440	0.047	-	-
mix 5/1 ppm	$^{57}Fe/^{56}Fe$	0.199484	0.001	0.198803	0.01	-	-
	$^{54}Fe/^{56}Fe$	0.063443	0.001	0.063465	0.01	-	-
nat. Fe/100 ppb	$^{57}Fe/^{56}Fe$	-	-	0.023135	0.22	0.023094	-
	$^{54}Fe/^{56}Fe$	-	-	0.063703	0.11	0.063703	-
nat. Fe/1 ppm	$^{57}Fe/^{56}Fe$	-	-	0.023068	0.03	0.023094	-

	Ratio	Neptun	rsd	Nu Plasma	rsd	natural	rsd
	^{54}Fe/^{56}Fe	-	-	0.063703	0.008	0.063703	-
IRMM 014 100ppb	^{57}Fe/^{56}Fe	0.023835	0.070	-	-	0.023096	0.31
	^{54}Fe/^{56}Fe	0.063700	0.020	-	-	0.063700	0.42
IRMM 014 1ppm	^{57}Fe/^{56}Fe	0.023821	0.006	-	-	0.023096	0.31
	^{54}Fe/^{56}Fe	0.063700	0.004	-	-	0.063700	0.42

Tab. 24 Results for fe isotope measurements of synthetic mixtures

	Neptun			Nu Plasma		
Signal stability [% rsd]	^{57}Fe	^{56}Fe	^{54}Fe	^{57}Fe	^{56}Fe	^{54}Fe
100 ppb	0.8	0.7	0.7	1.0	1.0	1.0
1 ppm	1.0	1.0	1.0	0.9	0.9	0.9
Sensitivity [mV/ppb]	0.0061	0.0059	0.0055	0.0021	0.0020	0.0019

Tab. 25 Signal stabilities and sensitivities for Fe measurements

S isotope measurements

	Ratio	Neptun	rsd [%]	Nu Plasma	rsd [%]	natural
1 ppm S	^{34}S/^{32}S	0.04871	0.06	0.04508	0.05	0.04519
	^{33}S/^{32}S	0.00863	0.57	0.00799	0.44	0.00801

Tab. 26 Results for S isotope measurements (data not mass bias corrected)

	Neptun			Nu Plasma		
Signal stability [% rsd]	^{34}S	^{33}S	^{32}S	^{34}S	^{33}S	^{32}S
	2.1	2.8	2.1	1.5	1.8	1.5
Sensitivity [V/ppm]	0.2540	0.2532	0.2351	0.2083	0.1994	0.1910

Tab. 27 Signal stabilities and sensitivities for S measurements

Sr Isotope data concerning investigation of archaeological tooth samples

Data for Gars Thunau

Sample #	Enamel		Dentine	
	^{87}Sr/^{86}Sr	SE	^{87}Sr/^{86}Sr	SE
1	0.71473	0.00002	0.71523	0.00001
2	0.71032	0.00002	0.71561	0.00001
7	0.71532	0.00002	0.71750	0.00002
18	0.71383	0.00002	0.71669	0.00002
19	0.71405	0.00002	0.71569	0.00002
20	0.70998	0.00002	0.71551	0.00001
21	0.71831	0.00003	0.71490	0.00004
22	0.71402	0.00001	0.71635	0.00001
23	0.71155	0.00002	0.71542	0.00002
24	0.71185	0.00002	0.71607	0.00002
26	0.71161	0.00002	0.71669	0.00001

29	0.71528	0.00002	0.71427	0.00002
30	0.71773	0.00001	0.71690	0.00002
32	0.71199	0.00001	0.71697	0.00002
43	0.72709	0.00006	0.71664	0.00002
46	0.71151	0.00002	0.71669	0.00003
48	0.71130	0.00002	0.71646	0.00001
51	0.72709	0.00006	0.71658	0.00001
52	0.72214	0.00003	0.71946	0.00002
53	0.71081	0.00002	0.71507	0.00002
54	0.71049	0.00001	0.71470	0.00002
56	0.71081	0.00001	0.71524	0.00002
69	0.71106	0.00002	0.71600	0.00001
70	0.71506	0.00002	0.71606	0.00001
72	0.71286	0.00001	0.71464	0.00001
73	0.78579	0.00017	0.71666	0.00004
75	0.71212	0.00002	0.71613	0.00002
76	0.71230	0.00002	0.71681	0.00002
78	0.71401	0.00002	0.71676	0.00002
79	0.71170	0.00002	0.71657	0.00002
81	0.71463	0.00002	0.71648	0.00002
82	0.71027	0.00002	0.71602	0.00002
88	0.71159	0.00002	0.73117	0.00005
90	0.70931	0.00001	0.71433	0.00002
92	0.71064	0.00001	0.71528	0.00002
96	0.71222	0.00002	0.71657	0.00003
101	0.71138	0.00002	0.71531	0.00002
102	0.71199	0.00002	0.71233	0.00002
114	0.71139	0.00001	0.71175	0.00002
124	0.71139	0.00002	0.71489	0.00001
126	0.71098	0.00001	0.71010	0.00002
128	0.71081	0.00002	0.71419	0.00002
129	0.71337	0.00002	0.71517	0.00002
130	0.71086	0.00002	0.71674	0.00001
132	0.71150	0.00002	0.71605	0.00002
133	0.71061	0.00001	0.71523	0.00001
135	0.71357	0.00002	0.71609	0.00002
136	0.71205	0.00001	0.71544	0.00001
137	0.71057	0.00002	0.71544	0.00001
138	0.70965	0.00002	0.71500	0.00002
139	0.71248	0.00002	0.71625	0.00002
146	0.71155	0.00002	0.71526	0.00003

Tab. 28 ^{87}Sr/^{86}Sr isotope data for Gars Thunau

Measurement uncertainties are quoted as standard error as provided by the "Nu Instruments Calculation Editor".

Data for Hainburg, Mannersdorf and Prellenkirchen

Sample #	Enamel $^{87}Sr/^{86}Sr$	SE	Dentine	$^{87}Sr/^{86}Sr$
1	0.70931	0.00001	0.70963	0.00001
2	0.71135	0.00001	0.71103	0.00001
3	0.71015	0.00001	0.71013	0.00001
4	0.71133	0.00001	0.70950	0.00001
5	0.70943	0.00001	0.70949	0.00001
8	0.70975	0.00001	0.70926	0.00001
10	0.70986	0.00001	0.70995	0.00001
11	0.71190	0.00001	0.71042	0.00003
12	0.70902	0.00005	0.70966	0.00001
13	0.71062	0.00001	0.70951	0.00001
14	0.71015	0.00001	0.70954	0.00001
15	0.71258	0.00001	0.71009	0.00001
16	0.71009	0.00001	0.71044	0.00001
18	0.70940	0.00001	0.70975	0.00001
19	0.70980	0.00001	0.70930	0.00001
20	0.70930	0.00001	0.70981	0.00001
21	0.71038	0.00001	0.70940	0.00001
22	0.70929	0.00001	0.70937	0.00001
23	0.70878	0.00001	0.70951	0.00001
24	0.71120	0.00001	0.71029	0.00001
25	0.70890	0.00001	0.70979	0.00002
26	0.70942	0.00001	0.70949	0.00001
27	0.70984	0.00001	0.71023	0.00001
28	0.70856	0.00001	0.70941	0.00001
29	0.70918	0.00001	0.70945	0.00001
30	0.71086	0.00001	0.70952	0.00001
31	0.70904	0.00001	0.70952	0.00001
32	0.70884	0.00001	0.70956	0.00001
33	0.70970	0.00001	0.70981	0.00001
34	0.70925	0.00001	0.70967	0.00001
35	0.71215	0.00001	0.70990	0.00001
36	0.70986	0.00002	0.70969	0.00001
37	0.71193	0.00001	0.70996	0.00001
38	0.70934	0.00001	0.70968	0.00001
39	0.71186	0.00001	0.71028	0.00001
40	0.70898	0.00001	0.70957	0.00001
41	0.71116	0.00001	0.70963	0.00002
42	0.71149	0.00001	0.71026	0.00001
43	0.71107	0.00001	0.70975	0.00001
44	0.70893	0.00001	0.70966	0.00001
45	0.71048	0.00001	0.71010	0.00001
46	0.70914	0.00001	0.70957	0.00001
47	0.71412	0.00001	0.70993	0.00001
48	0.71373	0.00001	0.71034	0.00001
49	0.70940	0.00001	0.71015	0.00001
50	0.70955	0.00001	0.71032	0.00001
51	0.70935	0.00001	0.70964	0.00001
52	0.70945	0.00001	0.70977	0.00001
53	0.71012	0.00001	0.70991	0.00001

54	0.70916	0.00001	0.70951	0.00001
55	0.70849	0.00001	0.70929	0.00001
56	0.70883	0.00001	0.70945	0.00001
57	0.70912	0.00001	0.70946	0.00001
58	0.70926	0.00001	0.70999	0.00001
59	0.70853	0.00001	0.70922	0.00001
60	0.70923	0.00001	0.70940	0.00001
61	0.70889	0.00001	0.70946	0.00001
62	0.70907	0.00001	0.70964	0.00001
63	0.70889	0.00001	0.70944	0.00001
64	0.71152	0.00001	0.71000	0.00001
65	0.70977	0.00001	0.70952	0.00001
66	0.70907	0.00001	0.70979	0.00001
67	0.70896	0.00001	0.70951	0.00001
68	0.71125	0.00001	0.71019	0.00001
69	0.70894	0.00001	0.70956	0.00001
70	0.70915	0.00001	0.70949	0.00001
71	0.71376	0.00001	0.70972	0.00001
72	0.71129	0.00001	0.71050	0.00001
73	0.70921	0.00001	0.70998	0.00001
74	0.70900	0.00001	0.70941	0.00001
75	0.71012	0.00001	0.70986	0.00001
76	0.71034	0.00001	0.71036	0.00001
77	0.70926	0.00001	0.71013	0.00001
78	0.71061	0.00001	0.71036	0.00001
79	0.70929	0.01530	0.71016	0.00001
80	0.71126	0.00001	0.70971	0.00001
81	0.70960	0.00001	0.70994	0.00001
82	0.70924	0.00001	0.71006	0.00001
83	0.71060	0.00001	0.70970	0.00001
84	0.70892	0.00001	0.70972	0.00001
85	0.70916	0.00001	0.70958	0.00002
86	0.70917	0.00001	0.71000	0.00002
87	0.70910	0.00002	0.70997	0.00001
88	0.71130	0.00001	0.70999	0.00002
89	0.70905	0.00001	0.71040	0.00001
90	0.71147	0.00001	0.70998	0.00001
91	0.71083	0.00001	0.70981	0.00002
92	0.71062	0.00001	0.70999	0.00001
93	0.71065	0.00001	0.70988	0.00001
94	0.70832	0.00001	0.70941	0.00001
95	0.70871	0.00001	0.71008	0.00001
96	0.70876	0.00001	0.70972	0.00001
97	0.71009	0.00001	0.71019	0.00001
98	0.70990	0.00001	0.71018	0.00001
99	0.70979	0.00001	0.71013	0.00002
100	0.71202	0.00001	0.71080	0.00002
101	0.70972	0.00002	0.70983	0.00001
102	0.71060	0.00001	0.71020	0.00001
103	0.71044	0.00001	0.71037	0.00001
105	0.71179	0.00002	0.71101	0.00001
106	0.71179	0.00001	0.71034	0.00001
107	0.70993	0.00001	0.71042	0.00001

108	0.71058	0.00001	0.71022	0.00001
109	0.71126	0.00001	0.71048	0.00002
110	0.71117	0.00002	0.71065	0.00002

Tab. 29 ^{87}Sr/^{86}Sr isotope data for Hainburg, Mannersdorf and Prellenkirchen

Relevant publications and publication drafts

Publication titles in order of appearance:

"Development of an on-line flow injection Sr/matrix separation method for accurate, high-throughput determination of Sr isotope ratios by multiple collector-inductively coupled plasma-mass spectrometry"
Galler P., Limbeck A., Boulyga S.F., Stingeder G., Hirata T., Prohaska T.
Analytical Chemistry, 2007, **79**, 5023-9.

"Automation and miniaturization of an on-line flow injection Sr/matrix separation method for accurate, high throughput determination of Sr isotope ratios by MC-ICP-MS"
Galler P., Limbeck A., Üvevges M., Prohaska T.
Publication draft submitted to the *Journal of Analytical Atomic Spectrometry*.

"Identification of Marchfeld asparagus using Sr isotope ratio measurements by MC-ICP-MS"
Swoboda S., Brunner M., Boulyga S.F., Galler P., Horacek M., Prohaska T.
Analytical and Bioanalytical Chemistry, 2007, **390**, 487-94.

"Non-destructive determination of $^{87}Sr/^{86}Sr$ isotope ratios in early Upper Palaeolithic human teeth from the Mladeč Caves – preliminary results"
Prohaska T., Teschler-Nicola M., Galler P., Přichystal A., Stingeder G., Jelenc M., Klötzli U.
Early Modern Humans at the Moravian Gate, ed. Teschler-Nicola M., Springer-Verlag, Vienna, 2006, 505-14.